

LA-4842-MS

AN INFORMAL REPORT

CIC-14 REPORT COLLECTION
**REPRODUCTION
COPY**

e. 3

LAMPF Neutrino Facility Proposal

LOS ALAMOS NATIONAL LABORATORY
3 9338 00362 8467



los alamos
scientific laboratory
of the University of California
LOS ALAMOS, NEW MEXICO 87544

UNITED STATES
ATOMIC ENERGY COMMISSION
CONTRACT W-7405-ENG. 36

This report was prepared as an account of work sponsored by the United States Government. Neither the United States nor the United States Atomic Energy Commission, nor any of their employees, nor any of their contractors, subcontractors, or their employees, makes any warranty, express or implied, or assumes any legal liability or responsibility for the accuracy, completeness or usefulness of any information, apparatus, product or process disclosed, or represents that its use would not infringe privately owned rights.

This report, like other special-purpose documents in the LA. . .MS series, has not been reviewed or verified for accuracy in the interest of prompt distribution.

Printed in the United States of America. Available from
National Technical Information Service
U. S. Department of Commerce
5285 Port Royal Road
Springfield, Virginia 22151
Price: Printed Copy \$3.00; Microfiche \$0.95

LA-4842-MS

An Informal Report

UC-28 and 34

ISSUED: December 1971



LAMPF Neutrino Facility Proposal

K. Lande* and D. C. Potter, University of Pennsylvania
F. Reines*, H. Chen, and W. R. Kropp, University of California - Irvine
C. Cowan and H. Uberall, Catholic University of America
R. Davis, Brookhaven National Laboratory
E. Fenyves, University of Texas - Austin
E. Fowler, Purdue University
H. Frauenfelder, University of Illinois
V. Hughes and P. Nemethy, Yale University
S. L. Meyer, Northwestern University
R. L. Burman*, MP-7, D. R. F. Cochran, MP-6, and D. Nagle, MP-DO, LASL



*Written by K. Lande and F. Reines, compiled by R. L. Burman



PREFACE

Neutrino interactions have been observed at energies below a few MeV and in the GeV range. The Los Alamos Meson Physics Facility offers the first practical opportunity to study neutrino reactions at intermediate energies.

The neutrinos originating in the LAMPF beam stop have a typical energy of 40 MeV. This energy is below the threshold for producing muons and pions from muon-neutrinos. Electron-neutrino interactions can therefore be studied without interference from the muon-neutrino processes which dominate neutrino events at the high energy synchrotrons. Compared to reactor experiments the higher energy of the neutrinos is a distinct advantage, for it implies higher cross sections and some improvement in background rejection.

One may envisage a varied and serious program of neutrino experiments at LAMPF. This program could include a test of muon-conservation, a measurement of neutrino cross sections on chlorine with implications for neutrino astrophysics, studies of giant-resonance and exclusion principle effects on inverse-beta decay reactions with nuclei, and elastic neutrino-electron scattering.

All these experiments have in common the following features. They can use the LAMPF beam stop without modifications as a neutrino source; they require a well-shielded counting room and some five to six meters of iron shielding between this room and the beam stop. We feel that such a general neutrino facility is very desirable as it would permit investigation of a number of fundamental questions in weak interactions and in astrophysics.

TABLE OF CONTENTS

	<u>Page</u>
I. INTRODUCTION	1
II. PHYSICS	1
III. EXPERIMENTAL FACILITY	2
IV. SUMMARY	3
APPENDIX - Neutrino Experimental Proposals	5
No. 20 - "Neutrino Experiment," B. Hahn, G. Czapek, and P. G. Seiler	5
No. 24 - "Neutrino Experiments at LAMPF," E. Fenyves, K. Lande, and D. C. Potter	14
No. 31 - "A Neutrino Experiment to Test Muon Conserva- tion," V. W. Hughes, P. Nemethy, J. Duclos, R. Burman, and D. Cochran	21
No. 38 - "Neutrino Physics Program," H. Chen, M. F. Crouch, W. R. Kropp, J. Lathrop, F. Reines, and H. Sobel	28
No. 53 - "Observation of the Electron-Neutrino at LAMPF," R. Davis, E. Fowler, and S. Meyer	43

LAMPF NEUTRINO FACILITY PROPOSAL

by

R. L. Burman, H. Chen, D. R. F. Cochran, C. Cowan,
R. Davis, E. Fenyves, E. Fowler, H. Frauenfelder,
V. Hughes, W. R. Kropp, K. Lande, S. L. Meyer,
D. Nagle, P. Nemethy, D. C. Potter, F. Reines, and H. Uberall

I. INTRODUCTION

The advent of LAMPF makes practical the study of electronic neutrino interactions. An intense source of intermediate energy ν_e occurs at LAMPF as the end product of a chain involving pion production by protons in the LAMPF beam stopper and subsequent pion and muon decay. We estimate that 1/2 ma of incident protons gives rise to $1/4 \times 10^{15} \nu_e/\text{sec}$ with energies between 0 and 53 MeV. The ν_μ that accompany them do not have enough energy to produce muons and so by the presently accepted form of the lepton conservation law are sterile.

The other terrestrial neutrino sources are fission reactors that produce $\bar{\nu}_e$ ($3 \times 10^{13} \bar{\nu}_e/\text{cm}^2/\text{sec}$) with energies ~ 3 MeV, and high energy proton accelerators (AGS, CERN, Serphukov, and NAL) that produce neutrino beams predominantly muonic in character. The fission reactor presents the difficulty of looking for low energy secondaries in the presence of naturally occurring backgrounds. The increase of neutrino energy from the 3 MeV typical at reactors to the 30 MeV at LAMPF increases neutrino-electron cross sections by one order of magnitude and neutrino-nucleus cross sections by two orders of magnitude. In addition, the problems associated with natural radioactivity backgrounds decrease enormously because of the increase in the energy of the interaction secondaries. The high energy accelerators, in addition to the muonic nature of their neutrino source, have neutrinos (ν_e and ν_μ) of such an energy that the inelastic processes (production of π , N^* , etc.) swamp the elastic and charge exchange interactions. The LAMPF neutrino program

complements those at high energy accelerators (NAL, etc.) in that LAMPF aims mainly at a study of four fermion interactions, while the high energy interests are directed toward intermediate boson searches and inelastic reactions. The major source of ν_e in the universe is the stellar fusion process. Although we receive $\sim 6 \times 10^{10} \nu_e/\text{cm}^2/\text{sec}$ from the sun, the low average energy of these neutrinos makes them difficult to detect by any known direct counting technique.

II. PHYSICS

The availability of ν_e at LAMPF will permit the investigation of a number of fundamental questions in weak interactions, and will illuminate such basic astrophysical phenomena as stellar evolution and supernova explosions.

The areas of investigation that have been suggested for the initial program are: neutrino-electron interaction, determination of the form of the lepton conservation law, search for anomalous neutrino interactions, study of neutrino induced nuclear interactions, and study of the solar neutrino detector.

A. Neutrino-Electron Interaction

A most important question is the observation and study of $\nu_e + e^-$ scattering. This (and the equivalent $\bar{\nu}_e + e^-$ scattering) is the only diagonal purely weak interaction that can be studied and as such is not restricted to the same coupling constant as the nondiagonal weak interactions.¹ It is also the only other purely leptonic first order weak interaction other than muon decay available for study.

The cross section for this process is predicted by the universal V-A theory to be²

$$\sigma(\nu_e + e^-) = \frac{2G^2}{\pi} M_e \left(\frac{2E_\nu^2}{M_e + 2E_\nu} \right).$$

For $E_\nu \gg M_e c^2$

$$\sigma(\nu_e + e^-) \approx \frac{2G^2}{\pi} M_e E_\nu.$$

The critical questions to be answered by this study are:

1. Does the process exist?
2. Is there any anomaly in the value of G ?
3. Is the energy dependence linear?
4. What is the shape of the electron recoil spectrum?

Not only is this interaction fundamental to weak interactions, its existence and rate are also very important for the understanding of energy transfer mechanisms in stellar evolution³ and supernova formation.⁴

B. Lepton Conservation Law

The presently available data are consistent with four different lepton conservation laws. If we assign $L_e = +1$ to e^- and ν_e , $L_e = -1$ to e^+ and $\bar{\nu}_e$, $L_\mu = +1$ to μ^- and ν_μ and $L_\mu = -1$ to μ^+ and $\bar{\nu}_\mu$ then these four possible lepton conservation laws can be summarized as:⁵

1. ΣL_e and ΣL_μ separately conserved;
2. $\Sigma(L_e + L_\mu)$ and $(-1)^{\Sigma L_e} (-1)^{\Sigma L_\mu}$ separately conserved;
3. $\Sigma(L_e + 2L_\mu)$ conserved, and
4. $\Sigma(L_e - L_\mu)$ conserved.

Because of the characteristics of the π and μ decay the LAMPF neutrino source is ideally suited to distinguish between these four possibilities. Version (1) (additive law) permits only $\mu^+ + e^+ + \nu_e + \bar{\nu}_\mu$ while version (2) (multiplicative law) also permits $\mu^+ + e^+ + \bar{\nu}_e + \nu_\mu$. The observation of $\bar{\nu}_e$ from the LAMPF beam stop would indicate the validity of the multiplicative law while the absence of $\bar{\nu}_e$ would eliminate the multiplicative law from contention.⁶

Version (3) is indistinguishable from the additive law if there are only two leptons. Version (4) (subtractive law) would give rise to anomalous ν_μ interactions.

C. ν_μ Interactions

The LAMPF beam stop produces monoenergetic ν_μ from the decay of stopped pions, $\pi^+ \rightarrow \mu^+ + \nu_\mu$ ($E_{\nu_\mu} = 30$ MeV), and muonic anti-neutrinos with $0 \leq E \leq 50$ MeV from μ^+ decay. These ν_μ are energetically incapable of producing muons in either electron or nucleon interactions. A most surprising and spectacular situation could arise if the ν_μ produced electrons in electron or nucleon interactions. The two-body kinematics associated with 30 MeV ν_μ would make this process readily recognizable.

D. Neutrino Induced Nuclear Interactions

The neutrinos generated in the LAMPF beam stop can only engage in elastic or inverse beta decay interactions with electrons and protons since they are not energetic enough to produce muons or pions. In interactions with nuclei, however, they can induce nuclear transitions via the inverse beta decay interactions.⁷ These transitions involve energies considerably larger than are usual in beta decay and can excite states that are not observed to beta decay, and so may permit the study of the transition matrix elements involved in regions not previously accessible.

E. Study of the Solar Neutrino Detector

The search for solar neutrinos⁸ via the reaction $\nu_e + \text{Cl}^{37} \rightarrow \text{Ar}^{37*} + e^-$ has established an upper limit for energetic ν_e from the sun considerably below the predictions of present solar models.⁹ LAMPF provides the only terrestrial ν_e source capable of producing this reaction and might provide a verification of the sensitivity of this detector. Such a verification would enable one to set an upper limit for the temperature in the interior of the sun considerably below that obtained from the present solar models and might eventually challenge the presently assumed mechanisms for stellar energy generation.

III. EXPERIMENTAL FACILITY

Pions are produced as the protons slow down in the beam stop. About half of these pions interact before coming to rest. The remaining π^+ decay at rest into $\mu^+ + \nu_\mu$, and the resulting μ^+ , in turn decay into $e^+ + \nu_e + \bar{\nu}_\mu$. Most of the π^- come to rest and are captured by nuclei. About 1% of the stopping π^- decay, giving rise to μ^- that in

turn come to rest and are captured by nuclei. The ratio of μ^- to μ^+ decays is $\approx 1/7000$, so that virtually the only neutrinos emitted by the LAMPF beam stop come from the $\pi^+ \rightarrow \mu^+$ decay chain. We estimate that one ν_e is produced for every twelve protons incident on the beam stop.

The experimental facility is simple. It consists of massive shielding between the beam stop and the neutrino detection apparatus to absorb the radiation associated with the beam stop region, and shielding around the detection apparatus to attenuate cosmic rays and scattered radiation from other experimental areas. We estimate that five meters of steel will attenuate sufficiently the beam stop radiation and that 1 to $1\frac{1}{2}$ meters of steel will serve as an adequate enclosure shield. It should be emphasized that this facility does not require the magnets, horns or other beam transport apparatus characteristic of other accelerator neutrino facilities. The entire facility consists mostly of shielding -- some arranged to form an experimental enclosure and some located between that enclosure and the beam stop. An enclosure about six meters square and about five meters high appears adequate to accommodate the presently proposed experiments.

A convenient location would be the area immediately south of the main proton-line beam dump. Fig. 1 shows a schematic outline of the facility; it fits without modifications into the current beam dump design. Most of the 5-6 meters of direct shielding steel is already present as part of the beam dump. The rest of the direct shielding and a possible enclosure, also constructed of steel shielding blocks, is shown by the dashed lines in the drawing.

A typical neutrino detector would consist of a target containing about $0.3 - 1.0 \times 10^{30}$ protons, and an equal number of electrons. For a $\nu_e + e^-$ cross section of $6 \times 10^{-43} \text{ cm}^2$ and a flux of about $10^8 \nu_e/\text{cm}^2/\text{sec}$, we have about 2 to 6 interactions per day or probably one observed interaction per day. If the beam stop also emits $\bar{\nu}_e$ (due to the multiplicative law, for example) we expect about 10^2 times as many nucleon interactions as electron interactions.

Because of the small cross sections inherent in neutrino interactions and because of the interrelated nature of the contemplated experiments it is anticipated that most of these experiments could be done

in parallel. All the experiments, with the exception of the Cl^{37} experiment, can, in principle, be accommodated by a single detection apparatus.

The prime problem in the establishment of the neutrino experimental area is the construction of a suitably shielded enclosure. The construction and testing of this area will undoubtedly require a considerable period of time, and will be a major challenge in the execution of these experiments. The running time for the proposed program of experiments is dominated by the important $\nu_e + e^-$ scattering reaction, because of its relatively small anticipated cross section. Since the neutrino-nucleon cross sections are $\sim 10^2$ larger the data necessary to measure those reactions should be available in a significantly shorter time.

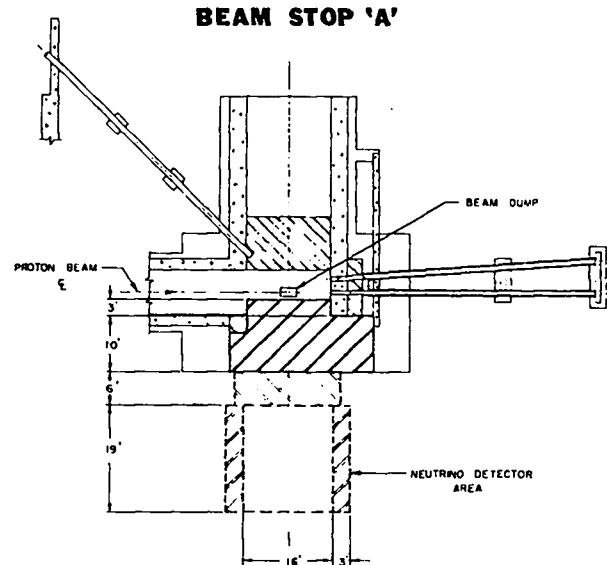


Fig. 1. Plan at beam elevation 6972 ft.

IV. SUMMARY

The proposed LAMPF neutrino facility would permit the investigation of an almost virgin area of physics that is of prime importance both to the understanding of weak interactions and to stellar evolution and energy generation. The required experimental facility is simple, consisting of a shielded enclosure. Since LAMPF is the only accelerator with the characteristics required for the study of ν_e interactions as well as the other fundamental questions

outlined above, we strongly urge the establishment and support of such a facility at LAMPF.

References

1. M. Gell-Mann, M. Goldberger, N. Kroll, and F. E. Low, Phys. Rev. 179, 1518 (1969).
2. R. P. Feynman and M. Gell-Mann, Phys. Rev. 109, 193 (1958).
3. E. E. Salpeter, Comments of Nuclear and Particle Physics 2, 1 (1968).
4. H. Y. Chiu, Annual Review of Nuclear Science 16, 591 (1966).
5. These possibilities and their implications are summarized by B. Pontecorvo, Sov. Phys. JETP 26, 984 (1968). Also see L. S. Kisslinger, Phys. Rev. Lett. 26, 998 (1971).
6. It would also be possible for $\bar{\nu}_e$ to arise from lepton nonconservation and an associated neutrino oscillation. A recent suggestion of the possibility of lepton nonconservation and its manifestation in double beta decay and C. P. violation has been discussed by H. Primakoff and D. H. Sharp, Phys. Rev. Letters 23, 501 (1969). The possibilities of neutrino oscillation have been considered by V. Gribov and B. Pontecorvo, Phys. Letters 28B, 493 (1969) and B. Pontecorvo - Kiev Conference on High Energy Physics (1970).
7. See for example, F. J. Kelly and H. Uberall, Phys. Rev. 158, 987 (1967).
8. R. Davis, D. S. Harmer, and K. C. Hoffman, Phys. Rev. Letters 20, 1205 (1968).
9. J. N. Bahcall and R. K. Ulrich, Astrophys. Jour. 160, L57 (1970).

APPENDIX

NEUTRINO EXPERIMENTAL PROPOSALS

No. 20 - "Neutrino Experiment," B. Hahn, Spokesman
G. Czapek, B. Hahn, and P. G. Seiler, University
of Berne

RESEARCH PROPOSAL

LOS ALAMOS MESON PHYSICS FACILITY

v-EXPERIMENT

Spokesman: B. Hahn

G. Czapek, B. Hahn, and P. G. Seiler
Physics Department, University of Berne

June 5, 1971

Original for SIN
March 3, 1970

SUMMARY OF EXPERIMENT

It is proposed to carry out a neutrino physics programme, which allows to study with the same apparatus:

- Lepton conservation law
- inverse β -decay on various target nuclei and
- neutrino-electron scattering.

The detector is made out of modules containing each 1 "massless" multiwire counter, 1 "massless" optical spark chamber and 1 target. One module has dimensions of 200 cm x 200 cm x 10 cm. 30 modules arranged in one row and fanned-out for photography will be used. 4-5 fold coincidences between successive multiwire counters trigger the spark chambers. The multiwire counters are also used to measure ionisation. The counting rates of good events will be of the order of 1-10 events per day at LAMPF. Angle and range of the particles can be determined. Additional information comes from multiple scattering. The target material will be C, CH₂, H₂O, D₂O, Al, Cl₂C₄ etc. The detector will be placed at 90° to the beam dump and behind approximately 8 m of iron shielding. A massive block-house around the detector is required against cosmic background. A quantitative study on the cosmic background, which is induced by energetic neutrons with a scaled down set-up is under way. These measurements will allow to determine the dimensions of the block-house. A cosmic ν -meson veto counter with a veto factor of 10^4 - 10^5 , possibly a liquid scintillator surrounding the apparatus will be a necessity. Our model apparatus also will be exposed to 35 MeV electrons of a betatron at Berne, in order to get experiences. An on line computer is used for data acquisition and detector control.

PROPOSAL INFORMATION

Beam Area: ν -area

Beam Requirements:

Type of Particle: Protons
Momentum Range: 700 \div 800 MeV
Intensity: Maximum possible, $> 600 \mu A$
Target(s): Dump

Running Time Required:

Installation Time Required (no beam): 3 months
Data Runs: Continuous 1 year *SHIELDING TESTS AND RUNNING IN: 3 months*

Scheduling:

Realistic date when User will have the non-LAMPF apparatus ready: January 1973 \div July 1973

Major LAMPF Apparatus Required:

Computer: on line Computer HP 2100
Electronics: standard fast electronics, power supplies

Shielding and Enclosures Required: ν -shielding, block-house, hole in experimental floor
Special Services Required: cosmic ray shield (P's)

Space Required:

$\sim 50 m^2$ + space for electronics and on line computer;
 $\sim 12 - 15$ racks

Special apparatus to be fabricated by LAMPF

- beam dump
- 8 m of Fe shielding, 4 m high, 4 m wide
- hole in experimental floor: 6.5 m long, 6 m wide, 3.5 m high
- shield against charged cosmic and machine background
- concrete blockhouse or earth mountain against cosmic and machine neutrals
- mass production of multiwire proportional detectors, spark chambers and target holders
- detector frame

1. Introduction

The intense proton beam of LAMPF after traversing several thin and thick targets finally will be stopped almost at its full energy and with approximately its half primary intensity in a beam dump and provide an almost point-like source of medium energy neutrinos. The greatest interest will be on the electron neutrinos of μ^+ -decay. The neutrinos have a maximum energy of 53 MeV. This energy range so far has not been accessible to experimental investigations. This range lies in between those of antineutrinos and neutrinos of reactors and the sun (< 10 MeV) and neutrinos from proton synchrotrons (> 500 MeV). The neutrino intensity will amount to several 10^{14} neutrinos/sec with isotropic angular distribution. The contamination of neutrinos from ν^- -decay will be negligible due to the high capture rate of ν^- and $\bar{\nu}^-$ in atomic nuclei. Muonneutrinos from τ^- and ν^- -decay have energies below the threshold of ν^- -production. The neutrinos from ν^- -decay will be important in several respects to study weak interactions.

1.1. Lepton Conservation

ν^+ -decay is so far the only pure leptonic process which has been accessible to the experiment. All information on ν -decay resides on observations done on the decay positron. Nothing is known experimentally on the nature of the accompanying neutral particles. These are most likely $\nu_e - \bar{\nu}_\mu$ -pairs or $\bar{\nu}_e - \nu_\mu$ -pairs. The second possibility with "interchanged" neutrinos corresponds with the multiplicative lepton conservation law as it has been formulated by Cabibbo and Gatto¹⁾²⁾ and by Weinberg³⁾⁴⁾. Experimental upper limits with respect to a multiplicative lepton conservation law have been given deduced from non-observation of muonium-antimuonium-conversion⁵⁾ from the process⁶⁾

$$e^+ + e^- \rightarrow \mu^- + \mu^+$$

and from the processes⁷⁾⁸⁾

$$\nu_\mu + Z \rightarrow Z + e^- + \mu^+ + \nu_e$$

All these experiments, however, so far are not sensitive enough to detect a coupling of the strength of the universal weak interaction⁹⁾.

In the proposed experiment $\bar{\nu}_e$ should be detected by the process

$$\bar{\nu}_e + p \rightarrow n + e^+$$

performing a $\text{CH}_2\text{-C}$ difference measurement. $\bar{\nu}_e$ should be detected in the process

$$\nu_e + d \rightarrow p + p + e^-$$

performing a $\text{D}_2\text{O-H}_2\text{O}$ difference measurement.

1.2. ν_e e^- -Scattering

The simplest process in weak interaction is the elastic scattering of electron neutrinos on electrons. This process has recently been discussed in the frame of a modified weak interaction theory by Gell-Mann, Goldberger, Kroll and Low¹⁰⁾. The coupling in ν_e - e scattering could deviate from universal coupling. Some evidence for the occurrence of $\bar{\nu}_e$ - e scattering has been announced recently at a reactor-experiment¹¹⁾. From the CERN 1964 neutrino experiment¹²⁾ an upper limit for a coupling constant $G_{\nu_e e}$ of $G_{\nu_e e} < 6G$ (G = coupling constant of β -decay) with 90% confidence has been deduced.

The astrophysical importance of ν - e coupling and its experimental evidence has been discussed by Stothers¹³⁾.

In ν - e scattering¹⁴⁾ it is expected that recoil electrons are ejected in a forward cone. The scattering cross section must be proportional to the electric charge of the target nucleus.

1.3. Neutrino Nucleus Scattering

So far inverse β -decay has been observed only on free protons by using reactor antineutrinos¹⁵⁾¹⁶⁾. Elaborate attempts to detect neutrinos from the sun by the reaction

$$\nu_e + \text{Cl}^{37} \rightarrow \text{Ar}^{37} + e^-$$

so far have been unsuccessful. At proton synchrotrons, however, in the multi-GeV energy range electron neutrino nucleus reactions have been observed, the neutrinos stemming from K_{e3} -decay¹⁸⁾.

In the energy range up to 53 MeV the neutrino cross sections on nuclei will strongly depend on nuclear structure. The cross sections will depend on the degree of the allowance of the transitions. Measurements with intermediate energy neutrinos on nuclei will be of great importance with respect to neutrino astrophysics¹⁹⁾²⁰⁾.

1.4. Experimental Technique

The expected event rates will be small (a few, or several ten events per day, depending on the process) even with a multiton detector. The neutrino experiment therefore requires continuous running during a long period. The interference with other experiments of a pion factory will be small because the experiments can be done with the remaining proton beam falling into the beam dump. The average beam intensity, however, should be above 500 μA . The shielding problem against neutrons, pions coming from the machine, beam dump and from cosmic radiation will be a major problem to be solved. The experimental set up for the detection of the electrons or positrons must be fully automated and the experiment must be done with a computer on line for data acquisition and detector control. The events will be photographed in optical spark chambers and immediately rescanned.

The project must be started not later than two years in advance to the actual experiment in order to allow the construction of the large detector as well as the anticounter system and the shielding.

A prestudy with respect to cosmic background and the performance of a model detector is under study. Recoil protons and pion production from cosmic neutrons is investigated and the model set up is exposed to an electron beam of 40 MeV energy of a betatron.

2. Neutrino Flux

Neutrinos are produced in the following way

$$\begin{aligned} p + \text{target} &\rightarrow \pi^+ + \dots \\ \pi^+ &\rightarrow \mu^+ + \nu_\mu \\ \mu^+ &\rightarrow e^+ + \nu_e(\bar{\nu}_e) + \bar{\nu}_\mu(\nu_\mu) \end{aligned}$$

Since π^+ and μ^+ will decay at rest, ν_μ will be below the threshold for μ -production. In order to estimate the number of stopped muons the probability for pion production by protons must be known. Since the production cross sections are roughly proportional to $A^{2/3}$, light targets e.g. carbon or water are preferable. Furthermore the loss of positive pions by the charge exchange process must be considered. Therefore the energy spectrum of the produced pions must be known too.

2.1. The Production of Positive Pions

The total cross section for the reaction

$$p + C \rightarrow \pi^+ + \dots$$

in dependence of the proton primary energy is given in the literature only incompletely. One finds in²⁴⁾

E_p	σ_{π^+}
350 MeV	5.5 mb
450 MeV	27.4 mb
660 MeV	37.9 mb

If one takes for the total cross section, by using the data of²³⁾,

$$\sigma_{\text{tot}} = 12^{2/3} \frac{\sigma_{\text{tot}}(\text{pp}) + \sigma_{\text{tot}}(\text{p}^{11})}{2}$$

the number of positive pions per proton (700 MeV), taking into account the ionisation energy loss of the protons in the target (C , approximately 150 g/cm²) amounts to

$$n_{\pi^+}/p = 0.15$$

With a proton beam of 500 μA the pion intensity will be

$$I(\pi^+) \approx 4.5 \cdot 10^{14} \text{ sec}^{-1}$$

2.2. The Production of Positive Muons and Neutrinos

The energy spectra of the pions in the forward direction are given in²³⁾. By averaging the spectra for the effective proton energies one finds the energy spectrum of the pions. This spectrum is shifted to higher energies relative to the true spectrum. Since pions emitted at large angles have smaller energies than those emitted in the forward direction, the calculated pion loss is overestimated. For the cross section of the reaction



the following relation has been assumed

$$\sigma_{ex}(\pi^+ + C) \approx \frac{A}{2} \sigma_{ex}(\pi^+ + n) \approx \frac{A}{2} \sigma_{ex}(\pi^+ + p)$$

Together with the data of²²⁾ this amounts to a pion loss of approximately 30 %. The estimated intensity for positive muons then is

$$I(\mu^+) \approx 3 \cdot 10^{14} \mu^+ / \text{sec}$$

3. Lepton Conservation and ν^+ -Decay

3.1. Lepton Conservation

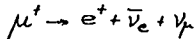
Based on experimental observations and on theoretical arguments¹⁾²⁾ 3)4) a lepton conservation law can be formulated in several ways using the following definition for L_e and L_μ :

particle	L_e	L_μ
ν_e, e^-	1	0
ν_μ, μ^-	0	1
$\bar{\nu}_e, e^+$	-1	0
$\bar{\nu}_\mu, \mu^+$	0	-1
others	0	0

The following formulations of lepton conservation can be discussed, whereby the following expressions should be conserved in all interactions

1. $\sum L_e, \sum L_\mu$
2. $\sum L_e - \sum L_\mu$
3. $\sum L_e - \sum L_\mu \pmod{4}$
4. $\prod (1 - 2L_\mu^i)$
5. $\sum L_e + \sum L_\mu, \prod (-1)^{L_e}$

All these formulations are in agreement with present experimental information, however have different content. The decay



is forbidden by law 1 and 2, but is not forbidden by laws 3, 4, 5.

3.2. The Energy Spectrum of the Neutrinos

Assuming V-A-theory and a two component neutrino the energy spectra of leptons and antileptons in ν^+ -decay can be calculated. Neglecting the electron-mass relative to the muon-mass one finds²⁴⁾²⁵⁾ (Fig. 3) the energy spectra

$$\text{For leptons } w(E) = \frac{192}{m_\mu^6} E^2 \left(\frac{m_\mu}{2} - E \right)$$

$$\text{for antileptons } w(E) = \frac{64}{m_\mu^6} E^2 \left(\frac{3m_\mu}{4} - E \right)$$

The kinetic energy lies inbetween

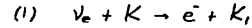
$$0 \leq E \leq \frac{m_\mu}{2}$$

The average energy of the leptons is smaller than the average energy of the antileptons. The neutrinos will be emitted isotropically with respect to the laboratory system.

4. Neutrino Nucleus Cross Sections

4.1. In General

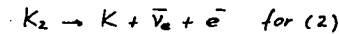
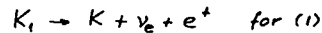
Considering the scattering processes



whereby K, K_1, K_2 are complex nuclei. One finds analogous to the Fermi-theory of β -decay for the cross section²⁶⁾ (Fig. 2)

$$\sigma = \frac{1.00 \cdot 10^{-40}}{ft_{1/2}} E_e p_e \quad [\text{cm}^2]$$

where E_e is the kinetic energy of the electron in MeV, p_e is the momentum of the electrons in MeV/c, $ft_{1/2}$ is the ft-value of the β -decay:



$p_e E_e$ corresponds to the phase space factor for the considered scattering process. $ft_{1/2}$ is inversely proportional to the transition matrix element of the nuclei ($K \rightarrow K_1$, resp. $K \rightarrow K_2$). The neutrino nucleus scattering cross section is¹⁵⁾²⁷⁾

$$\sigma(\nu_e n) = \sigma(\bar{\nu}_e p) = 8 \cdot 10^{-44} p_e E_e \quad [\text{cm}^2]$$

The cross section on deuterium might be suppressed by a factor²⁸⁾. The formulas do not contain a final state Coulomb correction. For the secondary electrons isotropy is assumed.

4.2. Cross Sections for Neutrinos from ν^+ -Decay

An average cross section is obtained by folding with the energy spectrum:

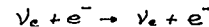
$$\bar{\nu}_e + p \rightarrow e^+ + n: \quad \bar{\sigma} = 1.1 \cdot 10^{-40} \text{ cm}^2$$

$$\nu_e + Al^{27} \rightarrow e^- + Si_{\text{ground}}^{27}: \quad \bar{\sigma} = 2.3 \cdot 10^{-41} \text{ cm}^2$$

Aluminium which occurs naturally as a pure isotope, is an interesting target for the study of neutrino nucleus interaction, because of the small ft-value of Si^{27} ground state ($ft_{1/2} = 10^{3.6} \text{ sec}$). It is difficult to estimate the contribution of excited states of Si^{27} to the cross section. With the available energy also breakup of nuclei is possible³⁰⁾.

5. Neutrino-Electron Cross Section

The total cross section for the reaction



in dependence of the neutrino energy E_ν can be calculated with universal coupling¹⁴⁾³¹⁾ (Fig 2).

$$\sigma \approx 1.7 \cdot 10^{-48} E_\nu \quad [\text{cm}^2, \text{MeV}]$$

The energy spectrum of the secondary electrons is constant in the interval

$$0 \leq E_e \leq E_\nu / (1 + \frac{2m_e}{E_\nu})$$

The uniform energy distribution corresponds with a strong forward peaking of the electrons. Taking into account the energy spectrum of the neutrinos an average cross section is obtained:

$$\sigma = 5.3 \cdot 10^{-43} \text{ cm}^2$$

In a E_e, θ_e -diagram, events only are possible by kinematics in the dashed area of Fig. 5. The energy spectrum integrated over the solid angle is approximately

$$W(E_e) \approx \frac{10}{3m_p} \left[1 - 4 \left(\frac{2E_e}{m_p} \right)^3 + 3 \left(\frac{2E_e}{m_p} \right)^4 \right]$$

The scattering of antineutrinos will not be discussed further, the cross sections being approximately three times smaller and the secondary electrons have smaller energies.

6. Experimental Technique

6.1. Detector

The event rates which will be given in the next section have been calculated under the assumption of a target surface of 120 m^2 . The detector will consist of 30 subunits (modules) each composed of a target, a trigger counter and an optical spark chamber. The subunit has an area of 2.2 m^2 and a thickness of 7 cm. The whole detector volume will be approximately 12 m^3 and will have a mass of approximately 3,3 tons. Photography is done from below viewing directly the fanned-out spark chambers without using mirrors. The detector is surrounded by a heavy concret shielding. The detector has the important feature that by interchanging the target material all the experiments listed in the introduction can be made with the same apparatus, one after the other.

6.2. Target Material

In two successive experiments under the same conditions the target materials CH_2 and C will be used. The hydrogen in CH_2 serves as a proton target for the antineutrino from the decay

$$\mu^+ \rightarrow e^+ + \bar{\nu}_e + \nu_\mu$$

i.e. the amplitude of the process violating the additive lepton number conservation of ν^+ -decay is determined by the CH_2/C -difference event rate. For various reasons it is expected that the cross section of the $\bar{\nu}_e$ -C reaction and the ν_e -C reaction will be appreciably smaller than the cross section for $\bar{\nu}_e$ -p and ν_e -n reactions. Should therefore the ν^+ -decay predominantly occur according to the equation

$$\mu^+ \rightarrow e^+ + \nu_e + \bar{\nu}_\mu$$

only a very small number of events should remain from the CH_2 -C-measurement. For the detection of ν_e a difference measurement between D_2O and H_2O will be performed. This experiment at the same time allows a comparison between experimental and theoretical²⁸⁾ ν_e -d cross section. In the following an experiment with aluminium targets as well as other targets (e.g. C_6Cl_2) will be done. At the same time data are accumulated which should contain also neutrino electron scattering. The separation of such events should be possible due to the strong forward peaking (Fig. 5). In addition the event rate for ν_e -scattering must be proportional to the atomic number of the target nucleus.

6.3. Target Thickness and Trigger Conditions

In order to suppress short range particles as well as accidental coincidences an m-fold coincidence of successive trigger counters is required. On the other hand due to the finite range of the electrons m should not be too large. An optimum with respect to the event rate is reached approximately at

$$\frac{m t}{R_{\text{max}}} \approx 0.4$$

m: number of successive trigger counters in coincidence
t: target thickness
 R_{max} : maximum range of electrons (measured in the same units as t) (Fig. 4, 6).

With this condition one observes approximately 40 % of all neutrino reactions; for carbon and $m = 5$ one obtains $t = 1.8 \text{ g/cm}^2$. For further optimisation Monte Carlo calculations are needed.

6.4. Trigger Counters

Plastic scintillators are not suitable as trigger counters because of the high density and the chemical composition. Therefore large area³⁵⁾ "massless" multiwire proportional counters are in development. These counters have somewhat larger response time as well as a time jitter. For the small event rate expected this can be tolerated.

6.5. Anticounter

In order to reduce the trigger rate by cosmic muons down to $10^{-3}/\text{sec}$. a veto factor of the anticounter of several times 10^4 is required. The possibility is studied to use large area multiwire counters instead of plastic or liquid scintillators.

6.6. Spark Chambers

Optical three-electrode spark chambers with small mass of the mesh type will be used.

6.7. On line Computer

Since the experiment with its low counting rate needs a long exposure time, a certain degree of automation should be reached, e.g. the efficiency of the trigger counters should be supervised by on line computer technique. For each event the trigger pattern and digitized pulseheights measured by the proportional counters (trigger counters) are recorded on magnetic tape. Periodically measured single rates as well as information about the beam conditions will be stored on disc.

6.8. Evaluation

Only a small fraction of the pictures will show neutrino events. Cosmic ray muon tracks will be eliminated by introducing a reduced fiducial volume. Electrons can be clearly distinguished from protons from multiple scattering measurements. Fig. 7 shows the expectation value calculated according to³²⁾ of the projected scattering angle in carbon for a target thickness of $t = 1.8 \text{ g/cm}^2$ in dependence of the rest range. As can be seen stopping protons and stopping electrons can be distinguished at a high confidence level. The separation of stopping protons and 50 MeV electrons which leave the detector after 5 subunits, however, is less good. In this latter case one loses with a track length of 6 double sparks 50 % of all electrons when 90 % of the protons are eliminated.

7. Event Rates

$$r = \frac{I_\nu \cdot \sigma \cdot L \cdot t \cdot F \cdot q}{A \cdot 4\pi \cdot c^2} \cdot \begin{cases} 1 & \text{for } (\nu - K) \\ Z & \text{for } (\nu - e) \end{cases}$$

where

I_ν neutrino flux
 σ average cross section
 Z atomic number of the target
 A mass number of the target

- t target thickness
- F total target area
- s average distance between detector and the neutrino source
- L Avogadro's number
- q probability to observe an interaction

Especially for $F = 120 \text{ m}^2$, $s = 10,0 \text{ m}$ (this corresponds to 8 m iron shielding instead of the 5 m quoted by the LAMPF Neutrino Users Group), $t = 1,9 \text{ g/cm}^2$ $q = 40$ % the following event rates can be expected.

reaction	assumed decay ratio $\frac{\mu^+ \rightarrow e^+ \bar{\nu}_e \nu_\mu}{\mu^+ \rightarrow e^+ \bar{\nu}_e \nu_\mu + \bar{\nu}_\mu \nu_e}$	event rate day ⁻¹
$\bar{\nu}_e + p \rightarrow e^+ + n$ (in CH_2)	1/2	8
$\nu_e + e^- \rightarrow e^- + \nu_e$ (in Al)	0	0.3 (with Fermi Coupling)
$\nu_e + \text{Al}^{27} \rightarrow e^- + \text{Si}^{27}_{\text{ground}}$	0	1.0
$\nu_e + d \rightarrow e^- + p + p$ (in D_2O)	0	5

8. Shielding

8.2. Shielding Between Beam Dump and Detector

In view of the small neutrino event rate of some ten events per day the secondary neutrino flux from the dump must be reduced to a few events per day at the detector. Neutrons above 100 MeV can produce in the detector recoil protons which can trigger the detector and which can produce tracks similar to those of electrons. Neutrons above 300 MeV can create pions which stop in the target and are undergoing the ν -e-decay sequence. This electron source must be completely eliminated. In the beam dump there will be produced per incoming proton approximately one neutron with energy larger than 100 MeV, i.e. at 500 μA proton current approximately $2 \cdot 10^{15}$ neutrons per second will be produced in the forward direction. The energy spectrum of the neutrons has a maximum at approximately 400 MeV with a half width of approximately 100 MeV. Perpendicular to the proton beam direction the neutron intensity will be reduced by approximately a factor of 5 and the average energy will be smaller by approximately 100 MeV. The required reduction factor of the neutron flux is approximately 10^{17} . As shielding material only iron is in question. For the computation of the absorption length the inelastic n-Cu cross section (taking from³³, Fig. 8) is used and recomputed for Fe with an $A^{2/3}$ ratio.

$$\lambda_{\text{Fe}}^{\text{inel}} = 17.7 \text{ cm}$$

After the first inelastic reaction the neutrons are not lost completely, they are however reduced in energy by a factor of approximately 0.65. In three steps the average energy is below 150 MeV and after that the neutron can be considered to be lost completely as the cross section is increasing rapidly with decreasing energy. After the thickness x of the absorber the neutron intensity is

$$N(x) = N_0 \left(1 + \frac{x}{\lambda} + \frac{x^2}{2\lambda^2}\right) e^{-x/\lambda} \approx N_0 \frac{x^2}{2\lambda^2} \cdot e^{-x/\lambda}$$

In order to obtain a reduction factor of 10^{17} approximately 8 m of iron (density $7,8 \text{ g/cm}^3$) will be necessary. An additional reduction in neutron flux by elastic scattering processes is to be expected, but has not been taken into account. The height of the shielding must be approximately 3 m. Precautions must be taken to avoid neutrons penetrating the detector from above or below the shielding. Adequate re-inforcement of the shielding on top and at the bottom must be provided. In order to reach an optimum thickness of the shielding the last few meters must be adjusted accordingly during the first phase of the experiment.

8.2. Blockhouse

The detector will be put inside a blockhouse for protection against low energetic neutrons of the machine against gamma-radiation from π_0 -decay and neutrons from cosmic rays.

8.2.1. Low Energy Neutrons

Individual neutrons below 100 MeV are incapable to produce triggers, however, the low energetic neutron flux on the level of the biological tolerance dose of 10 neutrons/cm²/sec is too high by a factor of 100, since they produce random sparks in the spark chambers as well as random coincidences. An attenuation factor of 10^4 is required which easily can be achieved.

8.2.2. Gamma Rays

Indirect gamma rays with energies larger 10 MeV must be shielded carefully since they are producing electron pairs or compton electrons which can simulate neutrino events. Gamma rays must be absorbed by adequate lead shielding of the targets and the beam dump.

8.2.3. Cosmic Neutrons

The cosmic neutron flux with energies above 100 MeV is approximately $2 \cdot 10^{-3}$ neutrons per cm²/sec³⁴). With an effective surface of the detector of approximately 20 m², $4 \cdot 10^7$ neutrons per day will reach the detector. This background is under study at our laboratory.

9. Pre-experiments and Additional Experiments

In order to check some of the most important computations and estimations a model set up scaled down in the ratio of 1:4 has been built. A subunit of the model set up consists of a thin wall aluminium spark chamber (0,4 g/cm²), a plastic trigger counter (1 cm thick) and space for targets of different materials. The whole model is surrounded by plastic scintillators which serve as anticounters. The spark chambers are triggered by 2:6 successive scintillators. The following measurements will be made:

- a) Range of electrons with the target materials C, CH₂, H₂O, D₂O, aluminium and heavier material for various energies up to 45 MeV.
- b) Calibration measurements on discrimination between electrons and protons by means of multiple scattering measurements
- c) Determination of the frequency of proton triggers resulting from cosmic ray neutrons
- d) Determination of frequency of pion triggers resulting from cosmic ray neutrons
- e) Study of the background nearby a beam dump of 600 MeV protons (e.g. CERN Isolde)
- f) Determination of an upper limit of the frequency of electron tracks resulting from steep muons (δ -rays) and resulting from stopping muons (decay electrons).

References

- 1) N. Cabibbo and R. Gatto, *Phys.Rev.Lett.* 5, 114, 1961
- 2) N. Cabibbo and R. Gatto, *Nuovo Cimento* 19, 612, 1961
- 3) G. Feinberg and S. Weinberg, *Phys.Rev.Lett.* 5, 381, 1961
- 4) T.D. Lee and C.S. Wu, *Ann.Rev.Nucl.Sci.* 15, 390, 1965
- 5) G.G. Amato, P. Crane, J.E. Rothberg and P.A. Thompson, *Phys.Rev.Lett.* 21, 1709, 1968
- 6) W.C. Barber, B. Gittelman, D.C. Cheng and G.K. O'Neill, *Phys.Rev.Lett.* 22, 902, 1969
- 7) C.Y. Chang, *Phys.Rev.Lett.* 24, 79, 1970
- 8) K. Borer, B. Hahn, H. Hofer, H. Kaspar, F. Krienen and P.G. Seiler, *Physics Lett.* 29B, 614, 1969
- 9) E. Lohrmann, *Proc.Lund Int.Conf.Elem.Part.* 1969, 16
- 10) M. Gell-Mann, M. Goldberger, N.M. Kroll and F.E. Low, *Phys.Rev.* 179, 1518, 1969
- 11) F. Reines and H.S. Gurr, *Univ. Calif., Irvine Report Nr.UCI10,19*
- 12) H.J. Steiner, *III.Phys.Inst.Techn.Hochsch.Aachen, Int.Rep-ort* 1970
- 13) R.D. Stothers, *Phys.Rev.Lett.* 24, 538, 1970
- 14) W. Hauer, *III.Phys.Inst.Techn.Hochsch.Aachen, Int. Report Nr. 27*, 1968
- 15) F.A. Nezrick and F. Reines, *Phys.Rev.* 142, 852, 1966
- 16) C.L. Cowan, A.D. Mc Guire, F.B. Harrison, H.W. Kruse and F. Reines, *Phys.Rev.* 117, 159, 1960
- 17) R. Davis, D.S. Harmer and K.C. Hoffman, *Phys.Rev.Lett.* 20, 1205, 1968
- 18) J.K. Bienlein, A. Böhm, G. v. Dardel, H. Faisner, F. Ferrero, J.M. Gaillard, H.J. Gerber, B. Hahn, V. Kaftanov, F. Krienen, M. Reinharz, R.A. Salmeron, P.G. Seiler, A. Staude, J. Stein and H.J. Steiner, *Physica Lett.* 13, 80, 1964
- 19) H.Y. Chiu, "Neutrino Astrophysics", Gordon and Breach, London, 1965
- 20) E.E. Salpeter, *Comments Nucl.Part.Phys.* 2, 97, 1968
- 21) W. Hirt, E. Heer, M. Martin, E.G. Michaelis, C. Serre, P. Sarek and B.T. Wright, *yellow CERN-Report Nr. 69-24*, 1969. Quoted values from: W. Dudziak (350 MeV), E. Lillothun (450 MeV), A.G. Meshkovskii et al. (660 MeV)
- 22) V.S. Barashenkov, "Interaction Cross Sections of Elementary Particles", *Israel Progr.Sci.Transl.*, Jerusalem, 1968
- 23) Technical Proposal for an Isochronous Ring Accelerator for 500 MeV Protons, Part II
- 24) H. Ueberall, *Nuovo Cimento* 23, 219, 1962
- 25) G. Källen, "Elementarteilchenphysik", BI-Hochschultaschenbücher, Mannheim, 1965
- 26) F. Reines and R.M. Wood Jr., *Phys.Rev.Lett.* 14, 20, 1965
- 27) N. Cabibbo and R. Gatto, *Nuovo Cimento* 15, 304, 1960
- 28) F.J. Kelly and H. Ueberall, *Phys.Rev.Lett.* 16, 145, 1966
- 29) Y. Yamaguchi, *yellow CERN-Report Nr. 61-2*, 1961
- 30) H. Ueberall, *Phys.Rev.* 126, 1572, 1962
- 31) J.N. Bahcall, *Phys.Rev.* 136B, 1164, 1964
- 32) L. Marton, "Methods of Experimental Physics", Vol. 5A, 73-74, Academic Press, New York and London, 1961
- 33) V.S. Barashenkov, K.K. Gudima and V.D. Tonosov, *Fortschr. Physik* 17, 683, 1969
- 34) E.B. Hughes and P.L. Maraden, *Journ.Geophys.Rev.* 71, 1435, 1966
- 35) K. Borer, G. Czappek, H. Kaspar and P.G. Seiler, *Nuclear Instruments and Methods*, in press

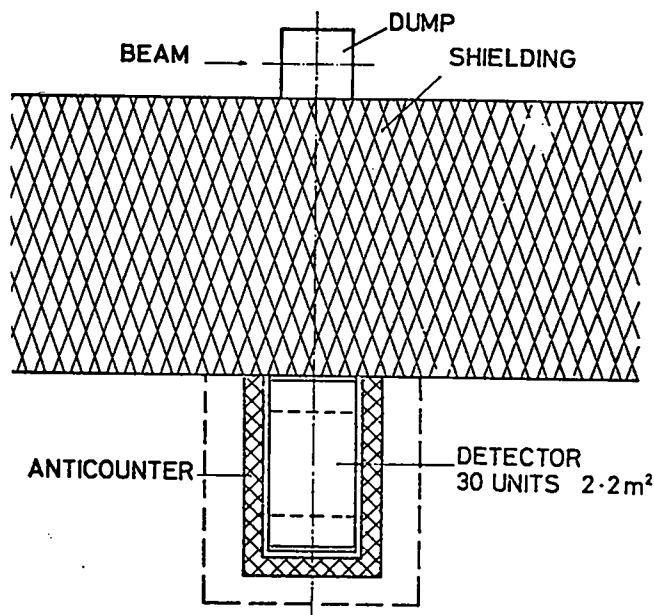


Figure 1a

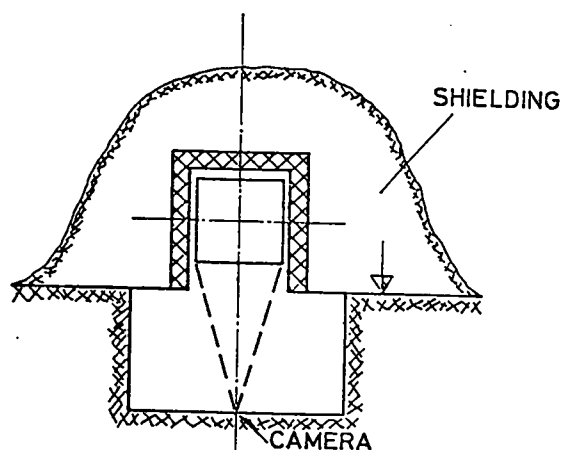


Figure 1b

1: Experimental lay-out, top- and side-view

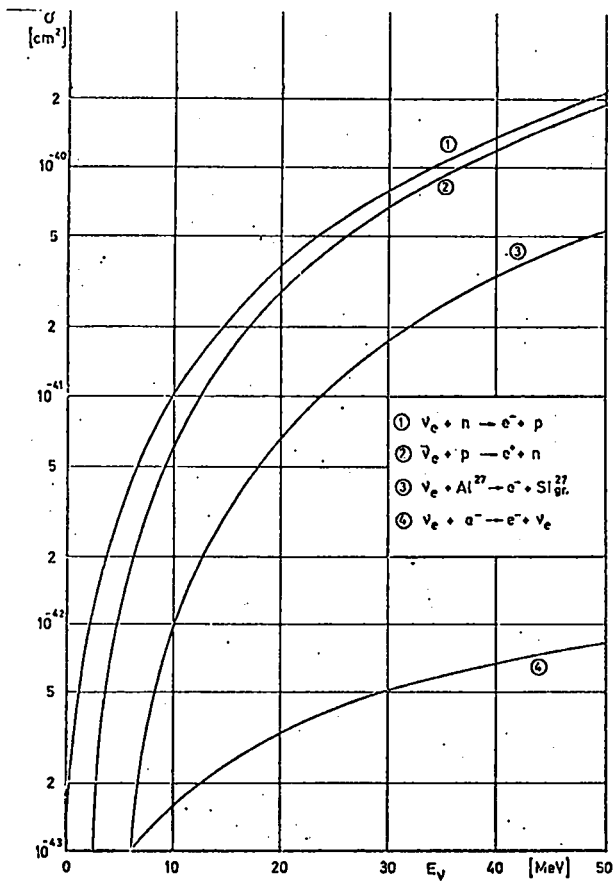
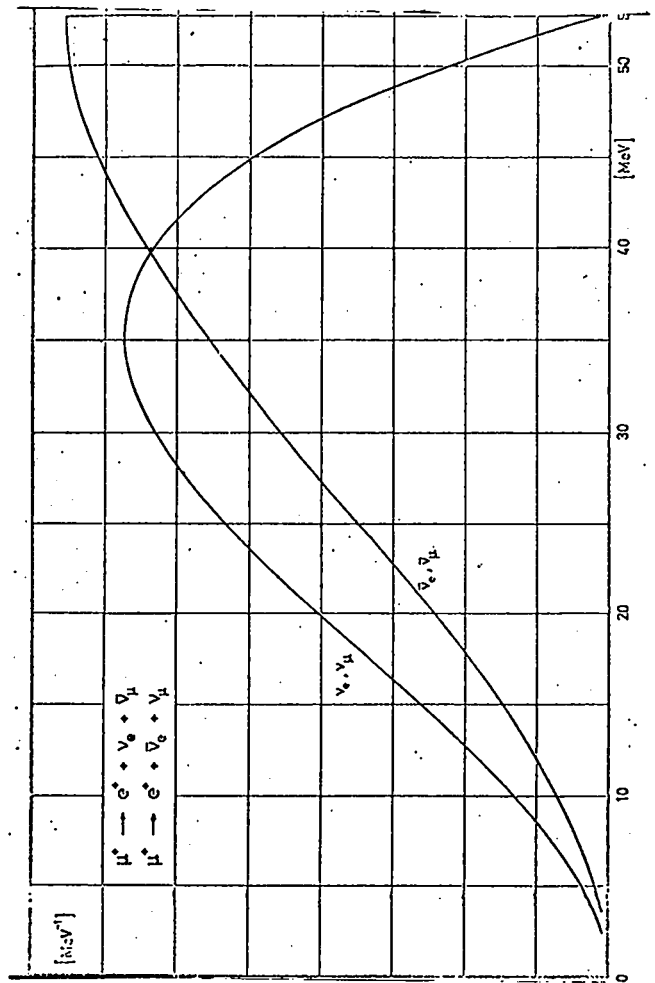


Figure 2

Neutrino cross sections versus neutrino energy



3. Normalised energy spectra of neutrinos from ν -decay

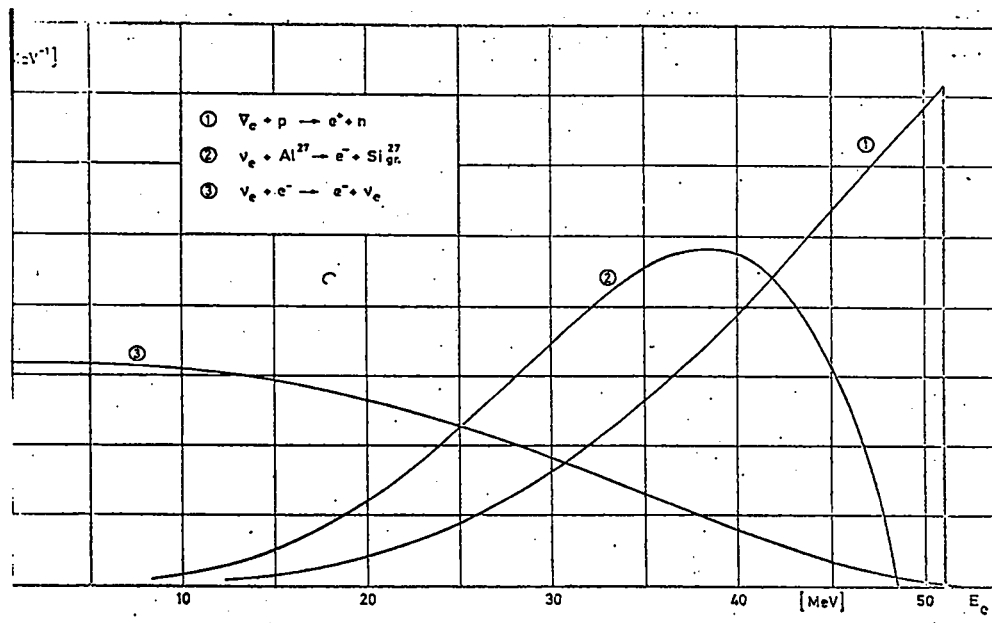
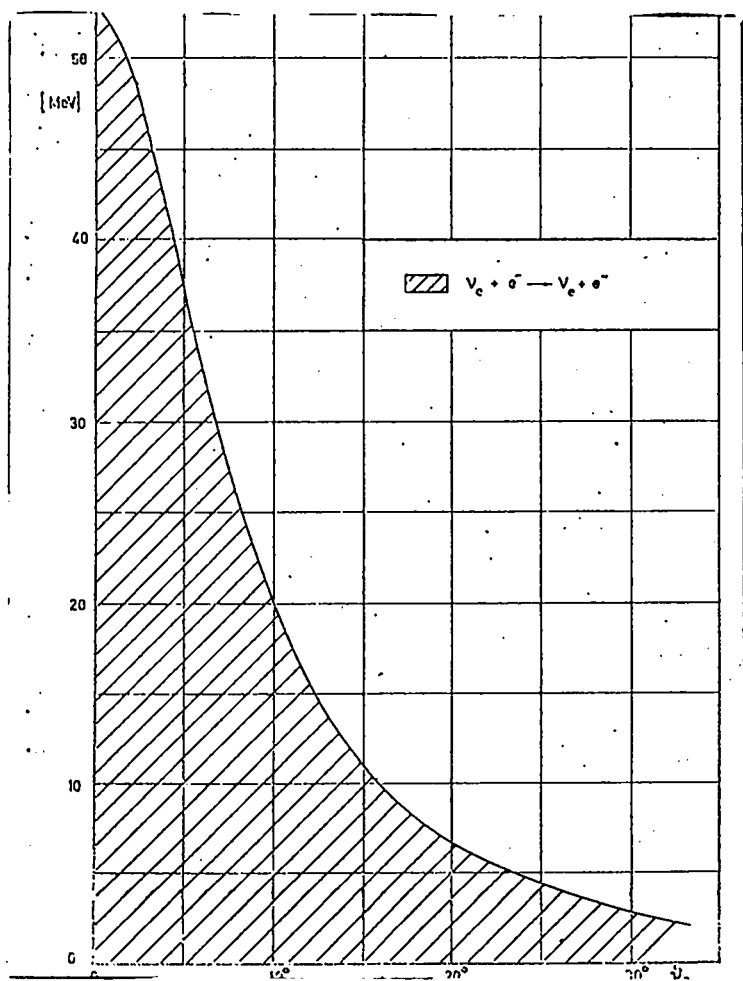


Fig. 4. Normalized energy spectra of the electrons in the inverse reaction taking into account the energy dependence of the cross sections and the energy spectra of neutrinos.



5: Kinematics of the elastic neutrino scattering. Due to the finite energy spectrum of the neutrinos from μ^+ -decay the dependence of energy and scattering angle is not unique.

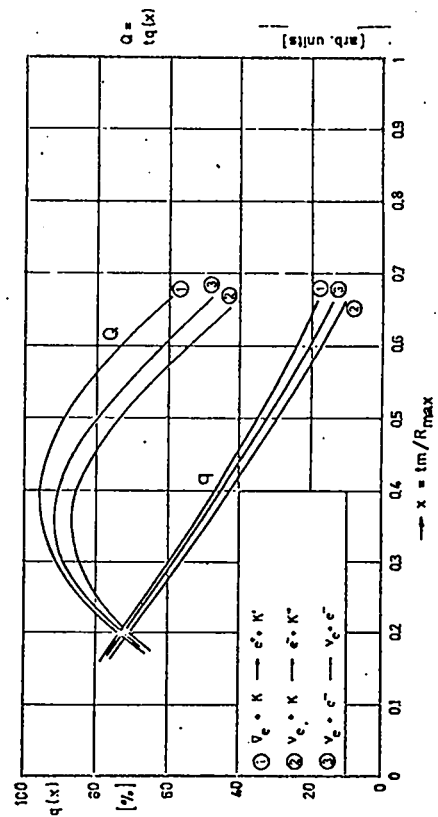


Fig. 6.

Optimisation of the target. q = the probability that interaction in a target produces a trigger signal. t = thickness of a target subunit. m = required number of coincidences. R_{\max} = the range of the most energetic electrons. Q = proportional to the observed event rate.

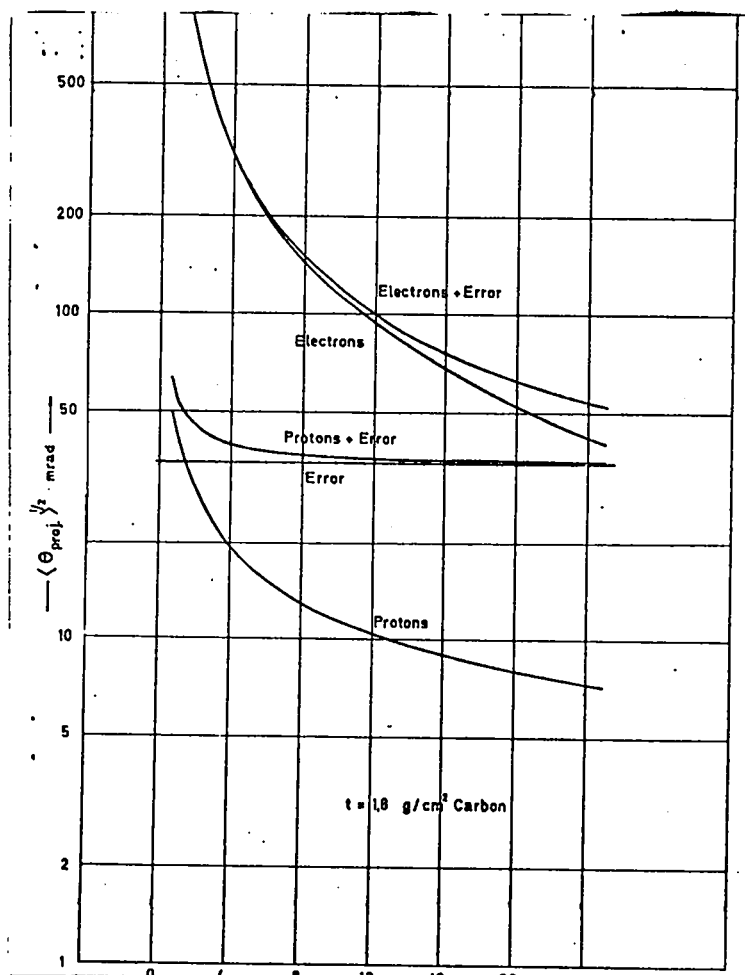


Fig. 7. Multiple scattering of protons and electrons in a detector containing carbon targets as a function of rest range.

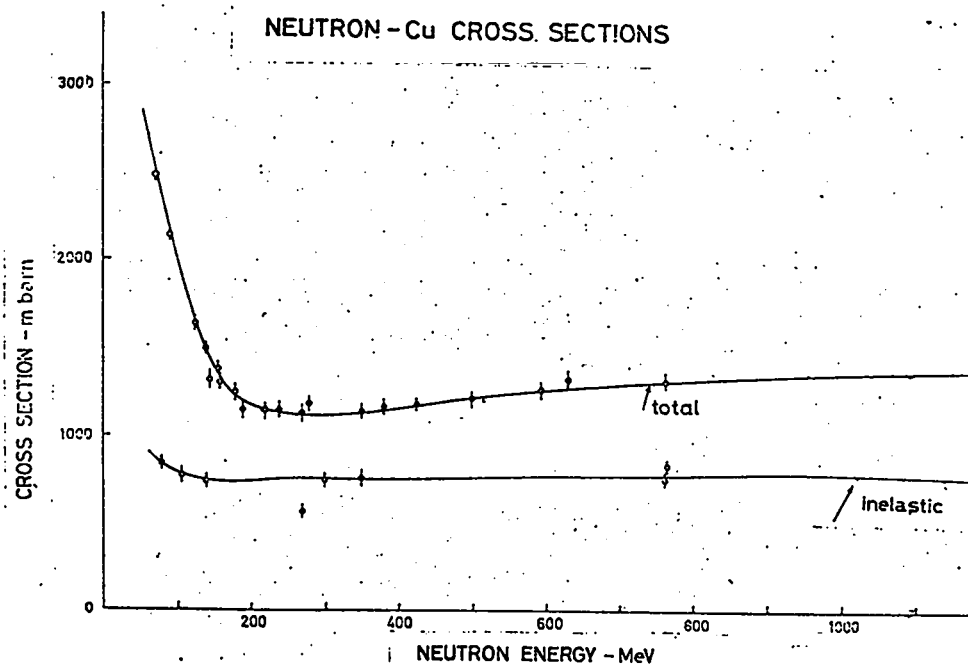


Fig. 8. Total and inelastic cross sections of neutrons on copper in dependence of energy.

No. 24 - "Neutrino Experiments at LAMPF," Kenneth Lande, Spokesman

E. Fenyves, U. of Texas-Dallas; Kenneth Lande and D. C. Potter, U. of Pa.

RESEARCH PROPOSAL

LOS ALAMOS MESON PHYSICS FACILITY

TITLE OF EXPERIMENT

Neutrino Experiments at LAMPF

Kenneth Lande, SPOKESMAN

PARTICIPANTS AND INSTITUTIONS

Ervin Fenyves

University of Texas at Dallas

Kenneth Lande and Donald C. Potter

University of Pennsylvania, Philadelphia

Date: January 29, 1971

SUMMARY OF EXPERIMENT

We propose to use the neutrinos arising from the decay of stopped π^+ and μ^+ mesons in the LAMPF beam stopper to:

- determine the form of the lepton conservation law;
- measure the rate and angular distribution of neutrino-electron scattering;
- look for anomalous ν_μ interactions; and
- search for lepton non-conservation and neutrino oscillations.

A liquid hydrogen Čerenkov counter will serve as:

- the target for neutrino interactions;
- an indicator of the electronic nature of the neutrino interaction secondaries; and
- a measure of electron energy loss in the target.

The polarity, direction and momentum of the electron (from ν -e interactions) and positron (from ν -p interactions) secondaries that emerge from the target will be measured with a spark chamber-magnet spectrometer.

Since the detector measures the electron energy as well as the neutrino-electron angle it kinematically constrains the interaction and so determines the neutrino energy.

The experiments that we think are most appropriate to LAMPF and that cannot be done properly at any other existing accelerator are:

- Test of the Multiplicative Lepton Number Conservation Law
- Search for ν_μ - e^- elastic scattering
- Measurement of the Rate of Diagonal Current-Current Interactions; i.e., cross section of ν_e - e^- scattering

- Search for neutrino oscillations and lepton non-conservation.

Although most of these problems have been discussed widely for some time, only in cases (1) and (3) have any measurements been made and these were inconclusive. The advent of LAMPF finally makes possible the resolution of these fundamental questions.

Our proposed experimental arrangement is designed to carry out all of these experiments simultaneously and with the same apparatus. In particular we intend to measure the polarity and momentum of electrons and positrons arising from neutrino interactions with the protons and electrons in a hydrogen target. In the LAMPF beam stopper region neutrinos arise from the decay of stopped π^+ mesons and the subsequent decay of μ^+ mesons. μ^- decays can be ignored since the ratio of μ^- decays to μ^+ decays in the LAMPF beam stopper is $< 10^{-3}$. The π^+ decays give rise to monochromatic ν_μ with $E = 30$ Mev. If the additive lepton number conservation law holds then the μ^+ decay gives rise only to ν_e and $\bar{\nu}_\mu$, while if the multiplicative law applies the μ^+ decays also give rise to an equal number of $\bar{\nu}_e$ and ν_μ . All the neutrinos from stopped muon decay have a broad energy spectrum extending from 0 to 53 Mev.

The results of the multiplicative law test will determine the kinds of neutrinos emanating from the μ^+ decays, and so specify the analysis of any neutrino interaction experiment; for example, neutrino-electron scattering or neutrino capture in Cl^{37} .

In particular, in analyzing the neutrino-electron interactions it must be realized that if:

- Lepton conservation law is additive and there are no anomalous interactions only ν_e should be considered,
- Lepton conservation law is multiplicative and there are no anomalous interactions both ν_e and $\bar{\nu}_e$ are involved in the interactions,
- If there are anomalous interactions then ν_μ and $\bar{\nu}_\mu$ are also involved in neutrino-electron interactions.

The above considerations are indicative of the inter-relationship between the analysis and results of the various proposed neutrino experiments.

II. Multiplicative Lepton Conservation Law

It is well known that all present experimental results^{1,2)} on leptons are consistent with the existence of either

a) an additive conservation law of electronic and muonic lepton numbers, in which the sums ΣL_e and ΣL_μ are separately conserved³⁾, or

b) a multiplicative conservation law⁴⁾, in which only the sum $\Sigma(L_e + L_\mu)$ and the sign $(-1)^{\Sigma L_e}$ (and consequently also the sign $(-1)^{\Sigma L_\mu}$) are separately conserved.

Several experiments have been carried out recently in order to decide which form of the lepton conservation law prevails. They resulted, however, in upper limits of C_μ (the weak-coupling constant only allowed by the multiplicative conservation law) that are very much larger than C_ν (the universal vector-coupling constant of beta decay).

The results given by the search for muonium-antimuonium conversion⁵⁾ and for the process $e^- + e^- \rightarrow \mu^- + \mu^-$ ⁶⁾ were:

$$C_\mu \leq 5800 C_\nu \quad \text{and} \\ C_\mu \leq 610 C_\nu, \quad \text{respectively.}$$

An analysis⁷⁾ of the recent CERN high-energy neutrino experiment⁸⁾, testing the conservation of the muonic lepton number, indicated that the upper limit of C_μ should be of the order of $5C_\nu$, if it is assumed that the neutral leptons and charged leptons behave identically in weak interactions.

The above approaches to the problem are presently inconclusive and do not promise significant improvement in sensitivity. Another approach to the problem, suggested by Pontecorvo⁹⁾, is more promising. He showed that the multiplicative conservation law can be tested directly by the investigation of the muon decay products.

According to the additive conservation law only the decay:

$$\mu^+ \rightarrow e^+ + \nu_e + \bar{\nu}_\mu \quad (1)$$

is allowed, while the multiplicative conservation law allows two equally valid channels:

$$\mu^+ \rightarrow e^+ + \nu_e + \bar{\nu}_\mu \quad (1)$$

$$\mu^+ \rightarrow e^+ + \bar{\nu}_e + \nu_\mu \quad (2)$$

It is obvious that the validity of the multiplicative conservation law can be tested by a search for decay mode (2). If the muons decay at rest, then ν_μ and $\bar{\nu}_\mu$ cannot interact with nucleons via any allowed current-current interaction channel because their energy is smaller than the muon mass, and the problem is reduced to the determination of the relative proportions of ν_e and $\bar{\nu}_e$ among the decay products.

Since $\bar{\nu}_e$ interact with protons according to the scheme

$$\bar{\nu}_e + p \rightarrow n + e^+ \quad (3)$$

whereas the reaction

$$\nu_e + p \rightarrow n + e^+ \quad (4)$$

is forbidden by any lepton number conservation law, reaction (3) with neutrinos from stopped μ^+ can be used as a test of the existence of the multiplicative conservation law.

The emergence of positrons from our hydrogen target would be indicative of the occurrence of reaction (3), while the absence of such positrons would demonstrate the validity of the additive law.

III. Search for ν_μ - e^- Elastic Scattering

The current-current interaction does not allow ν_μ - e^- elastic scattering. However, there have been various speculations about possible anomalous ν_e - e^- and ν_μ - e^- interactions⁽¹⁰⁻¹¹⁾. An observation of these processes would be most interesting.

The decay of stopped π^+ produces monochromatic ν_μ of 30 Mev total energy. The flux of such ν_μ is equal to that of ν_e arising from μ^+ decay. The ν_e energy spectrum, of course, extends from 0 to 53 Mev (Fig. 1). The ν_μ - e^- interactions can be recognized by an enhancement at 30 Mev in the neutrino energy distribution obtained from the reconstruction of the neutrino-electron interaction events, provided the ν_μ - e^- cross section is not much less than the ν_e - e^- cross section.

IV. ν_e - e^- Elastic Scattering

Although the current-current weak interaction completely specifies the rates for all four-lepton interactions, it has been pointed out^(11,12) that the diagonal interactions, i.e., elastic scatterings, are not necessarily constrained to the same coupling constant as the non-diagonal interactions.

The V-A theory predicts that⁽¹³⁾

$$\sigma(\bar{\nu}_e + e^- \rightarrow \bar{\nu}_e + e^-) = \frac{\sigma_0 E_\nu}{3 m_e c^2} \quad \text{and}$$

$$\sigma(\nu_e + e^- \rightarrow \nu_e + e^-) = \frac{\sigma_0 E_\nu}{m_e c^2}$$

$$\text{where } \frac{\sigma_0}{m_e c^2} = 1.67 \times 10^{-44} \text{ cm}^2 \cdot \text{Mev}^{-1}, \text{ and}$$

$$\frac{d\sigma}{dT}(\bar{\nu}_e + e^-) = \frac{\sigma_0}{m_e c^2} \left[1 - \frac{T}{E_\nu} \right]$$

$$\frac{d\sigma}{dT}(\nu_e + e^-) = \frac{\sigma_0}{m_e c^2}$$

where T is the kinetic energy of the recoil electron.

Using neutrinos from a fission reactor, Reines and Curr⁽¹⁴⁾ have established an upper limit for

$$\sigma(\bar{\nu}_e + e^- \rightarrow \bar{\nu}_e + e^-) \leq 2.5 \sigma_{V-A}$$

(the prediction of the V-A theory). There have been no studies of ν_e - e^- cross sections or of angular distributions for any neutrino-electron scatterings.

The cross section for $\nu_e + e^- \rightarrow \nu_e + e^-$ will be measured by the rate of negative electron emission from our liquid hydrogen target, and the angular distribution by the directions of the emitted electrons.

It should be noted that the neutrino-electron interaction study will be carried out in parallel with the multiplicative law test.

V. Search for Neutrino Oscillation

Pontecorvo⁽¹⁵⁾ has pointed out that if the leptonic charge is not exactly conserved then there can be transitions $\nu_{e,\mu} \rightleftharpoons \bar{\nu}_{e,\mu}$ and $\nu_\mu \rightleftharpoons \nu_e$. Such transitions are reminiscent of the weak transitions between K^0 and \bar{K}^0 due to non-conservation of hypercharge. Just as a \bar{K}^0 amplitude develops with time in a beam of initial K^0 , so a $\bar{\nu}_e$ or ν_μ amplitude can develop in a beam of ν_e . In the K^0 case, the time required for the growth of the \bar{K}^0 amplitude is determined by the K_1 - K_2 mass difference. In the neutrino case the oscillation period is determined by the mass difference of the neutrinos involved in the oscillation. Such an oscillation, of course, requires at least one massive neutrino.

The neutrino oscillation period, $\tau = \frac{2\pi}{(m_1^2 - m_2^2)v}$, could range from atomic to astronomic dimensions. If the oscillation length is much less than the flight path of our neutrinos then such an oscillation will produce effects mimicing those of the multiplicative lepton conservation law or of an anomalous neutrino interaction. Oscillation lengths comparable to our neutrino flight path or hydrogen target thickness will make the neutrino oscillation process recognizable. Very long oscillation lengths are beyond detection with terrestrial neutrino sources.

VI. Experimental Setup

The experimental setup consists of

- 1) a neutrino source in the beam stopper;
- 2) an iron filter to absorb charged particles, neutrons and gamma rays,
- 3) a liquid hydrogen target-magnet spectrometer to analyze the neutrino interaction secondaries;
- 5) an array of coincidence and anti-coincidence scintillation counters
- 6) an iron shield surrounding the detector array.

VII. Neutrino Beam

The 700 MeV protons of the LAMPF are stopped in an iron block which serves simultaneously as a target and a shield for all possible particles generated, except neutrinos. The range of primary protons in the iron block is about 35 cm. and the majority of these protons undergo nuclear interaction in the first two collision lengths, i.e., in about 26 cm.

The maximum energy pions produced by the interaction of protons have only slightly longer range than the protons, and the bulk of the pions are stopped in a much shorter distance. The same is valid also for the charged particles produced in secondary interactions by protons and pions. Thus the majority of pions are produced and slowed down in the first half meter of the iron block.

The intensity of neutrons generated by the primary protons is attenuated only by their nuclear interactions. The collision length for the maximum energy neutrons in iron is about 13 cm. Using an iron block of 2 m length in the direction of the proton beam and 5 m thick perpendicular to the proton beam (on one side of the beam, see Fig 2), the intensity of maximum energy neutrons is attenuated by a factor of about $5 \cdot 10^6$ in the forward direction and by a factor of about $5 \cdot 10^{16}$ perpendicular to it. The attenuation of neutrons having smaller energy, particularly those scattered almost perpendicular to the direction of the primary proton beam, is many orders of magnitude larger, mainly due to their smaller collision length.

Since 2 m or 5 m iron corresponds to 111 or 278 radiation lengths, respectively, the electron-photon component generated in the nuclear cascade processes is also totally absorbed.

According to the above considerations, a neutrino detector which is placed behind a 5 m thick iron block, perpendicular to the primary proton beam, and surrounded by, say, 2 m thick iron blocks from all sides, is shielded practically for all radiation except neutrinos.

The nature of the neutrinos reaching the hydrogen target depends on the pion and muon decays in the beam stopper. The number of ν^- produced is 1/7 that of π^+ produced. μ^- can only arise from π^- decay in flight since essentially all π^- that come to rest are absorbed by nuclei. μ^+ arise mainly from π^+ decays at rest. The probability of pion decay in flight is $\approx 1\%$. The probability that a μ^- stopped in iron can decay before capture is 10%. From these probabilities we have that for each μ^+ decay there are 1/7000 μ^- decays; 1/700 π^- decays in flight; 1/100 π^+ decays in flight and 1 π^+ decay at rest. According to this the only significant neutrino sources are π^+ and μ^+ decays at rest.⁽¹⁶⁾

VIII. Liquid Hydrogen Target - Čerenkov Counter

The major difference between the LAMPF neutrino beam and those at fission reactors is that the neutrinos at LAMPF have one order of magnitude higher energy than those at reactors. This feature permits a modification of the classical neutrino detection technique. In particular, it is now possible and, of course, desirable to detect the positrons and electrons in prompt coincidence and simultaneously observe their trajectories in a magnet-spark chamber spectrometer.

The key to the test of the multiplicative law is whether or not any of the neutrinos produced in the μ^+ decay will interact with protons to produce neutrons and positrons; i.e.

$$\bar{\nu}_e + p \rightarrow n + e^+ \quad (5)$$

In order to avoid any ν_e nuclear interactions which can produce electrons, $\nu_e + n \rightarrow p + e^-$, and could give rise to positrons through cascade processes we must use a liquid

hydrogen target. In addition, the large radiation length of hydrogen minimizes the chance of producing background electrons and positrons from gamma rays. This virtue of hydrogen is even more critical in suppressing backgrounds that would simulate $\nu_e - e^-$ elastic scattering, because of the appreciably smaller $\nu_e - e^-$ cross section.

In order to detect the production of an electron or positron as well as to determine the energy loss of that particle in the target, we intend to measure the Čerenkov radiation emitted in the target. The Čerenkov radiation pulse height combined with the magnetic spectrometer momentum and trajectory measurement will be used to reconstruct the kinematics of the interaction, i.e., determine the neutrino energy and angle between the neutrino and electron.

The thickness of the hydrogen target, as determined by the average electron range, will be about 1 meter. The transverse dimensions of the target will be 2 meters high and 4 meters wide.

IX. Magnet - Spark Chamber Spectrometer

The spectrometer is required to have an aperture properly matched to the dimensions of the hydrogen target (Fig. 2) and capable of measuring momenta of electrons between 5 and 50 Mev/c.

The magnet will have an aperture 1 meter high and 4 meters wide. Since only a relatively small bending power is needed to analyze these small momenta, the magnet can be quite thin, 5 cm. The total weight of the magnet will be 17,300 lbs.

In setting the bending power of the magnet it is desirable to have the angle of deflection in the magnet considerably larger than the multiple scattering angle.

The relevant formula is:

$$\frac{\theta_{\text{mag}}}{\theta_{\text{scatt. proj.}}} = \frac{\int H \cdot dl}{5} \sqrt{\frac{L_{\text{Rad}}}{L}} \quad (6)$$

where $\int H \cdot dl$ = the bending power in gauss meters;
 L_{Rad} = the radiation length of the material the electron traverses and L = the path length of the electron. In order to have $\frac{\theta_{\text{mag}}}{\theta_{\text{scatt. proj.}}} \sim 10$ with our spark chamber system we must have $\int H \cdot dl \sim 200$ gauss-meters. To minimize the multiple scattering in the region between the spark chambers of our system a helium bag will be inserted.

The spark chambers will be of the conventional optical type and of dimensions appropriate to the system aperture.

X Counter System

The apparatus will be triggered by a coincidence between the H_2 - Čerenkov counter and two scintillation counters, one, C_1 , immediately downstream of the hydrogen target and the other, C_2 , after the spark chamber system, provided there is

no pulse in any of the counters forming the anti-coincidence shield, Fig. 2.

XI. Shielding

As indicated above there will be a 5 meter thick steel shield between the beam stopper and our apparatus to absorb non-neutrino particles from the accelerator. To shield the apparatus from scattered accelerator-produced radiation we plan to surround the apparatus with an ~2 meter thick steel shield.

The soft component of cosmic radiation will be screened by the steel shield, while triggers due to the penetrating component will be vetoed by the anti-coincidence shield.

XII. Rates

Protons of 700 Mev have a total cross section of ~850 mb per iron nucleus and ~130 mb for π^+ production per iron nucleus. From these numbers we expect 10^{13} π^+ per 6×10^{15} protons incident on the beam stopper. Of these $\pi^+ \sim 50\%$ will stop and decay rather than interact giving rise to 5×10^{14} π^+ decays/sec and the same rate of μ^+ decays.

With a 5 meter thick plug our target subtends a solid angle of 0.2. If the multiplicative law applies, then one-half of the electronic neutrinos from μ^+ decay will interact with protons in the hydrogen according to reaction (5).

Using a mean cross section of $1.2 \times 10^{-40} \text{ cm}^2$ we have in this case 1 neutrino interaction in our target every 400 sec or 9 interactions/hour.

The spectrometer subtends a solid angle of about 10% for positions originating in the H_2 target. From this we get about 1 magnetically analyzed neutrino-nucleon interactions per hour.

Additional rate losses due to positrons that do not leave the hydrogen target or are otherwise lost in the spectrometer will reduce this rate to about 15 events/day.

For $\nu_e - e^-$ scattering we have a mean cross section of $\sim 6 \times 10^{-43} \text{ cm}^2$. The angular distribution of this process is predicted to be peaked in the forward direction and so we expect an order of magnitude enhancement in the collection efficiency of our spectrometer.

If the additive law is operable we expect 1.5 events/day, whereas the multiplicative law gives only 1 event/day. The difference is due to the fact that $\sigma(\bar{\nu}_e - e^-)$ is predicted to be 1/3 of $\sigma(\nu_e - e^-)$.

XIII. Preparation for Experiment

We have constructed a 1/4 scale model of the magnet-spark chamber spectrometer, Fig. 3. In order to verify the precision with which it can analyze electron momenta we intend to calibrate it at an electron accelerator.

We also hope to estimate the likelihood that a cosmic

ray induced trigger gives rise to an acceptable track in the spectrometer system by operating the model spectrometer in a simulated experimental area environment.

XIV Installation of Apparatus

Although we feel quite confident in our shielding calculations we hope to verify them by a step-by-step installation of the shield. Although we intend initially to provide space for a 7 meter long shield in the neutrino beam we will study the dependence of the background on the thickness of this plug. At present we think that 5 meters is an adequate thickness, but if we can tolerate a thinner plug we can increase our solid angle for neutrino collection. Other aspects of the shield may also be varied during the installation period.

XV Order of Date-Taking

When the shielding has been completed and the apparatus has been fully tested we hope to begin with a two week run with a N_2 fill in the target. During this time we should be able to test the multiplicative law and to determine the $\nu_e - e^-$ scattering rate. It would then be desirable to put D_2 in the target and calibrate the neutrino source via the reaction



This calibration is necessary to interpret the data taken with the N_2 fill.

If we are unable to borrow sufficient D_2 from bubble chambers for this calibration, then it will be necessary to carry out this phase with a liquid N_2 or O_2 fill and make the appropriate exclusion principle corrections.

Finally we will replace the N_2 fill and continue taking data for the various neutrino-electron scattering experiments. This phase of the experiment may take about one year.

XVI. Construction of Apparatus

The hydrogen target represents the most costly and dangerous element of our apparatus. It would be most desirable if the Los Alamos Scientific Laboratory could undertake the construction of the target and be responsible for the cryogenic aspects of its operation.

The construction of the 1/4 scale magnet-spark chamber spectrometer was a simple, straight forward operation. We anticipate no difficulties in the construction of the full scale system. The counters and electronics are all of conventional design, some of which presently exist and the rest can be readily acquired.

Expect for the hydrogen target, whose construction schedule we cannot easily estimate, we see no obstacles that

will prevent the construction of the apparatus by the fall of 1972 (except money).

Of course, we hope that LAMPF can obtain adequate amounts of steel or other appropriate shielding.

XVII. Additional Neutrino Experiments Appropriate to this Apparatus

A) The Pauli Exclusion Principle restricts the p to n or n to p transition in complex nuclei with very small momentum transfers.⁽¹⁷⁾ This drastically reduces the probability that a ν_e can produce a forward electron in collisions with complex nuclei.

This prediction has been interrogated by a $\nu_\mu - Fe$ interaction experiment⁽¹⁸⁾ at Argonne with uncertain results. The interpretation of their results is clouded by the difficulty of separating purely four-fermion events from those that produce a π^0 , say via N^* production. Again, the LAMPF neutrino energy range is ideal for overcoming this problem. We could verify the Exclusion Principle predictions by filling our target with liquid O_2 and observing the angular distribution of the outgoing electrons.

Since we may, in any case, fill our target with O_2 or N_2 during the initial testing or calibration phases this observation may not even require any additional running time.

B) Within the framework of the V-A theory, the non-isotropy of the angular distribution of electrons and positrons emitted in neutrino-nucleon collisions is determined by the value of $\frac{PA}{PV}$. Although $\frac{PA}{PV}$ has been determined from the measurement of the neutron lifetime and some other decays, it would be interesting to verify that its value in the region of momentum transfer available to us is the same as in those other processes.

This observation could be performed with our apparatus provided we rotate it by 90°. This experiment would require additional running time of about one month.

References

- 1) S. P. Rosen and H. Primakoff: Alpha, Beta and Gamma-ray Spectroscopy, North-Holland Publ. Co., Amsterdam, 1965.
- 2) T. D. Lee and C. S. Wu, Ann. Rev. Nucl. Sci. 15, 381 (1965).
- 3) Other possible versions of the additive conservation law are discussed by B. Pontecorvo, Soviet Physics JETP 26, 984 (1968).
- 4) G. Feinberg and S. Weinberg, Phys. Rev. Letters 6, 381 (1961).
- 5) J. J. Amato et al., Phys. Rev. Letters 21, 1709 (1968).
- 6) W. C. Barber et al., Phys. Rev. Letters 22, 902 (1969).
- 7) C. Y. Cheng, Phys. Rev. Letters 24, 79 (1970).
- 8) K. Borer et al., Physics Letters 29B, 614 (1969).
- 9) Nguyen Van Hieu and B. Pontecorvo, JETP Letters 7, 105 (1968).
- 10) F. Reines, UCI-10P19-29, 1969.
- 11) D. Yu. Bardin, S. M. Bilenky and B. Pontecorvo, Physics Letters 32B, 68 (1970).
- 12) M. Gell-Mann, M. Goldberger, N. Kroll and F. Low, Phys. Rev. 179, 1518 (1969).

- 13) R. P. Feynman and M. Gell-Mann, Phys. Rev. **109**, 193 (1958), Leon Heller-LAMS-3013 (1963).
- 14) F. Reines and H. Gurr, Phys. Rev. Letters **24**, 1448 (1970), and private communication.
- 15) B. Pontecorvo, Soviet Physics JETP, **26**, 984 (1968) and Proceedings of the Kiev Conference (1970).
- 16) A detailed calculation showed that the rate of neutrinos produced in all other processes, like the decay of (1) kaons, (2) $\pi^- \rightarrow e^- + \bar{\nu}_e$ decays in flight and (3) muons decaying in flight can be neglected.
- 17) B. Goulard and H. Primakoff, Phys. Rev. **135**, B1139 (1964).
- 18) R. L. Kustom et al., Phys. Rev. Letters **22**, 1014 (1969).

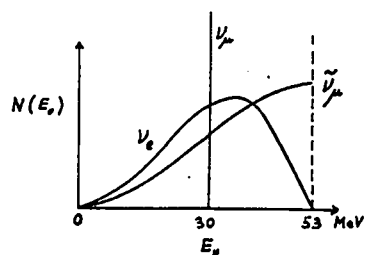
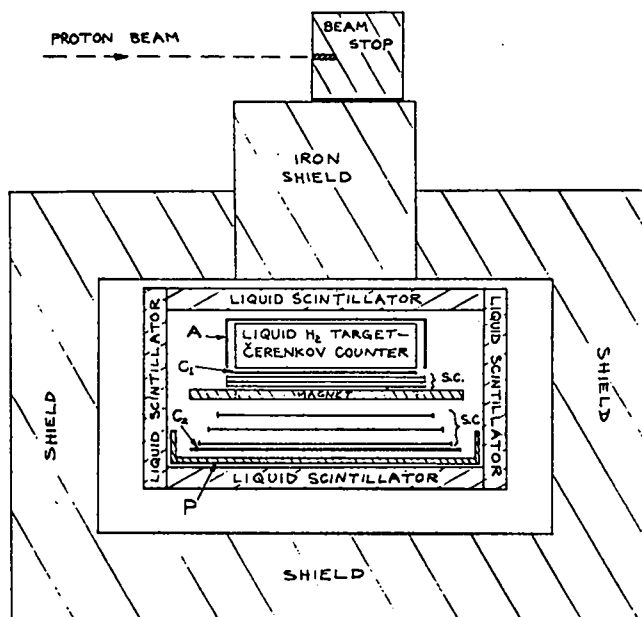


Fig. 1 Neutrino spectra for $\pi^+ \rightarrow \mu^+ + \nu_\mu$ and $\mu^+ \rightarrow e^+ + \nu_e + \bar{\nu}_\mu$ decays



A = ANTICOINCIDENCE COUNTER
 C_1, C_2 = COINCIDENCE COUNTERS
 SC = SPARK CHAMBERS
 P = LEAD ELECTRON ABSORBER

Fig. 2 The experimental arrangement

APPENDIX I

Estimation of the Background

We have to consider the following sources of background for the proposed experiments:

- (1) For the test of the Multiplicative Lepton Conservation Law we have to take into account
 - (a) Cosmic Rays
 - (b) Accelerator Muons
- (2) For the various neutrino-electron scattering experiments we have to take into account the same background sources and, in addition, if the Multiplicative Law holds the background given rise by the reaction



The expected rate of the latter events has been estimated about 20 times larger than the rate of neutrino-electron scatterings. The positrons produced in reaction (1) can be, however, easily distinguished from the electrons given rise in scattering processes by measuring the curvature of their tracks except of very unfortunate scatterings in the material of the spark chambers. The probability of such simulated electron events is, however, about 10 times smaller than the expected rate of neutrino-electron scatterings (and appears only in the case of the multiplicative law).

(a) Cosmic Ray Background

The cosmic ray background was estimated by using the experimental data of Reines obtained with a $3m^2$ liquid scintillation slab at LANS in 1954 (see "Neutrino Experiment at LAMPF", F. Reines 1970). Taking into account the duty cycle of LAMPF and an anticoincidence factor of about 10^6 Reines concludes that the cosmic ray background for a neutrino detector of the same projected area can be reduced to $< 1/\text{day}$. The projected area of our detector is almost of the same size as that of the above detector. We are detecting, however, only electrons emitted into the solid angle of the magnetic spectrometer. Due to the fact that the axis of the spectrometer is horizontal we have a strong angular selection against cosmic ray particles which decreases the rate of this background to < 0.1 .

(b) Accelerator Muons

Muons generated by the accelerator in targets or other materials upstream to the neutrino detector may generate background events. The rate of this events can be, however, experimentally determined by varying the thickness of the shielding around the detector and can be reduced to a reasonable value with suitable shielding and anticoincidence detectors.

Appendix II

Time schedule of neutrino experiments

1. $\frac{1}{2}$ scale model of magnet spectrometer completely tested at University of Pennsylvania May 1, 1971
2. Initiate design of liquid H₂ target Cerenkov counter in conjunction with Los Alamos Scientific Laboratory June 1, 1971
3. Test measurements carried out on the $\frac{1}{2}$ scale model of magnet spectrometer irradiated with electrons from stopped cosmic ray muons Sept. 1, 1971
4. Final plan of the experimental arrangement for spectrometer and target Cerenkov counter Nov. 1, 1971
5. Magnet - spark chamber spectrometer with anti-coincidence shield designed May 1, 1972
6. Magnet - spark chamber spectrometer with anti-coincidence shield built Aug. 1, 1972
7. Neutrino Source, iron filter and liquid H₂ target Cerenkov counter built at LAMPF Aug. 1, 1972
8. Study of background and completion of shielding Nov. 1, 1972
9. Start of data taking Jan. 2, 1973

Appendix III - Responsibility for Apparatus

We suggest that the following division of responsibility between LAMPF and the university participants.

- 1) Liquid H₂ Cerenkov counter
 - a) Cryogenics - LAMPF
 - b) Electronics and Optics - University of Pennsylvania
- 2) Magnet - University of Texas at Dallas
- 3) Spark Chamber System - University of Texas at Dallas
- 4) Trigger Counter System - University of Texas at Dallas
- 5) Readout System - University of Pennsylvania
- 6) Shielding Enclosure - LAMPF
- 7) Anti-coincidence Counter Shield - University of Texas at Dallas

If, as we hope, additional collaborators participate in this experiment, we would anticipate an appropriate, mutually satisfactory redistribution of the responsibilities.

Appendix IV

Budget Estimate for Neutrino Experiment

<u>Item</u>	<u>Sub-total</u>
1) Liquid H ₂ Cerenkov Counter	
a) Cryogenics:	
cryostat	\$50,000.
cryogenic instrumentation	10,000.
safety	20,000.
refrigerator *	(60,000.)
b) Electronics	
Photomultipliers	65,000.
H-V distribution	10,000.
	75,000.
2) Magnet	20,000.
3) Spark Chamber System	20,000.
4) Trigger Counter System	10,000.
5) Readout	20,000.
6) Shielding Enclosure	147,000.
7) Anti-coincidence Counter Shield	30,000.
Total	402,000. + (60,000.)

* We hope that an appropriate cryogenic refrigerator can be borrowed for this experiment from another laboratory and that we can avoid its purchase.

No. 31 - "A Neutrino Experiment to Test Muon Conservation," Peter Nemethy, Spokesman

V. W. Hughes, Peter Nemethy, Yale U.; Jean Duclos, Saclay Laboratory; R. L. Burman and D.R.F. Cochran, LASL

RESEARCH PROPOSAL
LOS ALAMOS MESON PHYSICS FACILITY

A NEUTRINO EXPERIMENT TO TEST MUON CONSERVATION

Vernon W. Hughes and Peter Nemethy,	Yale University
Jean Duclos,	Saclay Laboratory
Robert Burman and Donald Cochran,	Los Alamos Scientific Laboratory

March 15, 1971

Peter Nemethy, Spokesman

ABSTRACT

We propose a neutrino experiment to determine whether "muon conservation" is an additive or a multiplicative law. We search for exotic muon decay,

$$\mu^+ \rightarrow e^+ \nu_e \bar{\nu}_\mu$$

which is allowed by the multiplicative law but prohibited by the additive one. In order to distinguish this process from the usual muon decay ($\mu^+ \rightarrow e^+ \nu_e \bar{\nu}_\mu$) we detect the electron-anti-neutrino from the exotic decay, using the inverse-beta reaction,

$$\bar{\nu}_e p \rightarrow n e^+$$

on free protons in water. Our neutrino detector is a 6 m³ water Cerenkov counter. The nonfocusing total absorption counter has an energy resolution of 10% at 40 MeV, the typical positron energy.

We use the LAMPF proton beam stop as an intense source of positive muons decaying at rest. Six meters of heavy neutron shielding separate our detector from the beam stop.

The experiment can be run in a parasitic mode, with all upstream targets operating. With one third of the full proton beam arriving at the beam stop we expect a rate of 60 events/day if the multiplicative law holds.

PROPOSAL INFORMATION

BEAM AREA: Proton Beam Dump.

SECONDARY BEAM REQUIREMENTS: None.

PRIMARY BEAM REQUIREMENTS: 1/3 mA or more of the primary proton beam arriving at beam stop with an energy greater than 700 MeV.

RUNNING TIME: Installation and Tune up Time: 4 months.

Data Runs: 800 hours.

SCHEDULING: Non-LAMPF apparatus can be ready on Dec. 31, 1972.

LAMPF APPARATUS REQUIRED: Standard Fast Logic Electronics, Interface and Storage Device.

SHIELDING AND ENCLOSURES REQUIRED: 6 meters of iron barrier shielding between beam stop and apparatus, with matched dirt earth-shine and sky-shine protection.

SPECIAL SERVICES: The loan of 1500 gallons of heavy water, to be returned after the experiment.

SPACE REQUIRED: A cubic volume 3m x 3m x 3m.

I. INTRODUCTION

Neutrino interactions have been observed¹ at energies below a few MeV and in the GeV range. The Los Alamos Meson Physics Facility offers the first practical opportunity to study neutrino reactions at intermediate energies.

The neutrinos originating in the LAMPF beam stop have a typical energy of 40 MeV. This energy is below the threshold for producing muons and pions from muon-neutrinos. Electron-neutrino interactions can therefore be studied without interference from the muon-neutrino processes which dominate neutrino events at the high energy synchrotrons. Compared to reactor experiments the higher energy of the neutrinos is a distinct advantage, for it implies higher cross-sections and some improvement in background rejection.

One may envisage a varied and serious program of neutrino experiments at LAMPF. This program could include a test of muon-conservation, a measurement of neutrino cross-sections on chlorine with implications for neutrino astrophysics, studies of giant-resonance and exclusion principle effects on inverse-beta decay reactions with nuclei, and elastic neutrino-electron scattering.

All these experiments have in common the following features. They can use the LAMPF beam stop without modifications as a neutrino source; they require a well-shielded counting room and some six meters of iron shielding between this room and the beam stop. We feel that such a general neutrino facility is very desirable and that it would justify the necessary investment in shielding by extending the range of interesting physics that can be done at the LAMPF.

We propose a neutrino experiment specifically designed to determine whether muon conservation is an additive or a multiplicative law. We believe that this experiment, with limited aim, reasonably high event rate and fairly simple apparatus, could be an early one in any neutrino program. Incidentally, information about the backgrounds encountered in this experiment may well be useful in the detailed design of more ambitious and difficult projects.

The form of the law of conservation of muonness is of some importance to the theory of weak interactions. It was the absence of the reaction

$$\mu^+ \rightarrow e^+ + \gamma, \quad (1)$$

allowed by lepton conservation, that first prompted speculation about a new conservation law; a speculation based on the attractive idea that any process which is not forbidden will occur. This hypothesis, muon conservation, was subsequently confirmed by the discovery of the muon-neutrino which cannot produce electrons by the inverse beta decay process

$$\bar{\nu}_\mu + Z \rightarrow Z' + e, \quad (2)$$

and therefore is distinct from the electron-neutrino².

Feinberg and Weinberg³ pointed out in 1951 that there are two possibilities for the conservation of "muonness" in weak interactions. The classical one is an additive law. Choosing a muon-number $L_\mu = +1$ for μ^- and $\bar{\nu}_\mu$, $L_\mu = -1$ for μ^+ and ν_μ , and $L_\mu = 0$ for anything else, we require

$$\sum_i L_\mu(i) = \text{constant}.$$

The other possibility is a parity-like multiplicative conservation law. Let $P_\mu = -1$ for μ^+ , μ^- , ν_μ , $\bar{\nu}_\mu$, and $P_\mu = +1$ for anything else. Then we require

$$\prod_i P_\mu(i) = \text{constant}.$$

Either conservation law prohibits reactions (1) and (2); both allow all our established lepton reactions. The predictions are different only for reactions involving an even number of electron-like and muon-like particles. Of the two laws the additive one is stronger. In particular it prohibits the following four-lepton interactions allowed by the multiplicative law:³

$$\mu^+ e^- \leftrightarrow \mu^- e^+ \quad (3)$$

and

$$\mu^+ \rightarrow e^+ \bar{\nu}_e \nu_\mu. \quad (4)$$

Reaction (3), muonium-antimuonium conversion, requires a neutral current which could possibly be associated with a new interaction which is stronger than weak interactions. Amato et al.⁵ have looked for muonium-antimuonium conversion in an argon atmosphere and have put an upper limit of $C_M/C_V \leq 5800$ for the process, where C_M and C_V are the coupling constants for reaction (3) and for the weak interaction respectively. Barber et al.⁶ have searched for the equivalent process, $e^+ e^- \rightarrow \mu^+ \mu^-$ to obtain the upper limit $C_M/C_V \leq 610$. Both limits are at the 95% confidence level.

The other test process, exotic muon decay (4) proceeds by a charged current. It contributes to muon decay, so that its coupling constant cannot exceed C_V . Chang⁷ has examined a CERN neutrino experiment⁸ for evidence of inverse exotic muon decay, $\nu_\mu + Z \rightarrow Z \mu^+ e^- \nu_e$, and finds that the level of background is 150 times the maximum rate of the process. To have a background sufficiently low for this particular test of the "muonness" law, the $\bar{\nu}_\mu$ contamination in the high energy ν_μ beam would have to be less than 2×10^{-5} .

There is, therefore, no present experimental evidence that would allow us to decide between the two conservation laws for weak interactions. The additive law is pleasing because of its similarity to lepton, baryon and charge conservation. Furthermore

it does not tamper with weak interaction universality. The attraction of the multiplicative law is the natural way in which it is associated with a world of exactly two lepton families. A multiplicative world would allow us to understand better why the muon exists and why it seems to be the only heavy electron.³ There is a price to pay: we would have to reexamine our ideas of universality. If the muon can decay into two channels ($\mu^+ \rightarrow e^+ \nu_e \bar{\nu}_\mu$ and $\mu^+ \rightarrow e^+ \bar{\nu}_e \nu_\mu$) then the effective strength of μ -decay is due to a primitive four-lepton coupling summed over the two channels; therefore, it is not the primitive muon coupling constant which is equal to the vector constant in beta decay.³

II. THE EXPERIMENT

A. Design. Let us recapitulate our present understanding of muon decay. It is a pure V-A interaction involving two distinct, massless neutrinos of opposite helicity: $\mu^+ \rightarrow e^+ \nu \bar{\nu}$. The energy spectra for positron, neutrino and anti-neutrino are shown in Fig. 1. The neutrino spectrum is different from the common spectrum of positron and anti-neutrino. The subscripts of the two neutrinos depend on the "muonness" selection rule. The additive law specifies $\nu = \nu_e$ and $\bar{\nu} = \bar{\nu}_\mu$; the multiplicative law allows the above assignment, but also its inverse, $\nu = \nu_\mu$ and $\bar{\nu} = \bar{\nu}_e$.

A priori we expect the two channels to have equal strength⁹ and we can summarize muon decay in the following table:

	Additive	Multiplicative	
$\mu^+ \rightarrow e^+ \nu_e \bar{\nu}_\mu$	100%	50%	(5)
$\mu^+ \rightarrow e^+ \bar{\nu}_e \nu_\mu$	0%	50%	(6)

In our experiment we search for the second of these reactions (exotic μ -decay). We look for inverse beta decay on a free proton in a water Cerenkov counter,

$$\bar{\nu}_e + p \rightarrow n + e^+. \quad (7)$$

The corresponding inverse beta reaction for usual μ -decay (5), $\nu_e + p \rightarrow X e^+$, is forbidden by charge conservation; there is no need to determine the sign of the lepton if a free proton is identified as the target nucleus.

What makes the experiment feasible with a water target is the fact that there is no significant confusion between the free proton reaction (7) and neutrino events on oxygen. (See section III.A.)

By choosing water as our neutrino converter we avoid the cost and cryogenic effort associated with a large liquid hydrogen detector. The free proton density in water is 50% higher than that in liquid hydrogen, so that there is a gain, rather than a loss, in counting rate/unit volume.

We have designed the experiment for operation in the presence of a substantial neutron flux, since we expect the residual neutron background not to be negligible in the neutrino area. This is why we have chosen a Cerenkov detector; its discrimination against neutrons is much superior to that of a scintillation counter. It is for the same reason that we do not rely on a delayed coincidence in identifying our events, for such a technique requires low probabilities of accidental neutrons in a delayed gate.

While 50% - 50% is the natural relative branching ratio between processes (5) and (6) in a "multiplicative world", we expect to be sensitive to any exotic contribution exceeding 10% of all muon decays.

B. Cerenkov Detector. Our neutrino detector, shown in Fig. 2 is a nonfocusing total-absorption Cerenkov counter. A cube of 180 cm size contains 6000 liters of water, viewed from all sides by 96 five-inch photomultipliers. Optical contact and water seal are provided directly by the photocathode envelopes. The counter is lined with a diffuse reflector. A wavelength shifter is added to the water in order to improve its performance. The gain of the counter will be about 5 photoelectrons/MeV for particles with $\beta=1$.

The angular distribution of positrons in the inverse beta process (7) is isotropic to within 10%. The positron energy spectrum is shown in Fig. 3. Because the cross-section is proportional to E_ν^2 , there is a fairly sharp peak at 53 MeV. The average energy of the positrons is 42 MeV. At 42 MeV the counter will have an energy resolution $\sigma = 10\%$. Energy losses due to edge effects and radiation will add a small low energy tail to the response curve, but will not increase the width at half-height.

The detector is surrounded by a 4 π solid angle cosmic ray anti-coincidence shield. This shield consists of a set of 24 liquid scintillation counters, 220 cm long by 55 cm wide. Each scintillator is viewed by a phototube from each end.

C. Muon Source and Event Rate. Our source of positive muons decaying at rest is the LAMPF proton beam stop. About one half will slow down without nuclear interactions and decay at rest. This decay produces slow μ^+ which in turn stop and decay. On the other hand, nearly all the ν^- are captured by nuclei before they can decay. The μ^- contamination of our μ^+ source depends somewhat on the composition of the beam stop but will be less than 1%.

With the full 1 mA 750 MeV proton beam absorbed in the beam stop, the expected yield is $7 \times 10^{14} \mu^+/\text{sec}$.⁹ If we assume a multiplicative law, we have $3.5 \times 10^{14} \bar{\nu}_e/\text{sec}$ emitted isotropically from the beam stop.

The mean energy of the $\bar{\nu}_e$ is $E_{\text{MOS}} = 39 \text{ MeV}$. The cross-section for reaction (7) is given by¹¹

$$\sigma_e = \left(\frac{\hbar}{mc}\right)^2 \frac{1}{2} G^2 |K|^2 \left[\sqrt{e^2 - 1} - 2.06 + 10^{-40} \left(\frac{E_\nu}{50 \text{ MeV}}\right)^2 (1 - 2.6/E_\nu)\right] \text{cm}^2, \quad (8)$$

where $e = E e^+ / m_e$. This expression yields a mean cross-section $\langle \sigma_e \rangle = 1.2 \times 10^{-40} \text{ cm}^2$ for our neutrinos. The corresponding event rate is found from

$$N(\text{events})/\text{sec} = N(\bar{\nu}_e)/\text{sec} \frac{d\Omega}{4\pi} L \frac{dN}{dV} (\text{protons}) \langle \sigma_e \rangle.$$

The above calculation gives

$$N(\text{events}/\text{Day Ton Water}^{-2}) = 17500, \quad (9)$$

where M_{etor} refers to the mean source-to-detector distance and Ton to the mass of protons in the detector.

The proposed layout of the experiment is shown in Fig. 4. The neutrino room is separated from the beam stop by six meters of shielding. The average beam-stop-to-detector distance is 8 meters. Our water Cerenkov counter contains 0.7 tons of free protons. Using (9), we obtain an event rate of 180/day with the full beam.

The experiment can therefore be run in a parasitic mode with all upstream targets operating. With one third of the beam arriving at the beam stop we still have a respectable 60 events/day.

D. Event Runs and Calibrations. We consider 1000 events (for a fifty-fifty multiplicative law) a reasonable goal for the experiment. This corresponds to 17 days or about 400 hours of beam at 1/3 intensity.

To provide a check on the experiment, we propose to repeat this run with heavy water replacing the water in our Cerenkov counter. Kelly and Uberall¹² have shown that the cross-section and e^- distribution in process $\nu_e D \rightarrow p p e^-$ are nearly equal to the free nucleon cross-section and distribution. We may, therefore, consider this process as an inverse beta reaction on a free neutron in the presence of a spectator proton:



The deuterium in heavy water therefore allows the electron-neutrino from normal μ^+ decay (5) to initiate the inverse beta process. In fact the total "free nucleon" inverse beta decay rate is independent of the choice of the muon conservation law; this fact makes such a calibration particularly desirable. To perform it we need the loan of 1600 gallons of heavy water for a two-week period. The total amount of time we need for the two data runs is 800 hours at 1/3 intensity.

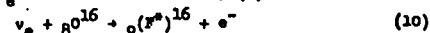
Before we engage in data taking, we have to build up the shielding to a point where the backgrounds are tolerable. While the larger part of the barrier shield can be a fixed installation, the last few interaction lengths should be variable; we should also allow flexibility for the rest of the neutrino house. We can then check the source and size of different background contributions by varying the shielding and find the final shielding configuration required. The exploratory nature of this operation makes predictions of the required time risky, if not impossible. With this reservation we estimate that the installation and optimization of shielding and detector may take about 4 months, with intermittent parasitic beam use at variable intensity.

An independent measurement of the μ^+ production rate in the beam stop would be useful. We may be able to obtain this number by building a mock-up of the water and copper plate beam stop and viewing it with phototubes. We would stop protons of 750 MeV in the mock-up at some minimal rate. Knowing the characteristic muon lifetime, we would obtain the μ^+ to proton ratio by observing the time distribution of counts from our mock-up counter after each incident proton.

For our muon conservation experiment it is not strictly necessary to have both the μ^+ production rate and the heavy water calibration. Either one will provide the necessary normalization. However, doing both would give a measurement of the absolute cross-section for inverse beta process (9). Though it has never been seen, this reaction is not expected to offer any surprises; its cross-section would be a good consistency check on our experiment.

III. BACKGROUNDS

A. Neutrinos. The oxygen in our water allows the inverse beta-reaction for the ν_e from normal muon decay (5):



This reaction is a potentially serious background, since we do not determine the sign of the electron. However, the maximum energy

of the electron in (10) is lower by ~15 MeV than that of the positron in reaction (7). Free proton events can therefore be identified by their energy: the distinctive e^+ peak at 50 MeV is above the cutoff for oxygen events. For reaction (7) $E_{\text{max}}(e^+) = 53$ MeV and $\langle E(e^+) \rangle = 42$ MeV; for reaction (10) $E_{\text{max}}(e^-) = 38$ MeV, $\langle E(e^-) \rangle < 23$ MeV; we have very different spectra indeed.

The total cross-section for process (10) on carbon, $\nu_e + {}^{12}\text{C} \rightarrow {}^{12}\text{N} + e^-$, as a function of neutrino energy has been calculated by Überall¹³ using two different sets of carbon wavefunctions. Messiah¹⁴ has calculated the cross-section for (10) on oxygen at a neutrino energy of 40 MeV. In Fig. 5 we show these results together with the free nucleon cross-section (8). At our energies the two calculations on carbon and that on oxygen all give similar cross-sections: $\sigma_e(\nu\text{C})/\sigma_e(\nu\text{P}) = 1/3$; $\sigma_e(\nu\text{O})/\sigma_e(\nu\text{P}) = 1/5$.¹⁵

In water we have two free protons per oxygen nucleus; but the number of ν_e for an additive law is twice the number of $\bar{\nu}_e$ for a multiplicative one, so that the factors of 2 cancel each other. In Fig. 6 we compare the free proton and oxygen electron-energy spectra normalized to their predicted cross-sections. With our 10% energy resolution we could clearly separate the free proton events even if the predicted oxygen cross-section were too low by a factor of 5. An auxiliary result of our experiment will be the measurement of the cross-section for (10).

Positrons from cosmic ray muons stopping in our counter and observed between machine pulses give us the continuous and accurate energy scale calibration that we need.

Other neutrino backgrounds for the experiment are $\nu - e$ elastic scattering and the correct inverse beta reaction (7) with $\bar{\nu}_e$ from the contamination of μ^- decaying in the beam stop. These backgrounds amount to only 2% of our expected real neutrino rate.

B. Saclay Background Study. We have built a 250 liter water Cerenkov counter, and studied its response to monoenergetic positrons, and to backgrounds near the beam stop of the new 500 MeV 1/2 mA Saclay Electron Linear Accelerator.¹⁶

The Cerenkov counter was a 65 cm cube with 8 photomultipliers viewing it. Its construction was identical to that of our proposed counter (section IIIB), so that we can regard the Saclay counter as a 1/3 scale model of our proposed Cerenkov detector. The uniformity of response of the counter was excellent. The energy resolution at 50 MeV was $\sigma = 11\%$ for a photocathode to wall-surface ratio which was 2/3 that of our proposed detector. It is on the basis of the Saclay study that we predict our counter performance with some confidence.

C. Thermal Neutrons. If a thermal neutron is captured on a heavy nucleus near the detector, we may observe a capture - gamma ray of up to 8 MeV in the Cerenkov counter. This energy is well below

that of our neutrinos, so that only the resolution and pile-up tails can simulate high energy events. The response of our counter to thermal neutrons is shown in Fig. 7. Pileup effects are included, together with the resolution. The counting rate falls exponentially with increasing energy. A 30 MeV threshold will give a rejection factor of 10^{10} against this background. Therefore, we can allow a rate of up to 10^{11} capture-gammas/day in our detector.

D. High Energy Neutrons. The energies of proton recoils from 50 or 100 MeV neutrons cover the energy region of our real events. Unlike a scintillator, our counter does not detect these protons, since their β is below the Cerenkov threshold in water. A Cerenkov counter sees 50 MeV neutrons only by their radiative capture in flight, $N + Z \rightarrow Z' + \gamma \rightarrow Z' + e^+e^-$. The cross-section for radiative capture is 3 orders of magnitude below that for elastic scattering (proton recoils), therefore 5×10^4 neutrons/day in the 50 MeV range will give us ~25 background events a day.

E. Neutron Produced Pions. A neutron whose energy is over 250 MeV can produce a pion in the detector or near it. This is the most treacherous background, since muons from the positive pions emit positrons whose spectrum (Fig. 1) is nearly identical to that of our real events. Because we have no kinematical rejection at all against this background we want to keep it under 1/10th of the real neutrino rate. A 500 MeV neutron traversing the detector region will make a π^+ with a probability of about 1%. Therefore the rate of such neutrons through the detector has to be limited to < 1000 /day.

F. Neutron Shield. The limits on neutron rates at our detector are $\sim 10^{11}$ thermal neutrons, 5×10^4 "50 MeV" neutrons, and 10^3 "500 MeV" neutrons per day. Shielding which is sufficient to achieve the last condition is also enough for the first two; pion production at the detector will be the dominant neutron background for the experiment.

The number of cascade neutrons above 350 MeV is about 0.2/proton or 10^{20} /day at 1/3 mA beam current. The high energy neutron angular distribution is strongly peaked in the forward direction; this prompts the choice of 90° for the placement of the neutrino room. Assuming that the relative probability of emission at 90° to forward emission is 10^{-2} , and noting that our detector subtends a solid angle of 5×10^{-3} , we get an unshielded rate of the order of 10^{15} neutrons ($E > 350$ MeV). Therefore the barrier shield has to attenuate these neutrons by $\sim 10^{12}$. Six meters of steel is a generous estimate of the depth needed. With such high attenuation of direct neutrons, sky-shine and earth-shine neutrons become important. The flux of such neutrons has to be matched to that of the direct ones by sufficient dirt shielding and side walls. We are in the process of doing a detailed shielding calculation with a LANPP neutron code.

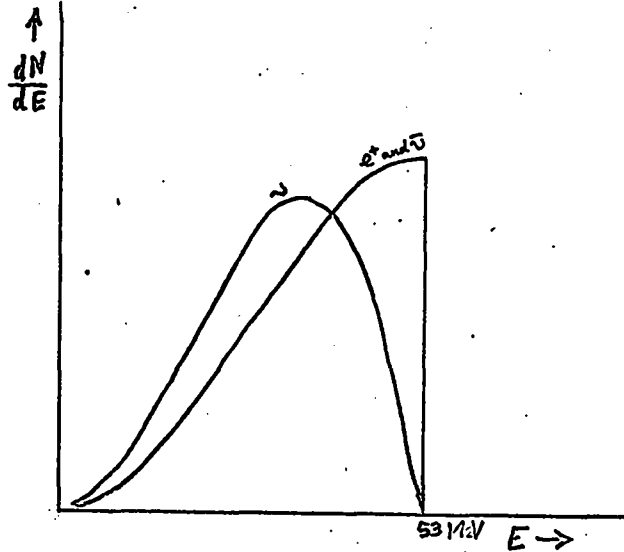
G. Cosmic Rays. Extrapolating our measurements made with the 250 liter counter, we predict cosmic ray pulses between 30 and 60 MeV at a rate of 2×10^5 /day in our proposed detector. The 6% beam duty cycle cuts down this rate to 1.2×10^5 /day. We estimate the inefficiency of our anti-shield to be no worse than 3×10^{-4} . This gives a cosmic ray rate under 36 events/day.

For those cosmic muons which seem to stop in our detector we generate a 20 μ s anti-gate to eliminate positrons from their decay. The dead-time loss associated with cosmic rays is insignificant. Finally, we note that the cosmic ray background rate and spectrum can be measured unambiguously between machine pulses; this allows a confident subtraction of any cosmic contribution.

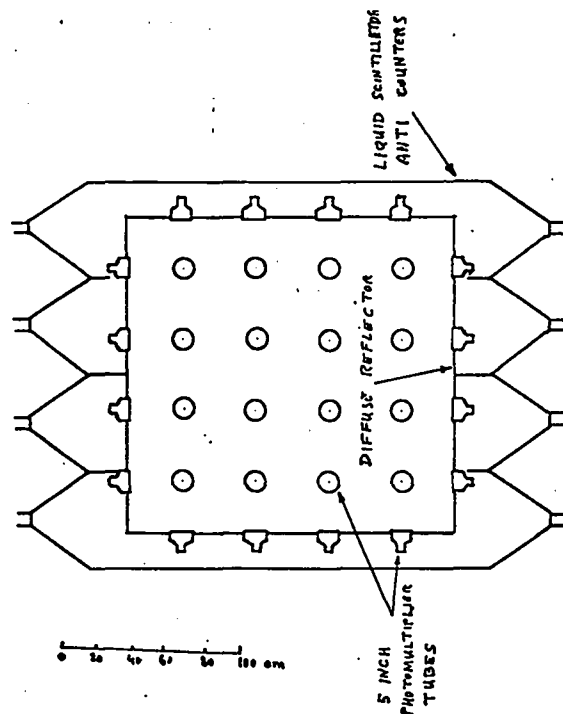
REFERENCES

1. Neutrinos were first detected by Reines and Cowan, Phys. Rev. 113, 273 (1959).
2. Danby, Gaillard, Goulianos, Lederman, Mistry, Schwartz, and Steinberger, Phys. Rev. Letters 2, 36 (1962).
3. Feinberg and Weinberg, Phys. Rev. Letters 6, 381 (1961).
4. An equivalent phrasing of the multiplicative law is the following: The sign of $(-1)^{L_u}$ or $(-1)^{L_e}$ is conserved, where L_u and L_e are the usual lepton numbers. See T.D. Lee and C.S. Wu, Ann. Rev. of Nuclear Science 15, 381 (1965).
5. Amato, Crane, Hughes, Morgan, Rothberg, and Thompson, Phys. Rev. Letters 21, 1709 (1968).
6. Barber, Fittleman, Cheng, and O'Neill, Phys. Rev. Letters 22, 902 (1969).
7. Chang, Phys. Rev. Letters 24, 79 (1970).
8. Borer, Hahn, Hofer, Kaspar, Kriemen, and Seiler, Phys. Letters 29B, 614 (1959).
9. Under a multiplicative law the reactions (5) and (6) are symmetric, so that an equal branching ratio is a natural though not a necessary choice. Universality of four-lepton interactions would assure the equality. Other, more exotic theories of the weak interaction have been suggested, such as $\nu_e \leftrightarrow \nu_\mu$ conversion fed by a finite ν_μ mass. (Pontecorvo, JETP 26, 984 (1968). The interpretation of mu-decay then has a wider latitude; the breaking of the additive law does not imply a straight multiplicative one. However, the first experimental question to pose is clear: does an appreciable fraction of μ^+ decays result in a $\bar{\nu}_e$, rather than a ν_e ?
10. Yale Study on High Intensity Proton Accelerators. Internal Report Y-12, October 1964. This rate may be uncertain by up to 50%.
11. Wu and Moszkowski, Beta Decay. (John Wiley and Sons, 1966).
12. Kelly and Überall, Phys. Rev. Letters 16, 145 (1966).
13. H. Überall, Phys. Rev. 137, B502 (1965); Kelly and Überall, Phys. Rev. 158, 987 (1967).
14. Albert Messiah, private communication.
15. In a private communication, Herbert Überall notes that the carbon cross-sections in Fig. 5 are probably too large by a factor of 2, since the same calculation over-estimates low energy photonuclear cross-sections by that amount. He then estimates the neutrino cross-section on oxygen from that on carbon by

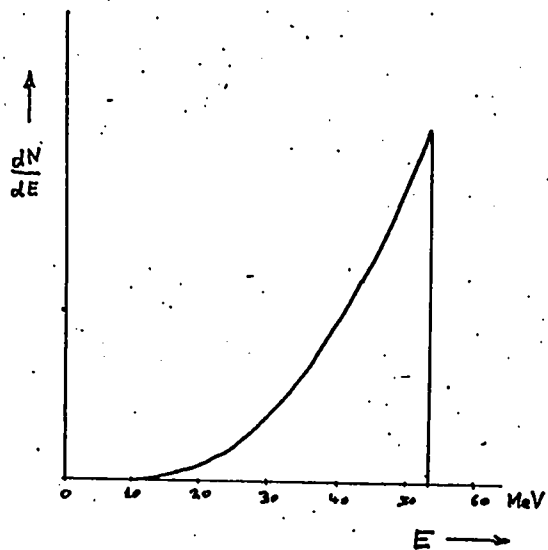
$$\sigma_T(\nu O) = \frac{Z(O)}{Z(C)} \times \sigma_T(\nu C) = \frac{4}{3} \sigma_T(\nu C).$$
 The result, $R = \sigma_T(\nu O)/\sigma_T(\nu P) \sim 1/4$, is in close agreement with A. Messiah's number, $R = 1/5$.
16. Dublos, Gerard, Miller, Morgenstein, Némethy and Picard; Saclay Report DPh-N/HE/71/2. Unpublished.



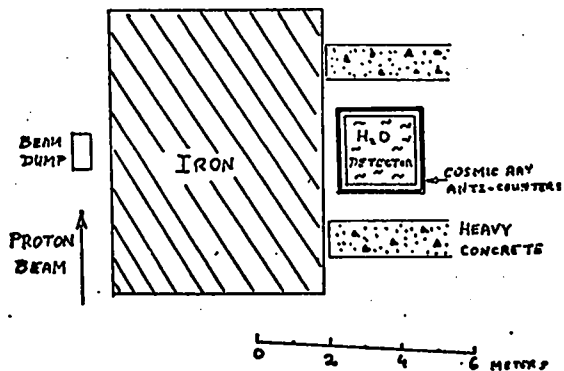
1. Energy spectra in muon decay: $\mu^+ \rightarrow e^+ \nu \bar{\nu}$.



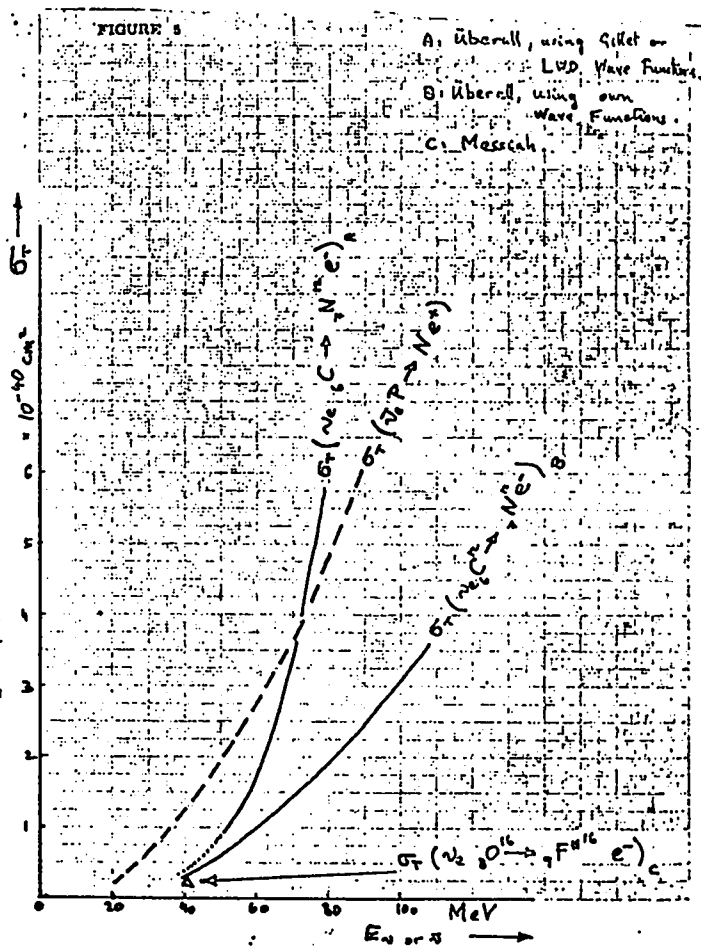
2. Water Cerenkov Detector.



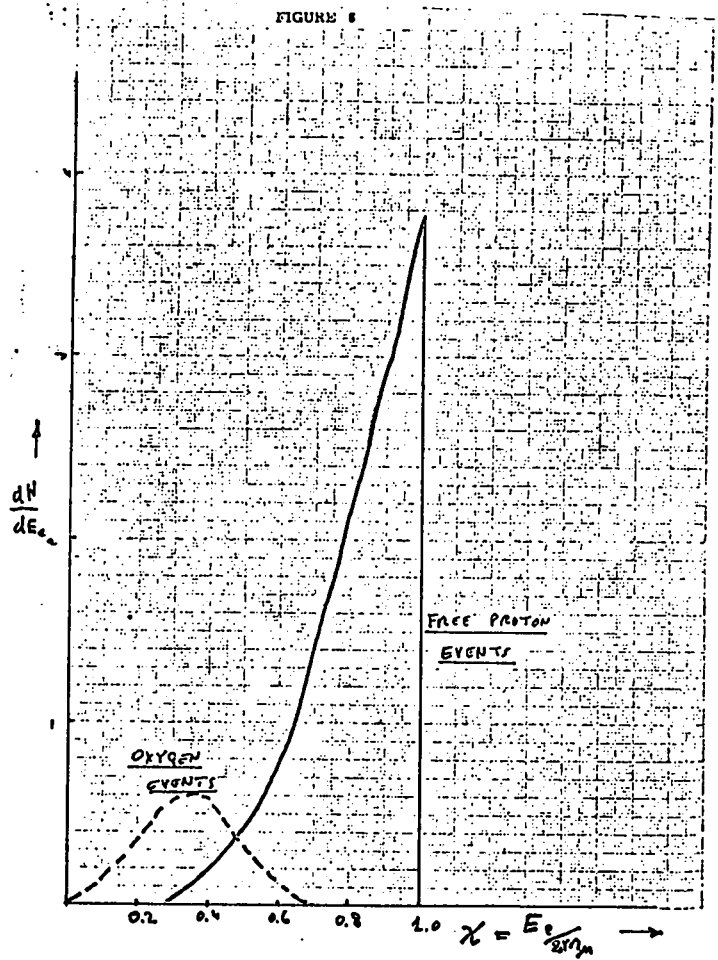
3. Energy spectrum of positron in the inverse beta decay:
 $\bar{\nu}_e + p \rightarrow n e^+$.



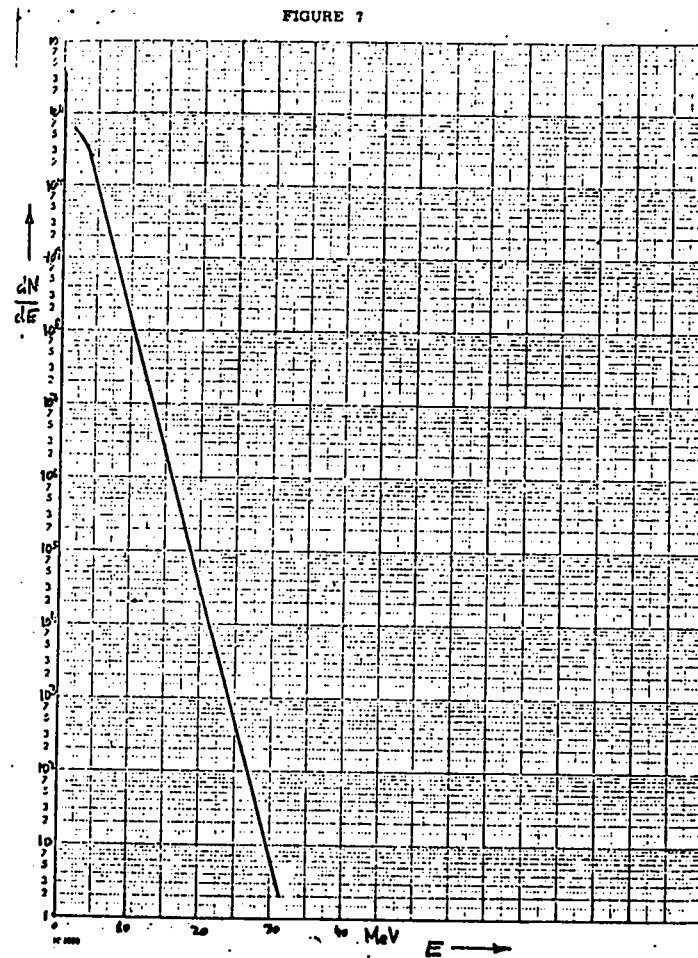
4. Layout of beam dump area and experiment.



5. Calculated inverse beta reaction cross-sections on oxygen and carbon, compared with free-proton cross-section.



6. Positron spectra from oxygen and free proton neutrino reactions.
Areas are proportional to calculated cross-sections.



7. Cerenkov counter response to capture gamma rays from thermal neutrons.

No. 38 - "Neutrino Physics Program: Elastic Scattering, Test of Multiplicative Law, Measurement of Neutrino Flux, Inverse β Decay,"
F. Reines, Spokesman

H. Chen, W. R. Kropp, J. Lathrop, F. Reines,
H. Sobel, U. of California-Irvine; and
M. F. Crouch, Case Western Reserve U.

RESEARCH PROPOSAL

LOS ALAMOS MESON PHYSICS FACILITY

Neutrino Physics Program: Elastic Scattering, Test
of Multiplicative Law, Measurement of Neutrino
Flux, Inverse β Decay

F. Reines, SPOKESMAN

PARTICIPANTS AND INSTITUTIONS

H. Chen	University of California, Irvine
M. F. Crouch	Case Western Reserve University
W. R. Kropp	University of California, Irvine
J. Lathrop	University of California, Irvine
F. Reines	University of California, Irvine
H. Sobel	University of California, Irvine

Date: March 30, 1971

SUMMARY

The series of experiments here proposed is designed to utilize the unique characteristics of LAMPF as a neutrino source to answer several key questions relating to the weak interaction. Among these questions are a test of the applicability of V-A theory to the elastic scattering of ν_e on e^- ; a test of the multiplicative vs additive law of lepton conservation in μ^+ decay; a measurement of the ν_e flux and a crude measurement of the ν_e spectrum.

Two classes of detectors, a large pot of scintillator and a more sophisticated slab array of scintillator spark chamber plus water (D_2O) target are considered in some detail so as to illuminate our reasoning in developing the preferred hybrid slab approach. The essential features of the slab array are total energy, rate of energy loss, sensitivity to delayed coincidences plus directional determination. In addition, the use of deuterated target inserts enable a determination of the ν_e flux via the well known inverse beta decay process $\nu_e + D \rightarrow p + e^-$.

The experimental design takes into account backgrounds due to cosmic rays and the machine and includes shielding and anticoincidence detectors. Typical signal rates are $\sim 1/\text{day}$ for detectors with a mass of several tons. These rates make the program here proposed one of 3 - 4 years duration with costs (excluding the bulk shielded experimental area) ranging from \$650,000 to \$900,000.

PROPOSAL INFORMATION

Beam Area: At right angles to beam stop and in the range 6 - 12 meters from the stop.

Secondary Channel (if known):

Beam Requirements: ν from μ^+ produced in beam stop with machine operated in the standard, advertized mode (~ 0.3 ma of 750 MeV protons on beam stop).

Primary Beam Requirements (State any requirements on the main accelerator beam, such as energy, intensity, or unusual pulse characteristics): Standard running configuration.

Running Time Required:

Installation Time Required (no beam): no constraint on beam (O.K. on or off).

Tune-up Beam (give intensity and hours needed): no special requirement.

Data Run (give realistic estimate of hours needed): a few years.

Scheduling:

Realistic date when User will have the non-LAMPF apparatus ready: 2 years

Give all information on other commitments of research group that may affect scheduling: no problems anticipated on this score.

Major LAMPF Apparatus Required:

Some electronics could be useful, but nothing major. In general, data analysis would be done at UCI.

Shielding and Enclosures Required: see attached sketches

Special Services Required (power, water, engineering, shop work, etc.): power requirements minimal ~ 50 kw.

Space Required (attach drawing giving layout): Electronics area $\sim 20' \times 30'$ located $\leq 100'$ from detector -- a trailer would do. Could even be accommodated within detector area (see sketch).

Experiment	Equipment (sandwich layers)	Estimated Run Time (50% accelerator duty cycle) ^{a)} (months)	Estimated Number of Events ^{b)}				
			e	H	D	C	O
Multiplicative Test	12	4	12 (6)	0 (90)	-	22 (22)	-
Elastic Scattering	32	12	100 (50)	0 (720)	-	400 (400)	-
Normalization	32 + 3 (D_2O)	7	70 (35)	0 (500)	100 (100)	280 (280)	66 (66)
Re-normalization	32 + 3 (H_2O)	7	70 (35)	0 (500)	-	280 (280)	66 (66)
Total		30	250 (125)	0 (1800)	100 (100)	1000 (1000)	130 (130)

a) 11 accelerator shifts/week.

b) 0.3 mA, 700 MeV proton beam and slab detector at a mean distance of 10.0 m.

Development of UCI Proposal

The rationale behind the UCI proposal is best described by a brief statement of its development. After a recognition of the unique characteristics of LAMPF for an investigation of various interesting features of the weak interaction via neutrinos:

- 1.) $\nu_e + e^- \rightarrow \nu_e + e^-$
- 2.) test of the multiplicative vs additive lepton conservation law
- 3.) a) intensity of neutrino flux from μ^+ decay
b) shape of neutrino spectrum from μ^+ decay (via $\nu_e + D$)
- 4.) more mundane interactions
a) $\nu_e + C^{12}$
b) $\nu_e + O^{16}$
- 5.) exotic interactions e.g. ν oscillations

We started with the simplest experimental arrangement which might be capable of accomplishing some of these objectives. As the limitations of the various approaches became apparent we moved on to increasingly sophisticated systems.

The first approach, simply a large pot of liquid scintillator ~ 5,000 gallons with an appropriate cosmic ray anticoincidence, continues to show promise as a method for observing (2), (4, a) and possibly (1.) Characteristic of the pot approach is excellent energy resolution (~2%), and the sensitivity to delayed coincidences and pulse shape. These features enable as little as a few percent admixture of multiplicative law to be seen via $\bar{\nu}_e + p \rightarrow n + e^+$. In addition, $\nu_e + C^{12}$ (on $\nu_e + C^{13}$) could be distinguished in the majority of cases via delayed coincidences involving ground state transitions of the product nuclei, N^{12} (or B^{12}). On the other hand, a very large admixture (50%) of $\bar{\nu}_e$ such as would result from a "maximal" multiplicative law would provide a most difficult, if not insoluble, background for the important $\nu_e + e^-$ signal.

The key problems to be faced in the pot approach relates to non neutrino associated backgrounds i. e. cosmic rays and machine. A realistic view shows that ~7 meters of iron shielding should eliminate backgrounds associated with machine neutrons. This conclusion is based on the energy discrimination available and the use of pulse shape to separate electrons from recoil protons. The latter factor is not known with any precision, although it might be as high as five. Cosmic rays present a real problem, requiring an inert shield of some 2.8×10^8 gm/cm² above the detector to remove nucleons as well as to attenuate the incident muons. Details of this possible approach are found in the Appendix.

In view of these questions, we were led to inquire as to the characteristics of the various reactions which were not utilized in the pot experiment: quite clearly the directionality and specific ionization played no role. Accordingly, a more sophisticated design incorporating the features of the pot plus a sensitivity to direction and specific energy loss was developed. As described in more detail below, it consists of a scintillating slab sandwich interspersed with very thin wall spark chambers. Since the spark chambers comprise a small fraction of the mass, the scintillators operate much like the pot except for a loss in energy resolution because of the less favorable geometry for the transmission of scintillation light to the photomultipliers. The dead time occasioned by the pulsing of the spark chambers does not seem too restrictive. In addition to these features, the segmented scintillator enables the specific energy loss to be inferred, a useful discriminator against recoil protons, for example. The excellent directional sensitivity of the interleaved spark chambers and track end information is most helpful in separating the sharply peaked recoil $\nu_e + e^-$ electron from backgrounds arising from cosmic rays and inverse beta decay. An additional feature of the slab sandwich is the attractive possibility of incorporating several thin, heavy water targets in the array so as to provide a normalization of the ν_e beam. In addition to reducing uncertainties in the beam intensity and spectrum such a direct measurement of the ν_e spectrum is of considerable interest in its own right. The appearance of visible tracks is a not unattractive feature.

Because of the excellent prospects for a successful global slab sandwich series of experiments as opposed to the more limited (and somewhat less costly) pot technique, it is proposed that advantage be taken of the modular approach which is natural to the slab sandwich so as to optimize the eventual configuration. So, for example, a quarter size slab array could be used as a pilot to determine backgrounds and, incidentally, achieve such goals as to test multiplicative vs additive lepton conservation in μ^+ decay. The design which is given below reflects an extremely conservative attitude, especially with respect to shielding against neutrons from both the machine and from cosmic rays, e.g. fewer than 100 neutrons traverse the detector per day from both sources.

Research Team

1.) The University of California, Irvine-Case Western Reserve group is currently engaged in an extensive investigation of high energy neutrino interactions two miles underground, using cosmic rays. The detector is a composite scintillation, flash tube hodoscope array consisting of 200 m² of slab scintillation detectors and 50,000 flash tubes, each tube 2 meters in length. This system, probably the most elaborate detector of its kind, is yielding results.

2.) We are, in addition, in the process of constructing a large cosmic ray muon detector at UCI for the purpose of studying the spectrum and interaction of muons in the TeV range. In this connection, we have designed and are constructing novel wire spark chambers with magnetostriuctive readout, each chamber containing 4 wire planes and having an area of 10 m².

3.) The group has been continuously engaged for a decade in investigations of low energy neutrino interactions using reactors. Currently we are attempting to detect the elastic scattering reaction $\bar{\nu}_e + e^- \rightarrow \bar{\nu}_e + e^-$, and are within a factor of 2 or so of the necessary sensitivity.

Research Team - Participation

The schedule is such that we would be able to make the LAMPF experimental program one of our major activities, substituting in large measure for the deep underground cosmic ray neutrino project which is nearing successful completion.

It is anticipated that a total of 4 physicists plus technicians would spend a major part of their time on the LAMPF activity either at the home institutions in preparation or data analysis or in residence at LAMPF. Those listed would be augmented by one or two others presently in the group or under active consideration as possibly joining us in this activity.

SPECIAL APPARATUS TO BE FABRICATED BY LAMPF (give full description including sketches and cost estimate):

A sketch of the shield configuration and experimental room suitable for this program is appended. It is hoped that this would be provided as part of the LAMPF facility and that appropriate detailed design and cost estimates and actual funding would be provided by LAMPF. It is anticipated that all other experimental equipment would be provided by the experimental group.

IDENTIFICATION OF HAZARDS ASSOCIATED WITH THE EXPERIMENTAL APPARATUS AND PRECAUTIONS TO BE TAKEN:

None. The system has standard high voltages and high flash point liquid scintillator.

THE SLAB METHOD

(M. H. CHEN AND J. F. LATHROP)

I. Introduction

The elastic scattering of electron neutrinos by electrons

$$\nu_e + e^- \rightarrow \nu_e + e^- \quad (1)$$

and the corresponding reaction with electron anti-neutrinos have not yet been observed. (2,3,4) This reaction is an example of a 'diagonal' interaction which has been the subject of much recent interest. The cross section for (1) can be predicted on the basis of Universal V-A theory. (5) However, it was pointed out by Gell-Mann et al. (6) that the divergence difficulties of higher order weak interaction for 'diagonal' interactions are of a more singular nature. The result is that reaction (1) cross sections could differ significantly from V-A. (7)

The advantages of using LAMPF as a source of electron neutrinos have been discussed. (8) We list and consider briefly some of the important points.

1) The flux of electron neutrinos at 10 meters from the beam dump has been estimated. For a 0.3 mA, 700-MeV, proton beam, it is about

$$1.7 \times 10^{12} \text{ cm}^{-2} \text{ day}^{-1}$$

2) Electron neutrinos are produced as follows. π^+ 's produced in nuclear interactions stop and decay within a volume with linear dimension 2'. These produce μ^+ 's which stop and decay. (9)

π^+ 's are absorbed. Thus

- i) ν_e 's are produced with essentially no $\bar{\nu}_e$'s.
- ii) ν_e spectrum is known. Its energy is in the range $0 \leq E_\nu \leq 53$ MeV, with mean energy of 32 MeV.
- iii) ν_μ 's from π and μ decay at rest are below threshold for any known reaction.
- iv) the inverse beta reaction on bound neutrons,



are suppressed by the Pauli Exclusion Principle at these energies. The selection of targets with a large Q value can further suppress reaction (2).

- v) the incident neutrino direction is known to $\pm 2^\circ$.
- vi) the electron angular distribution from reaction (2) is (roughly) isotropic; that from reaction (1) is sharply peaked in the forward direction.

3. With about a 20 MeV threshold for detection of recoil electrons, it follows that:

- i) one is far above backgrounds from natural radioactivity.
- ii) the electrons are minimum ionizing, and can be easily distinguished from other charged particles with the same range.
- iii) electrons from reaction (1) are constrained to be within 10° of the forward direction. With multiple scattering, these electrons are still constrained within a forward cone of about 15° (in the proposed detector).

We describe next a detector for reaction (1). The rate of events in this detector for reaction (1) from ν -A is expected to be one half event per day. The background from reaction (2) has been estimated and found to be smaller than the signal.

II. The Plastic Scintillator - Spark Chamber Detector (1)

The proposed detector would be a sandwich consisting of thick plastic scintillators and narrow gap thin foil spark chamber modules. It would have dimensions 10' (length) x 8' (width) x 4' (height) and would contain 3.75 metric tons of plastic scintillator. Each layer in the sandwich would contain 3.9 gm/cm² of plastic scintillator and less than 0.2 gm/cm² of foil spark chamber. There are 32 sandwich layers altogether.

The target electrons are in the plastic scintillator. This material was chosen because

- 1) the threshold for reaction (2) on bound neutrons is large, i.e. Q value is 18 MeV.
- 2) the radiation length is large, so that multiple scattering for electrons is minimized.
- 3) the energy of the electron can be measured via pulse height to better than $\pm 1\%$ once the location of the event in the counter is known.
- 4) dE/dx in one layer can be measured in order to isolate electrons from other charged particles.
- 5) The delayed coincidence method can be used to identify inverse beta reactions on C^{12} .

Each 4' x 8' scintillation plane would consist of four 2' x 4' x 1.5" counters with long side horizontal, and installed from either side.

The thin foil spark chamber modules are used to get spacial and angular information. There are four gaps in each spark chamber module. Each gap is of "canonical" width, i.e. 1 cm. The four gaps insure that angular information can be recorded to better than 5° in one spark chamber module. Each module is 4' x 8' x 2" also standing with the long side horizontal.

The trigger for an event occurs when three or more successive scintillation counter planes are in coincidence. (10) An event is defined by eight or more contiguous sparks. With spacial information provided by the spark chamber module one can determine

- i) dE/dx using the middle counter to identify the electron,
- ii) the energy of the electron from total pulse height (to $\pm 1\%$ or better).

With angular information provided by the spark chamber module, one can isolate reaction (1) from reaction (2). Taking 20 MeV as threshold (11), all events from reaction (1), because of kinematics, will be found within a 10° cone. With multiple scattering, the detected events from reaction (1) will be constrained within a 15° cone.

The efficiency of the detector, for reaction (1), integrated over the incident ν_e spectrum is a function of the threshold for detection of the recoil electron. We list the efficiency vs. threshold in Table I.

TABLE I

Threshold (MeV)	Efficiency (%)
10.0	68
15.0	53
20.0	39
25.0	27
30.0	17
35.0	9

Balancing off the increased efficiency at lower thresholds is the larger angle of recoil from the forward direction and the larger multiple scattering angle. The extent to which the threshold can be lowered depends on the signal to background ratio. The signal and background rates are estimated next.

III. Estimated Rate for Reaction (1)

We take the threshold for detection of reaction (1) to be 20 MeV. The detection efficiency of the apparatus will then be 40%. The average energy of the neutrino in the detected reaction is 38 MeV, thus the mean cross section for reaction (1) from ν -A is 6.2×10^{-43} cm². The event rate is

$$\begin{aligned}
 R &= (\nu_e \text{ flux } [\text{cm}^{-2} \text{ day}^{-1}]) \times (\text{number of electrons/gm } [\text{gm}^{-1}]) \\
 &\quad \times (\text{gms of target } [\text{gm}]) \times \\
 &\quad \times (\text{cross section } [\text{cm}^2]) \times (\text{detection efficiency}) \\
 &= (1.7 \times 10^{12}) \times (\frac{1}{2} \times 6 \times 10^{23}) \times (3.75 \times 10^6) \\
 &\quad \times (6.2 \times 10^{-43}) \times (0.40) \\
 &= 0.5 \text{ events/day.}
 \end{aligned}$$

Each event will have 8-32 contiguous sparks directed within a 15° cone of the neutrino source. The charged particles will be identified as an electron and its energy will be known to better than $\pm 1\%$.

IV. Estimated Rate for Reaction (2)

Essentially all the neutrons which are available in the detector in order for reaction (2) to proceed are found in C^{12} . The

reaction is



where " π^{12} " designates all possible final states of the inverse beta reaction on C^{12} .

Cross sections for reaction (3) are significantly suppressed as compared to σ_2 which is expected if the neutrons in C^{12} are free. The suppression occurs for two reasons; i) the Q value for reaction (3) is large, i.e. Q = 18 MeV, and ii) the Pauli Exclusion Principle restricts the final states which are available to the proton. A crude estimate of ii) can be made using the Fermi gas model for the nucleus. One gets the well known reduction factor:

$$\kappa(|\vec{q}|^2) = \frac{3}{2} \left(\frac{|\vec{q}|}{2p_F} \right) - \frac{1}{2} \left(\frac{|\vec{q}|}{2p_F} \right)^3 \quad \text{for } |\vec{q}| < 2p_F$$

$$= 1 \quad \text{for } |\vec{q}| > 2p_F$$

where $|\vec{q}|^2 = q^2 \left(1 + \frac{q^2}{4m_p^2} \right)$, m_p is the proton mass, $q^2 = (\nu_e - e)^2$ is the squared 4-momentum transfer and $p_F = 0.284 m_p$ is the Fermi momentum. Cross sections are given in Fig. 1 for reaction (2) on i) free neutrons, ii) neutrons with Q value of 18 MeV and iii) neutrons with Q value of 18 MeV and the reduction factor due to Pauli Exclusion principle. For $E_\nu = 40$ MeV, one sees that the cross section is reduced by a factor of about 35.

Since this cross section is roughly isotropic, one has to include only the fraction of the cross section in the 15° cone. A factor of two has to be included because the electron recoil in the backward cone would be confused with the forward cone. The effective background cross section is

$$\sigma_2^{eff} \sim (2) \times \left(\frac{1}{35} \right) \times (1.3 \times 10^{-40}) \times \left(\frac{0.034}{2} \right) \quad \text{cm}^2/\text{neutron}$$

$$\sim 1.3 \times 10^{-43} \quad \text{cm}^2/\text{neutron}$$

where the last factor is the fraction of solid angle in the 15° cone. The effective cross section for reaction (1) is

$$\sigma_1^{eff} \sim (6.2 \times 10^{-43}) \times \left(\frac{1}{2} \right) \quad \text{cm}^2/\text{electron}$$

$$\sim 3.1 \times 10^{-43} \quad \text{cm}^2/\text{electron}$$

where the last factor is the fraction of electrons with energy greater than 20 MeV in the lab for a 40 MeV incident neutrino. Thus one sees that the signal to background in the 15° cone is larger than 1. In order to determine the background in the 15° cone experimentally, one has to look at events outside the 15° cone.

We have also calculated the recoil electron spectrum for reactions (1) and (2) integrated over the incident ν_e spectrum. The differential cross section for reaction (1) is known; that for reaction (2), we take as follows

$$d\sigma_2 = \sigma_2^0 (T_e + Q - E_\nu) dT_e$$

i.e., that the electron carries all the available energy. The results are given in Fig. 2. Comparing curves 1 and 2, we see that it may be possible to lower the detection threshold since this background decreases rapidly with smaller electron kinetic

energy. With a 15.0 MeV threshold the estimated rate for reaction (1) will be increased from 0.5/day to about 0.65/day because the efficiency of the detector for reaction (1) has been increased.

V. Anomalous Reactions

(1) Multiplicative Lepton Conservation Law

If lepton number conservation is multiplicative, the positive muon can decay via either⁽¹²⁾

$$\mu^+ \rightarrow e^+ + \nu_e + \bar{\nu}_\mu$$

or

$$\mu^+ \rightarrow e^+ + \bar{\nu}_e + \nu_\mu$$

The electron anti-neutrino will be easily detected via the reaction

$$\bar{\nu}_e + p \rightarrow e^+ + n,$$

with protons in the plastic scintillator. From curve 4 of Fig. 2, (as an approximation) and taking the ratio of free protons to electrons, we see that a one percent contamination of $\bar{\nu}_e$'s in the neutrino flux can be easily detected using recoil electrons with energy greater than 35 MeV, and angular distribution information.

(2) Muon Neutrino Interactions

Muon neutrinos come from π and μ decay at rest. From π decay at rest the muon neutrino gets 30 MeV. Thus if the muon neutrino has an anomalous interaction one would expect to see either a peak in the recoil electron spectrum at 30 MeV or a sharp cutoff in the electron spectrum at 30 MeV. Both can be clearly detected with the present apparatus.

VI. Details of the Detector

(1) Shielding

A schematic of the experimental site is given in Fig. 3. The detector is placed 90° from the proton beam line and located as close as possible to the beam stop. To shield the beam stop, seven meters of iron is located in front of the detector. The last three meters of iron should be movable so that machine background can be studied. The detector itself is surrounded by an active anti-coincidence shield which removes the penetrating component of cosmic rays. This system is then surrounded by several meters of concrete which shields against thermal neutrons, and the soft component of cosmic rays.

(a) Iron Shield

High energy neutrons (with K.E. $> n^\circ$ threshold, 280 MeV) are produced in the beam stop by the incident proton beam and can cause a serious background in the detector. At 90° from the beam line the production of $\sim 10^{-3}$ neutrons/sr/proton⁽¹³⁾ occurs. The "removal" length for energetic neutrons is ~ 170 gm/cm².⁽¹⁴⁾ If we require no more than 50 neutrons/day incident upon the detector which subtends 3×10^{-2} sr, then 7.0 m of iron would be needed (for 0.3 mA primary proton beam).

Low level background radiation from slow neutrons can be important in producing accidental coincidences in the detector. Because the trigger occurs when a threefold coincidence exists, such accidental coincidence rates are low with the shielding provided by 7.0 m of iron. Nevertheless, 1.0 m of concrete shielding is included because the anti-coincidence shield, to be discussed later, may require it in order to decrease this low energy background.

(b) Concrete Shield

The detector is surrounded by several meters of heavy concrete ($\sim 1.2 \times 10^3 \text{ gm/cm}^2$) and is under a ceiling of 1.0 m of iron. This shield absorbs the soft component of cosmic rays, in particular neutrons. Without this shield, the number of energetic cosmic ray neutrons ($K.E. > 280 \text{ MeV}$) traversing the slab detector is approximately 700 sec^{-1} ($6 \times 10^7 \text{ day}^{-1}$).⁽¹⁵⁾ With 3.0 m of heavy concrete and 1.0 m of iron, this number is reduced by a factor 10^6 . The machine duty cycle further reduces this number by a factor of 16. This results in about 40 neutrons/day in the detector, a number that is comfortably small.

(c) Anti-coincidence Shield

The anti-coincidence house will have dimensions approximately 18' (length) x 15' (width) x 10' (height), and it is shown in Fig. 3. To act as a shield, it must have high efficiency while being relatively insensitive to low energy background. We think that liquid scintillator in acrylic slab tanks, similar to those used by the UCI group in the underground cosmic ray neutrino experiment, will meet these requirements.

With 3.0 m of heavy concrete ($\sim 1200 \text{ gm/cm}^2$) surrounding the detector, the cosmic ray muon intensity becomes slightly less ($\times 0.5$) than the standard sea level intensity. The number of muons traversing the detector is estimated to be 600 sec^{-1} (or $5 \times 10^7 \text{ day}^{-1}$).⁽¹⁶⁾ The number of stopping muons in the detector is estimated to be 20 sec^{-1} (or $1.6 \times 10^6 \text{ day}^{-1}$). We propose not to distinguish between the traversing and stopping muons in that the anti-coincidence shield will generate a 25 μsec gate for every anti-coincidence signal. With an anti-coincidence efficiency of one part in 10^4 and the machine duty cycle of 6%, the detector trigger rate is acceptably low. Because the detector trigger is defined by a triple coincidence in the upper or lower group of counters and because cosmic rays are mostly vertical, there is some additional automatic rejection of the cosmic ray signal. With spacial and angular information provided by the spark chambers, a discrimination factor of at least 30 is also to be included. Thus cosmic rays will be adequately shielded. We note that the number of muons traversing the anti-coincidence shield is approximately $2 \times 10^3 \text{ sec}^{-1}$. With a 25 μsec gate, the anti-coincidence deadtime is 8%.

(2) Scintillator Planes

Each scintillation plane is made up of 4 pieces of plastic scintillator with dimensions $2' \times 4' \times 1\frac{1}{2}"$, and each piece viewed from the short end with six 2" photomultiplier tubes. The schematic is given in Fig. 4. An estimate of cost is given in Table II. The scintillator resolution is estimated in Fig. 5. We see that the uncertainty in pulse height for the passage of a minimum ionizing particle through one slab is better than $\pm 20\%$. This is a sufficiently accurate dE/dx measurement to discriminate between electrons and other charged particles. The uncertainty in energy for a 20 MeV electron which is stopped is determined to be better than $\pm 1\%$. With NE110 or with a larger number of phototubes, the resolution can be significantly improved. We emphasize that the location of the event in the scintillator slab is known from analysis of the spark chamber data, and is used to counteract light attenuation in the slab, i.e. to get absolute normalization.

(3) Thin Foil Spark Chamber Modules

The thin foil spark chamber modules have sensitive areas of the same dimension as the scintillation planes. Each module will have five aluminum foils separated by 1 cm each. High voltage is connected to two foils to generate four active spark gaps. The total of four sparks provides for sufficient angular resolution in one module.

(4) Photography

The spark chambers are viewed by small angle stereo. Because the entire detector must be placed within an anti-coincidence shield against cosmic rays, it is necessary to minimize the volume within this shield. Possible approaches are shown in Fig. 6.

An alternate approach is to use either magnetostrictive, acoustical or wire spark chambers. These would decrease the cost of the anti-coincidence shield, but the cost of spark chambers and peripheral equipment would increase along with the added complications of the spark chambers.

(5) Electronics and Logic

The scintillation counters provide 128 channels of information. For each channel there would have to be a linear amplifier, a high level and a low level discriminator, analogy pulse height storage, and quick access storage. The standard electronics and logic is also required for triggering.

VII. Determination of Incident Neutrino Flux

Because the proposed method for studying reaction (1) is relatively clean and because it can provide over 100 events from reaction (1) in one year of data taking (assuming Universal V-A), the incident neutrino flux must be known accurately so that the absolute cross section for reaction (1) can be determined.

(1) A possible approach to take is as follows. Build two additional layers of the sandwich detector where instead of plastic scintillator slabs, one inserts "tanks" with dimensions $24" \times 48" \times 3\frac{1}{2}"$, filled with deuterated liquid scintillator. The container "tanks" are made from $\frac{1}{2}"$ plastic. These "tanks" hold approximately one half metric ton of $C_{10}D_8U_{10}$. The thickness of these "tanks" is not a handicap because the reaction looked for is



which is roughly isotropic. Thus multiple scattering is not a problem. These "tanks" must be inserted within the detector in order to detect backward events.

We estimate the event rate for reaction (4). The mean neutrino energy is $\sim 40 \text{ MeV}$ so that the inverse beta cross section on free neutrons is $\sim 1.3 \times 10^{-40} \text{ cm}^2$. The cross section for reaction (4) is $\sim \frac{1}{3}$ smaller.⁽¹⁷⁾ Thus

$$\begin{aligned} R &= (1.7 \times 10^{12}) \times \left(\frac{10}{148} \times 6 \times 10^{23} \right) \times (0.5 \times 10^6) \\ &\quad \times \left(\frac{1}{3} \times 1.3 \times 10^{-40} \right) \times (0.3) \\ &= 0.4 \text{ events/day} \end{aligned}$$

The last factor is the detector efficiency. This arises from assuming spark chamber efficiency to be zero for tracks greater than 45° . The overall rate is therefore comparable with that from reaction (1) even though the system is much smaller.

(2) A second much less costly approach has also been considered. One builds these layers as before, but the "tanks" are

filled with D_2O . With D_2O , one loses some energy resolution since the energy deposited in D_2O is unknown, but the cost of D_2O is relatively small (see Table II). The three layers are evenly distributed within the sandwich so that events initiated in reaction (4) in one "tank" does not penetrate into the other "tanks". The estimated event rate with the above configuration is ~ 0.9 events/day. The increase is due to the additional layer and due to a larger number of deuterium per molecule.

It is clear that with the above approaches it is possible to determine the incident neutrino flux to better than $\pm 10\%$ statistical accuracy. Using this experimentally determined flux, it is possible to determine reaction (1) cross section to $\pm 15\%$ (assuming Universal V-A).

VIII. A Proposed Program

Because it is desirable to locate the detector system as close as possible to the beam stop and because of the uncertainties with regard to the effects of neutron induced background, it is not clear what the optimum distance to the beam stop will be. In addition, the intensity of the ν_μ flux from μ^+ decay is not known to high accuracy ($\sim 10\%$). Such information is necessary for an accurate absolute normalization of the elastic scattering cross section if the reaction is observed.

A program which will provide answers to the above problems is proposed. The sequence is listed in column 1 of Table III. The required equipment and estimated run times are given in columns 2 and 3. The accelerator duty cycle refers to an average of 11 shifts/week accelerator on time. Estimated event rates for the different reactions are also given. The number in brackets assumes $50\% \bar{\nu}_\mu$'s from μ^+ decay as would result from a "maximal" multiplicative law. These estimates are based on a 0.3 mA, 700 MeV proton beam current with the slab detector located at a mean distance of 10.0 m from the beam dump. The expected number of events on Deuterium is somewhat higher than given. (17) Thus the estimated run time is $2\frac{1}{2}$ years.

With the proposed program, it appears possible to test the multiplicative lepton conservation law in four months. A $\bar{\nu}_\mu$ admixture of $\sim 10\%$ can be easily distinguished in this time. If the experiment progresses for 30 months, a $\sim 1\%$ admixture will be seen with the proposed apparatus. As to the ultimate goal of this experiment, i.e. the elastic scattering reaction, if the interaction is purely V-A, then it appears possible to determine this cross section to $\sim \pm 15\%$ in the proposed 30 months.

TABLE II
COST ESTIMATES (APPROXIMATE)

I. "Slab" Detector			
(1)	Plastic Scintillator (NE102 or NE110)		
	Size: 24" x 48" x 1 $\frac{1}{2}$ " x 4 x 32		
	Total Mass: 3.75 metric tons		\$60 K.
(2)	2" Phototubes (RCA-4518)		
	Total Number: 32 x 24 = 768		
	Unit Cost: \$73		\$56 K.
(3)	Lucite Lightpipes		
	Size: 24" x 6" x 1 $\frac{1}{2}$ " x 4 x 32		
	Total Mass: 0.47 metric tons		\$ 2 K.
(4)	Four gap thin foil spark chamber modules		
	Size: $\sim 48" \times 96" \times 2"$ x 32		\$50 K.
(5)	i) Electronics (Logic)	\$60 K.	
	ii) Photographic apparatus	\$ 5 K.	
	iii) Data reduction	\$50 K.	\$115 K.
II. Anti-coincidence Shield			
(1)	5" Phototubes*		\$20 K.
(2)	Anti-coincidence tanks (raw material, construction and scintillator*)		\$48 K.
III. ν_e Flux Detector*			
	D_2O (heavy water) @ \$28/lb.		
	Total Mass: ~ 0.75 metric tons		\$45 K.
IV. Contingency			
			\$40 K.
		Equipment Total	\sim \$440 K.
*These phototubes and some quantity of liquid scintillator are in hand from previous experiments.			
* $C_{10}H_8D_{10}$ (deuterated liquid scintillator) with a total mass of ~ 0.50 metric tons would cost \sim \$300 Kf.			
V. Manpower* (total duration of experiment including preparation, running and analysis)			
(1)	4 physicists @ 20 K/man yr. (4 yrs.)		\$320 K.
(2)	2 technicians-engineers @ 15 K/man yr. (4 yrs.)		\$120 K.
(3)	One scanner @ 10 K/man yr. (2 yrs.)		\$ 20 K.
		Manpower Total	\$460 K.
		Grand Total	\$900 K.

*This includes overhead expenses.

TABLE III

Experiment	Equipment (sandwich layers)	Estimated Run Time (50% accelerator duty cycle) ^{a)} (months)	Estimated Number of Events ^{b)}				
			e	H	D	C	O
Multiplicative Test	12	4	12 (6)	0 (90)	-	22 (22)	-
Elastic Scattering	32	12	100 (50)	0 (720)	-	400 (400)	-
Normalization	32 + 3 (D ₂ O)	7	70 (35)	0 (500)	100 (100)	280 (280)	66 (66)
Re-normalization	32 + 3 (H ₂ O)	7	70 (35)	0 (500)	-	280 (280)	66 (66)
Total		30	250 (125)	0 (1800)	100 (100)	1000 (1000)	130 (130)

a) 11 accelerator shifts/week.

b) 0.3 mA, 700 MeV proton beam and slab detector at a mean distance of 10.0 m.

APPENDIX

The "Pot" Method

(W. R. Kropp and H. W. Sobel)

The essential feature of the experiment is a large (5,000 gal.) hydrocarbon scintillator well shielded from the accelerator and provided with an efficient cosmic ray anticoincidence blanket, and an overburden of 2.8×10^8 gm cm⁻². Before discussing the experimental arrangement further, let us consider the reactions which can be produced in the scintillator by LAMPF neutrinos. Assuming that only $\bar{\nu}_e$'s are present in the decay spectrum (additive lepton conservation law) only two reactions are possible:

$$\bar{\nu}_e + e^- \rightarrow \bar{\nu}_e + e^- \quad (1)$$

and

$$\bar{\nu}_e + C^{12} \rightarrow N^{12} + e^- \quad (2)$$

In the case of the multiplicative law, $\bar{\nu}_e$'s are produced in equal numbers with ν_e and these additional interactions are possible:

$$\bar{\nu}_e + e^- \rightarrow \bar{\nu}_e + e^- \quad (3)$$

$$\bar{\nu}_e + p \rightarrow n + e^+ \quad (4)$$

$$\bar{\nu}_e + C^{12} \rightarrow B^{12} + e^+ \quad (5)$$

Background from reactions (2) and (5) leading to the ground states of N^{12} and B^{12} does not appear to be a serious problem because of the availability of a distinctive delayed coincidence between the inverse beta decay and the beta decay of the resultant nuclei:

$$N^{12} \rightarrow C^{12} + e^+ + \bar{\nu}_e \quad (6)$$

(17.6 MeV end point, $\tau_{1/2} = 11$ ms)

and

$$B^{12} \rightarrow C^{12} + e^- + \bar{\nu}_e \quad (7)$$

(13.4 MeV end point, $\tau_{1/2} = 19$ ms)

However, possible particle break up of excited N^{12} and B^{12} may seriously limit the energy below which such a background would mask electrons from the elastic scattering process.¹⁰

By raising the energy threshold for detection to 35 MeV (the maximum energy available to the electron in reaction (2)), this difficulty is surmounted (Fig. 8)¹⁰. Thus until further theoretical and experimental evidence is available, we conservatively choose this threshold and consider only reactions (1), (3) and (4).

The presence of $\bar{\nu}_e$ in the beam will be quickly revealed by the occurrence of reaction (4). This reaction is recognized by the e^+ spectrum and characteristic delayed coincidence between e^+ production and n capture.

Neutrino Fluxes:

The expected flux of electron neutrinos from LAMPF is $\sim 3 \times 10^7$ cm⁻² sec⁻¹ at 8.0 meters from the beam stop.¹¹ These arise from the decay of μ^+ produced by the reaction $\pi^+ \rightarrow \mu^+ + \nu_\mu$. As noted, the admixture of ν_e and $\bar{\nu}_e$ is determined by the nature of the lepton conservation law. The ν_e spectrum from μ decay is $\propto (E_\nu)^2$ while the $\bar{\nu}_e$ spectrum would be $\propto (E_\nu)^2$ (33 - $\frac{2}{3}E_\nu$). See Fig. 9.

Expected Signal Rates:

Folding together the spectra from μ decay and the recoil spectra from V-A theory, we obtain the cross-sections for the production of recoil electrons $\geq E_0$ for reactions (1) and (4). These are given in Table V.

E_0 (MeV)	$\sigma(\geq E_0)$ $\bar{\nu}_e + e^-$ (10^{-48} cm ² /electron)	$\sigma(\geq E_0)$ $\bar{\nu}_e + p$ (10^{-41} cm ² /proton)
25	1.45	9.03
30	0.904	8.45
35	0.482	7.46
40	0.203	5.92
45	0.051	3.72
50	0.005	0.80

Table V

The cross-sections for $\bar{\nu}_e + e^-$ are approximately 1/8 those for $\nu_e + e^-$ at energies characteristic of μ decay. Using these cross-sections, the rates per day in 5,000 gal located 11 m from the beam stop are given in Table VI for various energy thresholds. The 11 meter beam stop to detector distance is dictated by the required neutron shielding (see below).

E_0 (MeV)	Rate (day ⁻¹) in 5,000 gallons at 11 Meters		
	$\bar{\nu}_e + e^-$	$\bar{\nu}_e + e^-$ (approximate)	$\bar{\nu}_e + p$
25	1.13	0.07	81
30	0.70	0.04	76
35	0.37	0.02	67
40	0.16	0.01	53
45	0.04	0.002	34
50	0.004	0.0002	7

Table VI

(Allowance has been made for the equal admixture of ν_e and $\bar{\nu}_e$ in calculating the $\bar{\nu}_e + e^-$ and $\bar{\nu}_e + p$ rates. The $\bar{\nu}_e + e^-$ rate is calculated assuming all neutrinos are $\bar{\nu}_e$.)

From Table VI we see that an admixture of $\sim 3\%$ $\bar{\nu}_e$ in the beam will produce equal rates for reactions (1) and (4). Assuming a 90% neutron detection efficiency, a 21% contamination of $\bar{\nu}_e$ in the beam gives a signal to background of 1 for reaction (1). A 50% contamination (expected from the multiplicative law) would completely mask the elastic scattering signal.

Description of the Proposed Detector:

Fig. 10 gives a schematic of the proposed detector. The central portion of the detector consists of 5,000 gal. of CH₂ based scintillator in the form of a cylinder 2.88 m in diameter and 2.88 m high. This volume is viewed by ~ 400 5-inch photomultiplier tubes, through a 0.13 m thickness of non-scintillating, optically matching fluid.

The scintillator is chosen because it provides both electron and proton targets. In addition, the carbon target and optical matching fluid of the inner container has about as high a threshold for inverse beta decay as can be found.

The inert fluid serves a dual purpose. It minimizes the dependence of photomultiplier signal on event location and its ~ 20 MeV thickness for electrons discriminates against inverse beta decay events which take place outside the detector.

The 35 MeV cutoff for $\nu + C^{12}$ reactions (reaction (2)) places stringent requirements on detector resolution. It is necessary that the energy resolution of the detector be good enough to discriminate between

a > 35 MeV pulse from $\nu_e + e^-$ and a < 35 MeV pulse from the products of $\nu_e + C^{12}$. A resolution of 2% or 0.70 MeV should suffice for this purpose (Fig. 8).

Can such excellent energy resolution be achieved? In view of the many factors involved in determining the energy resolution of such scintillation detectors, we are fortunate to be able to scale performance from experience.²² A 580 gallon cylindrical detector 150 cm diameter and 120 cm high was painted with a white reflecting coat filled with mineral oil based scintillator (CH_2) and viewed by 100, 5-inch p.m. tubes. Its energy resolution for a centrally located gamma ray source (^{60}Co 2.0 MeV total energy) was 15% full width at half maximum. If variation of resolution with energy is governed by photon statistics, one would expect a resolution at 35 MeV of 4.2% full width at half maximum or $\pm 2\%$. Scaling the test detector to 5,000 gallons and allowing for the use of improved tubes with photocathode efficiency of ~25% (as compared with the test detectors tubes whose efficiency was ~15%) indicates ~330 tubes are required for 2% resolution.

Granting that the required energy resolution is achievable, it is still necessary to estimate the fraction of recoil electrons whose energy is totally absorbed, i. e. the detection efficiency for electrons with energy > 35 MeV. The point here is two fold: the electron track may not be entirely contained in the detector (edge effects) and some of the electron energy loss is in the form of bremsstrahlung.

Because of the great size of the detector under discussion (3 meters in diameter) these combined effects²³ are < 25%.

Neutron Background:

a.) n^0 Production

Accelerator neutrons of energy ≥ 280 MeV can make n^0 's in our sensitive volume. Since the interaction length for n^0 production is about 170 gm/cm², our tank is about 2 interaction lengths thick. We assume that all the neutrons in this range make n^0 's. The n^0 's decay into 2 gamma rays each with energy ≥ 70 MeV. At these energies the absorption length is about 50 gm/cm². On the average, we have therefore three absorption lengths for the gammas to traverse. This means that only a small fraction of the events will occur where both gammas escape without either depositing enough energy to exceed our discriminator of 53 MeV.

We, however, design our neutron shield to attenuate these neutrons to a level \leq the expected elastic scattering rate independent of the above considerations.

There are 6×10^{12} neutrons/sec. at energies ≥ 280 MeV at an angle of $\sim 90^\circ$ to the incident proton beam.²⁴ The removal mean free path in iron is 21.6 cm or equivalently the interaction length is 170 gm/cm². The center of our detector is 11 meters from the center of the beam stop and therefore subtends 8.2×10^{-3} sr. From these considerations, we see that there are 4.2×10^{10} neutrons day⁻¹ with an energy ≥ 280 MeV incident upon the tank. In order to reduce this rate to below the 0.4 day⁻¹ elastic scattering signal, 8.5 meters of iron are required. Since the facility to remove a portion of this shield is desirable if the background is as low as expected, a modular shield is necessary. A shield consisting of 7.1 meters of iron and 1 meter of lead would satisfy the above requirements. Fig. 11 gives a tentative sketch of the required shield.

b.) Knock-on Protons

Accelerator neutrons can impart energy to protons in the detector by means of an elastic collision. Since the relative response of the scintillator for protons is $\sim 1/2$ that for electrons, a neutron of energy ≥ 70 MeV would be necessary to exceed our lower threshold. The removal mean free path for neutrons ≤ 280 MeV decreases rapidly²⁵ and at 70 MeV for example λ_r is 12.8 cm as opposed to $\lambda_r = 21.6$ cm for 280 MeV neutrons. The attenuation, therefore, is enormously larger for these lower energies (a factor of $\sim 10^{13}$ for 70 MeV) and the shield correspondingly more effective. The spectrum of neutrons reaching the detector will, therefore, be very small below 280 MeV and peak at this energy, since the production spectrum is decreasing above 280 MeV. The higher the neutron energy, the smaller the probability that the knock-on proton will look like an electron in the 35-53 MeV energy range. If we therefore conservatively assume that all the neutrons are at 280 MeV, the maximum proton energy will look like 140 MeV in the detector. This means that only about 13% will be in our window. The shield as designed is, therefore, also conservative for this mechanism.

In addition, by looking at the pulse shape, we hope to be able to discriminate between protons and electrons.²⁶

c.) Low Energy Neutron Leakage

This consideration is simplified by our 35 MeV minimum energy requirement. Capture gamma rays are below this energy.

Cosmic Rays and Their Interactions in the Detector

a.) Cosmic Ray Muon Background

Using a $\cos^2 \theta$ angular distribution for cosmic rays, our cylindrical detector has an effective area of 20.5 m² sr. A fit to the differential muon spectrum as measured at mountain altitudes¹⁸ (3,200m) for energies greater than ~ 1.5 GeV is

$$I = .0562 E^{-2.57} \text{ cm}^{-2} \text{ sec}^{-1} \text{ sr}^{-1} \text{ GeV}^{-1}$$

If, for example, we had 10^8 gm/cm² of material above our detector, the resultant flux of muons would be

$$F = \int_{E_0}^{\infty} I dE$$

where E_0 is the minimum energy muon which can penetrate 10^8 gm/cm², in this case 1.8 GeV.

$$F = 1.42 \times 10^{-3} \text{ cm}^{-2} \text{ sec}^{-1} \text{ sr}^{-1}$$

The rate of muons through our detector in this case would be (20.5 m² sr) ($1.42 \times 10^{-3} \text{ m}^{-2} \text{ sec}^{-1} \text{ sr}^{-1}$) = $2.91 \times 10^{-2} \text{ sec}^{-1}$. Since the LAMPF duty cycle is 1/16 this is reduced to $1.82 \times 10^{-3} \text{ sec}^{-1}$. Our detector is about 500 MeV thick so the above rate would be spread out in a spectrum going from zero to about 500 MeV. We are, however, only concerned with that fraction of the muons which deposit between 35 and 53 MeV. We conservatively estimate this fraction to be about 18/500 by assuming equal probability from zero to 500 MeV. The rate in this energy range is thus (18/500) (1.82×10^{-3}) = $6.6 \times 10^{-5} \text{ sec}^{-1}$ = $5.7 \times 10^{-5} \text{ day}^{-1}$. In Table VII, the rate is evaluated for various thicknesses of absorber above the detector.

Thickness (gm/cm ²)	E_0 (GeV)	$F(\text{cm}^{-2} \text{ sec}^{-1} \text{ sr}^{-1})$	Rate (day ⁻¹)
1.0×10^3	1.8	1.42×10^{-3}	5.7×10^{-5}
1.5×10^3	3	6.38×10^{-4}	2.5×10^{-5}
2.0×10^3	4	4.06×10^{-4}	1.6×10^{-5}
2.5×10^3	5	2.86×10^{-4}	1.1×10^{-5}

Table VII

Some old data (February, 1965) taken in the basement of the Physics building at LASL with a 3 m² liquid scintillation slab (one of the original neutrino detectors used at Savannah River) allows us to check the above estimates. The rate seen in this detector in the 20-40 MeV range was $1.3 \times 10^6 \text{ day}^{-1}$. If we multiply this number by the duty cycle factor and normalize to our larger area we get a rate of $2.3 \times 10^6 \text{ day}^{-1}$. This number compares favorably with the above.

Since the elastic scattering rate is 0.37 day⁻¹, an overburden of 2×10^8 gm/cm² and an anti-coincidence factor of 10^3 would produce a background conservatively estimated to be 0.5 of the signal. Cosmic ray anti-coincidence factors of 10^3 have been achieved.²⁷

b.) Rate in Anti-Coincidence Detector

The effective area of the anti-coincidence shield for a $\cos^2 \theta$ angular distribution of cosmic ray muons is about 100 m² sr, with an overburden of 2×10^8 gm/cm², the rate is (100 m² sr) ($4.06 \times 10^{-4} \text{ sec}^{-1} \text{ sr}^{-1}$) = $4.1 \times 10^{-2} \text{ sec}^{-1}$. For one microsecond electronics, the dead time would be 0.4%.

c.) Stopping Muons

Stopping muons can simulate the elastic scattering signal, since the resulting electron is emitted some microseconds after the original muon signal. Muons can stop in the anti-coincidence shield, in the inert region near the phototubes inside the detector, or in the detector scintillator itself.

1.) Muons stopping in the anti-coincidence shield

Since most of the detector has a 20 MeV thick inert region surrounding it, the electron will be below threshold if it passes through this region. If the muon stops in the anti-coincidence regions below the sensitive volume, the electron signal will be accompanied by a second pulse in the anti-coincidence so vetoing the event.

2.) Muons stopping in the inert region

The number stopping in the inert region is estimated to be about 1×10^6 day⁻¹. Half of the electrons in this case will be going the wrong direction and only about half will be in the interval 35 to 53 MeV. When we also use the duty cycle of 1/16, the resultant number of electrons in the sensitive volume in our range is about 1.5×10^5 day⁻¹. These events, however, will be characterized by a muon entering the anti-coincidence and not leaving. An anti-coincidence factor of 10^3 would, therefore, be sufficient to eliminate this mechanism.

3.) Muons stopping in the sensitive volume

The detector is about 500 MeV thick, so the number that stop is

$$\int_{4.0}^{4.5} 0.0563 E^{-2.5} dE = 6.86 \times 10^{-4} \text{ cm}^{-2} \text{ sec}^{-1} \text{ sr}^{-1}$$

or $(6.86 \times 10^{-4} \text{ cm}^{-2} \text{ sec}^{-1} \text{ sr}^{-1}) (20.5 \text{ m}^2 \text{ sr}) (8.64 \times 10^4 \text{ sec day}^{-1})$
 $= 1.2 \times 10^3 \text{ day}^{-1}$

These events will be characterized by a large signal some microseconds earlier. If we veto every block of time 20 microseconds after such an event, our dead time would be only 0.4% and the mechanism is effectively eliminated.

d.) Neutral component

The flux of neutrons from cosmic rays at the LAMPF altitude is $6 \times 10^{-3} \text{ cm}^{-2} \text{ sec}^{-1} \text{ sr}^{-1}$ for energies above 200 MeV.¹² This implies a rate in our tank of $(6 \times 10^{-3}) (10^6) (20.5) = 1.23 \times 10^3 \text{ sec}^{-1} = 1.06 \times 10^4 \text{ day}^{-1}$. Dividing by the duty cycle, we get $6.6 \times 10^2 \text{ day}^{-1}$. To get this down to the level of our elastic scattering signal (0.4 day^{-1}) , we need an attenuation of $(6.6 \times 10^2) \times (2.65)$ or 1.75×10^3 . This implies an overburden of $2.8 \times 10^3 \text{ gm/cm}^2$.

Cost Estimates:

Cost estimates are given in Table VIII

EQUIPMENT			
Tubes	5,000 gallon detector	400 @ \$150	= 60 K
	anticoincidence	250 @ \$150	= 40 K
Scintillator liquid	5000 gallons	@ \$3	= 15 K
	anticoincidence ~ (13,000 gallons)		= 39 K
5,000 gallon tank detector			= 35 K
Anticoincidence tanks			= 25 K
Electronics			= 40 K
Contingency			= 15 K
	Subtotal		269 K
MANPOWER*			
	3 physicists @ 20K/man yr (4 yrs)		= 240 K
	2 technicians/engineers 15K/man yr (4 yrs)		= 120 K
	1 scanner 10K/yr (2 yrs)		= 20 K
	Total		380 K
	Grand Total		649 K

* includes all overhead

REFERENCES

- (1) M. H. Chen, (UCI-10P19-47, internal report).
- (2) H. J. Steiner, Phys. Rev. Letters **24**, 746 (1970).
- (3) F. Roines and H. Gurr, Phys. Rev. Letters **24**, 1448 (1970).
- (4) R. B. Stothers, Phys. Rev. Letters **24**, 538 (1970).
- (5) R. P. Feynman and M. Gell-Mann, Phys. Rev. **109**, 193 (1958); R. E. Marshak and E. C. G. Sudarshan, Phys. Rev. **109**, 1860 (1958).
- (6) M. Gell-Mann, M. Goldberger, N. Kroll, and F. E. Low, Phys. Rev. **179**, 1518 (1969).
- (7) From Universal V-A Theory, the differential cross section for reaction (1) is

$$d\sigma_1 = \frac{2G^2}{\pi} m_e dT_e = \sigma_0 \frac{dT_e}{m_e}$$

and the total cross section is

$$\sigma_1 = \frac{2G^2}{\pi} m_e \left(\frac{2E_\nu^2}{m_e + 2E_\nu} \right) = \sigma_0 \frac{2E_\nu^2}{(m_e + 2E_\nu)}$$

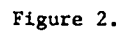
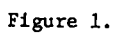
where

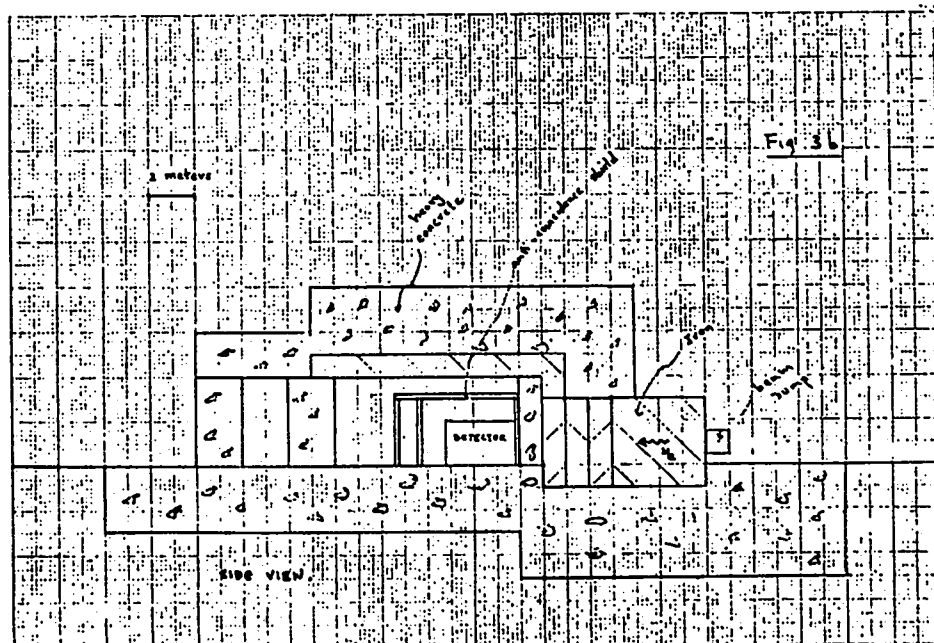
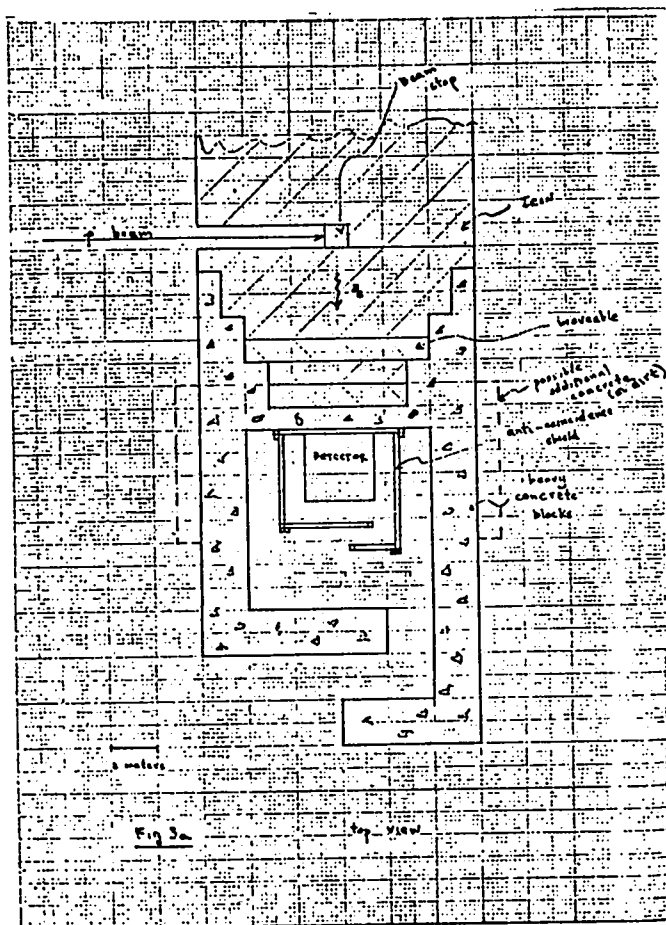
$$\sigma_0 = \frac{2G^2}{\pi} m_e^2 = 8.3 \times 10^{-45} \text{ cm}^2,$$

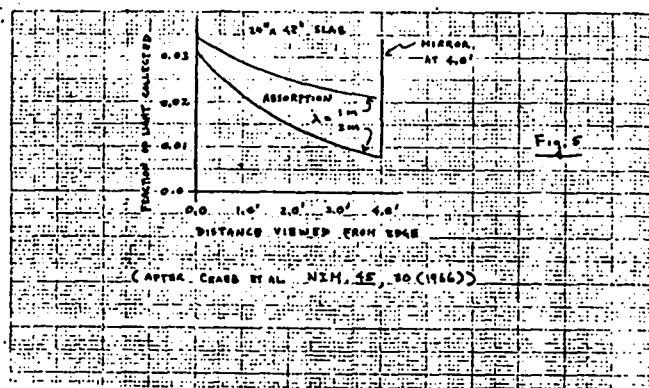
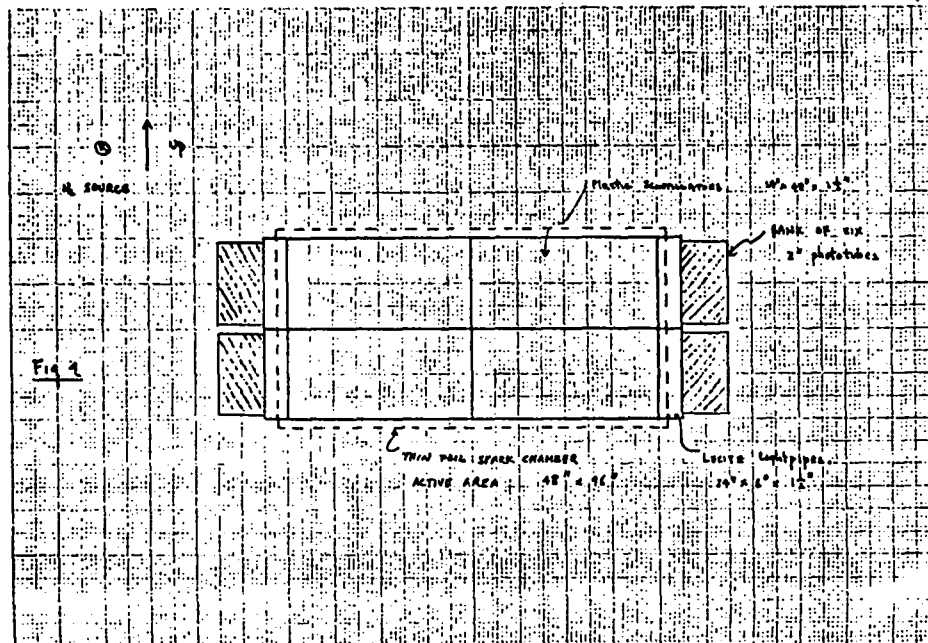
T_e is the lab kinetic energy of the recoil electron, E_ν is the lab energy of the incident neutrino, and G is the Fermi coupling constant.

- (8) Expected neutrino fluxes at LAMPF can be found in the original design book.
- (9) The fraction of π and μ decays in flight is small.
- (10) This requirement may be varied, e.g. one could require each counter to accept pulses from the passage of minimum ionizing particles (or smaller, down to some fixed threshold).
- (11) The threshold can be varied in analysis. With a threefold coincidence for triggering and minimum pulses of order 2 MeV from each counter, electrons with energy greater than 12 MeV will be accepted.
- (12) G. Feinberg and S. Weinberg, Phys. Rev. Letters **6**, 381 (1961).
- (13) Yale design report, Fig. B4, p. IV-92.
- (14) Yale design report, Table C1, p. IV-97.
- (15) B. Peters, Cosmic Rays, p. 9-225, Part 9, Chapter 12 of Handbook of Physics, edited by E. U. Condon and N. Odishaw (New York, McGraw-Hill, 1958); see also Khriyan et al., JETP **15**, 465 (1962).
- (16) S. Hayakawa, Cosmic Ray Physics, p. 374 (New York, Wiley-Interscience, 1969).
- (17) F. J. Kelly, and H. Überall, Phys. Rev. Letters **16**, 145 (1966). The fraction $\frac{1}{3}$ holds at $E_\nu \sim 15$ MeV. For higher neutrino energies, this fraction approaches 1. Thus the estimated rate can be as much as a factor of 3 larger.
- (18) Preliminary information indicates that as many as 30% of the reactions may go by particle emission. Kelley and Überall are currently in the process of extending their calculations to lower energies. (H. Überall, private communication).
- (19) The cross section used here to estimate the $\nu_e + C^{12}$ background was calculated by H. Chen (Ref. 1).
- (20) This assumes an 0.3 mA, 700 MeV proton beam reaches the beam dump. (LAMPF Users Group Newsletter, **2**, 1, March (1971)).
- (21) Yale design report, Fig. IV-13, p. IV-47.
- (22) L. V. East, Phys. Rev., **149**, 913 (1966).
- (23) The edge effect loss <10%, bremsstrahlung losses <20%. A precise measurement of these effects can be made using the actual detector to measure the muon decay electron spectrum with cosmic rays. Since the decay spectrum is peaked at 53 MeV, rather than decreasing to zero at this energy as does the ν_e recoil spectrum, its measurement is a most severe test. Such a measurement made with a relatively small detector (75 cm cylinder diameter) gave an efficiency of ~0.3 for decay electrons in the range 35 to 53 MeV.
- (24) Yale design report, Fig. B-4, p. IV-92.
- (25) Yale design report, Fig. C-1, p. IV-86.

- (27)







Attenuation of light pipe ($\times 0.36$) is included.

Assumes that photocathode area equals edge area.

Note: $\lambda = 2m$ is realistic for NE102 (footnote in Crabb et al.)

NE110 is supposed to be better.

We use $\lambda = 1.0m$ as the worst case.

View short edge with six 2" tubes (44 mm sensitive diameter,

20% photocathode efficiency)

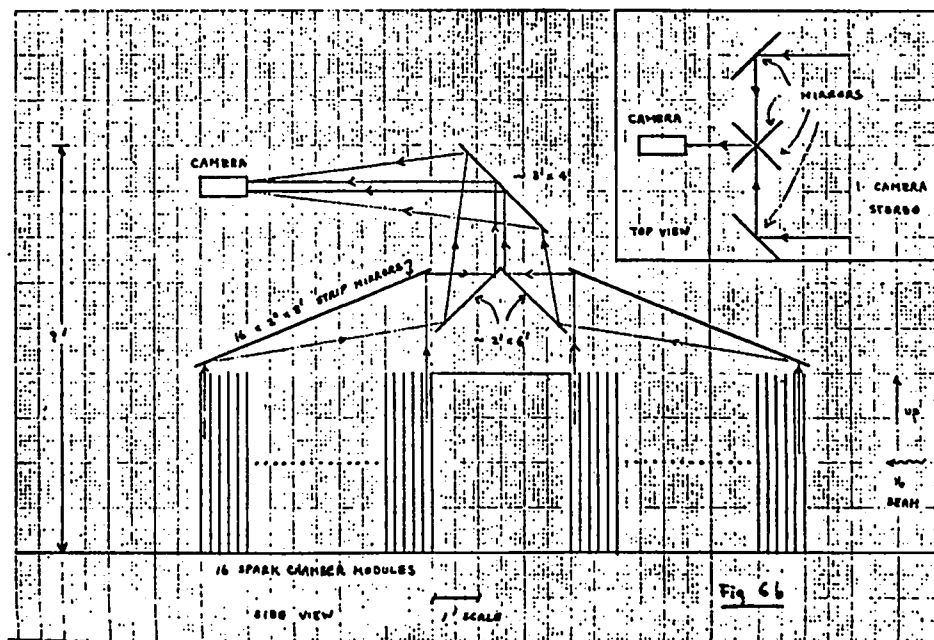
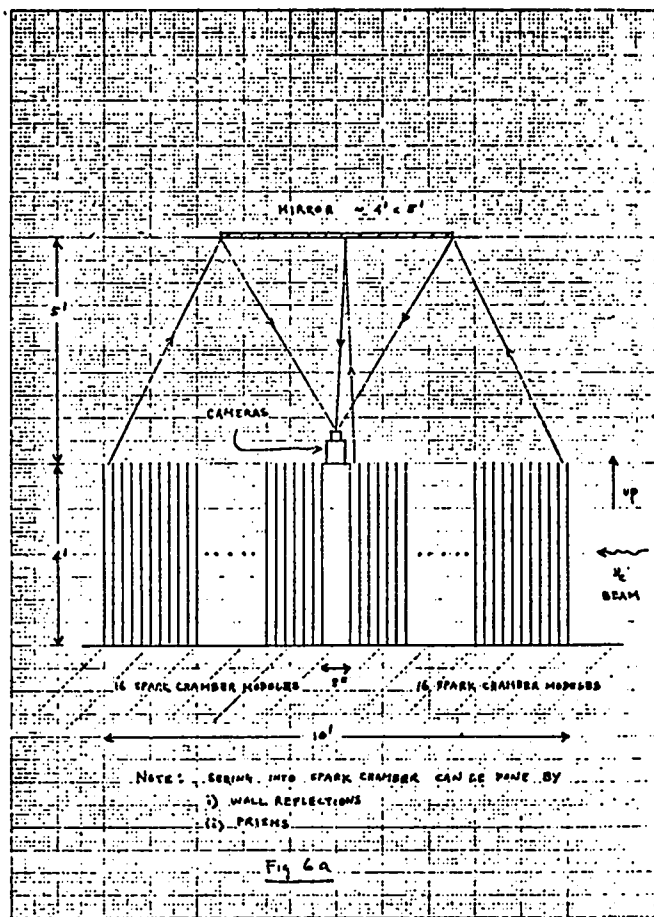
Ratio of area = $\frac{\text{Cathode area}}{\text{edge area}} = 0.37$

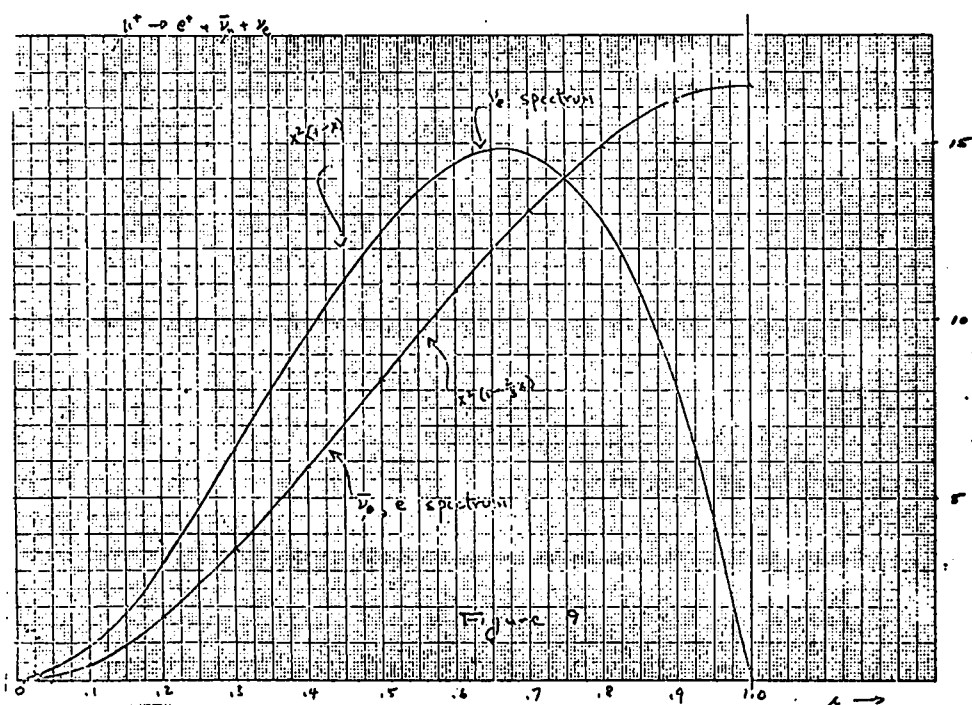
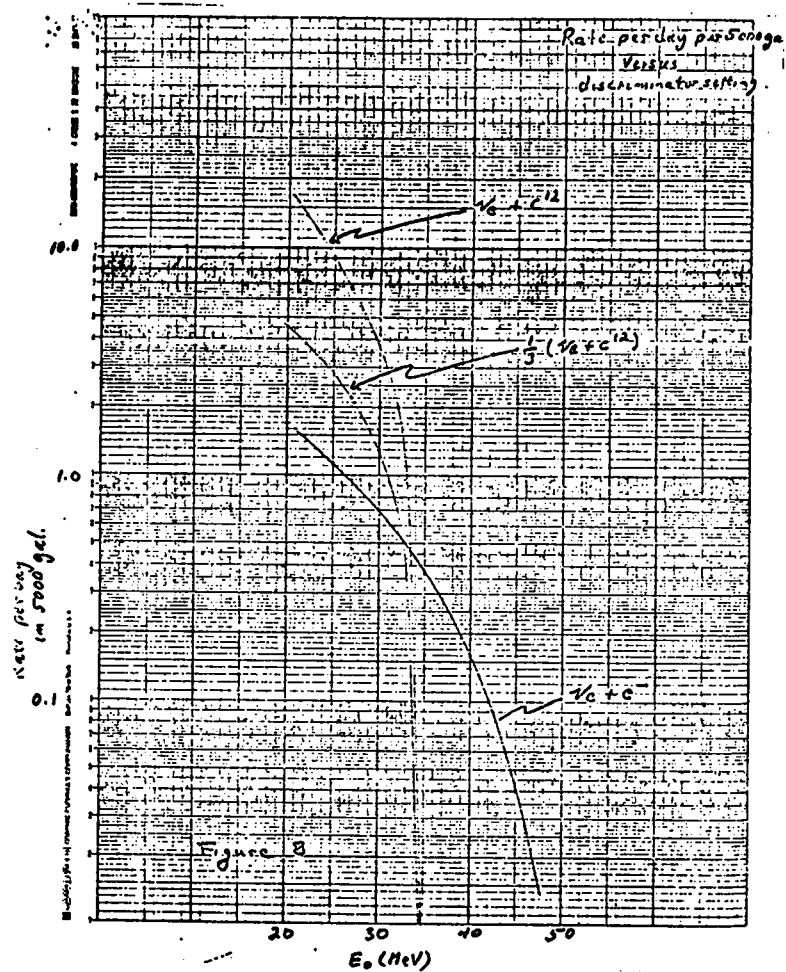
Number of photoelectrons = $(10^4/\text{MeV}) \times (0.01) \times (0.37) \times (0.2)$
 $= 7.4/\text{MeV}$ (worst case)

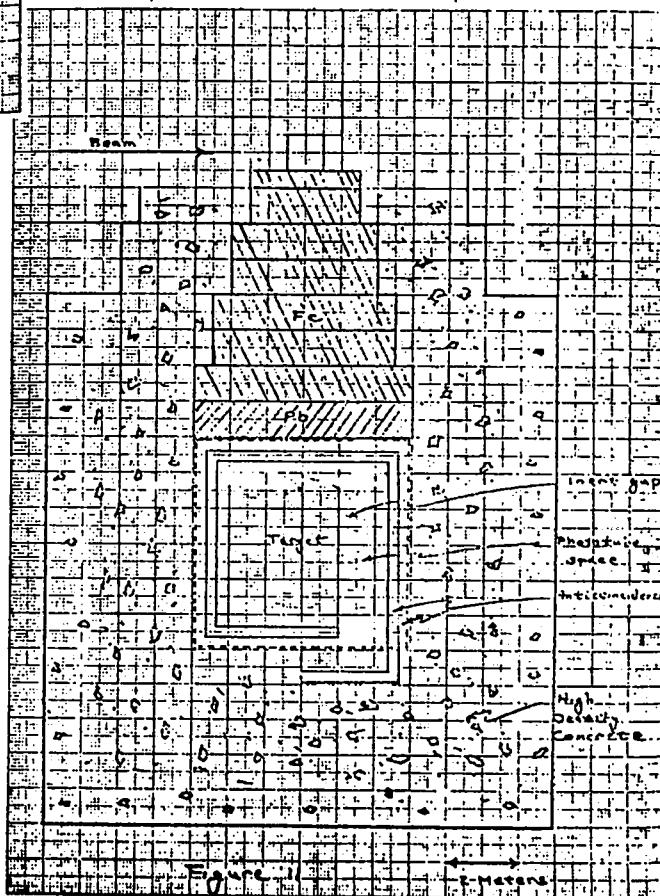
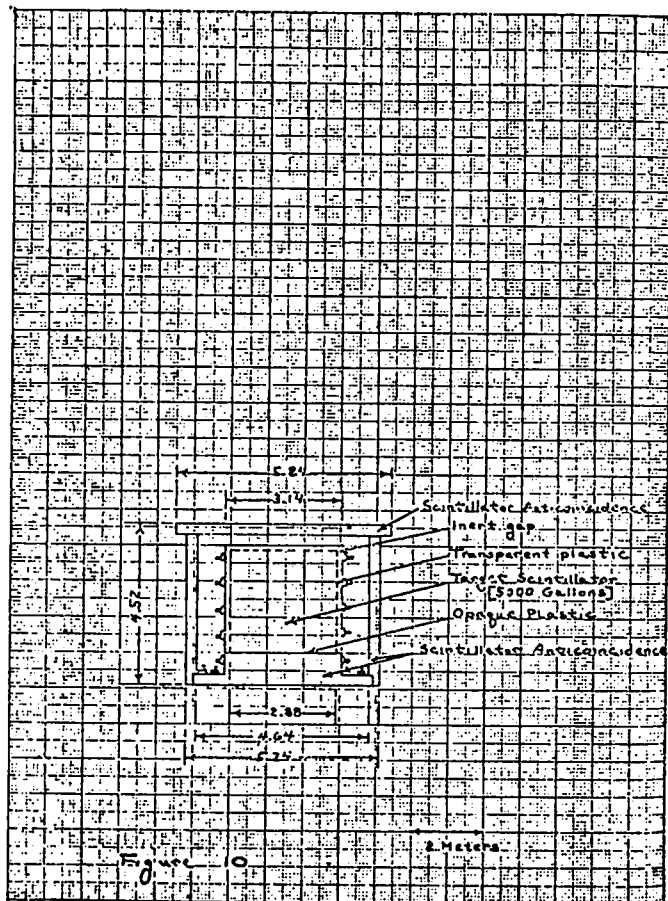
Decrease by factor of 2 to allow for uncertainties - 3.7 photons/MeV

7 MeV/slab (minimum ioniz.) = $\pm 20\%$

30 MeV electron (stopped) = $\pm 15\%$







No. 53 - "Observation of the Electron Neutrino at LAMPF"

R. Davis, BNL; E. Fowler, Purdue U.; and
S. L. Meyer, Northwestern U.

Research Proposal
Los Alamos Meson Physics Facility

Observation of the Electron Neutrino at LAMPF
Title of Experiment

Participants and Institutions

Raymond Davis, Brookhaven National Laboratory
Earle Fowler, Purdue University
Stuart L. Meyer, Northwestern University

Date: March 30, 1971

GENERAL DESCRIPTION

Beam Area:
Neutrino (beam dump area)
Secondary Channel (if known):
Beam Requirements:
Type of Particle:
Momentum Range:
Momentum Slice:
Solid Angle:
Spot Size:
Distance:
Intensity:
Beam Purity:
Target(s):
Primary Beam Requirements (State any requirements on the main accelerator beam, such as energy, intensity, or unusual pulse characteristics):
Maximum intensity, $E > 700$ MeV and steady
Machine Time Required:
Installation Time Required (no beam): 3 months
Turn-up Beam (give intensity and hours needed):
Data Runs (give realistic estimate of hours needed): 20-30 days per run
Scheduling:
Realistic date when User will have the non-LAMPF apparatus ready: July, 1972
Give all information on other commitments of research group that may affect scheduling:
Major LAMPF Apparatus Required:
Spectrometer, Magnets, Electronics, Computer
Shielding and Enclosures Required:
Neutrino area shielding as discussed
Special Services Required (power, water, engineering, shop work, etc.):
None
Space Required (attach drawing giving layout):
Modest

SUMMARY OF EXPERIMENT

We propose to utilize the reaction
 $\mu^+ + \text{Cl}^{37} \rightarrow \text{Ar}^{37*} + e^+$
to detect the electron-neutrino (as distinguished from the electron-antineutrino) and to study the question of whether the lepton conservation law is an additive law or a multiplicative law. This measurement will also provide a calibration of the neutrino flux from the decay of stopped positive muons in the beam stop as well as a check on the assumed energy spectrum of neutrinos from muon decay.

We propose to dispose a tank of several kilogallons of C_2Cl_4 around the LAMPF beam dump. We estimate a flux of $4 \times 10^7/\text{cm}^2\text{-sec}$ electron-neutrinos at a distance of 10 meters to produce a signal rate of 7.5 events/kilogallon-day. The equipment required is quite modest since the radiochemical technique is identical with that used in connection with the solar neutrino experiment and exists at Brookhaven National Laboratory. Required for the LAMPF installation is the necessary flushing and plumbing for several kilogallons and shielding from the beam stop adequate to eliminate the possibility of fast neutrons entering the tank as well as a sufficient number of interaction lengths (two meters iron-equivalent) to eliminate the muonic component of the cosmic radiation. The residual background due to cosmic-ray-muon-induced events is such that the beam time required to measure the cross-section of the reaction of interest to 5% is estimated to be 3.4×10^4 kilogallon-days. E.g. a 4000 gallon experiment could measure the cross-section to 20% in 21 days of running and about the same amount of off time.

DETAILED STATEMENT OF THE EXPERIMENT

The neutrino story spans almost precisely four decades of physics history. Pauli first introduced the idea of a penetrating neutral particle of very small mass at an American Physical Society meeting in June, 1931 and Fermi incorporated the neutrino into his theory of beta decay in 1934. The electron-antineutrino was directly detected by Reines and Cowan¹ in 1956. The fact that the electron-neutrino and the electron-antineutrino are distinct was shown by Davis in 1955 and by the absence of various double-beta-decay processes (ignoring the occasional citation of positive results for this latter series of experiments). The nonobservation of the electron-gamma and the three-electron decay modes of the muon indicated the possibility of the existence of two distinct neutrinos, electron-neutrinos and muon-neutrinos. The detection of muon-neutrinos as distinct from electron-neutrinos was accomplished by Danby, Gellard, Goulianos, Lederman, Mistry, Schwartz and Steinberger² in 1962. Since that time, muon-neutrinos and muon-antineutrinos have been experimentally detected.

Two experimental gaps currently exist. First, the electron-neutrino has not yet been positively identified to exist save as a possible background in experiments at high-energy accelerators. Second, the nature of the lepton conservation law which obtains in weak interactions is not yet clarified. The two possibilities which exist are the additive lepton conservation law and the multiplicative.³ At present, both are consistent with experiment. The detailed statement of the two possibilities is outlined in Appendix A but the salient results are as follows.

The additive law permits the decay

$$\mu^+ \rightarrow e^+ + \nu_e + \bar{\nu}_\mu \quad (1)$$

and forbids the decay

$$\mu^+ \rightarrow e^+ + \bar{\nu}_e + \nu_\mu \quad (2)$$

whereas the multiplicative law allows both and carries the implication that each decay mode is present 50% of the time.

The transition

$$\mu^+ + e^- \rightarrow \mu^- + e^+ \quad (3)$$

provides a test of the additive and multiplicative conservation laws since this "muonium-antimuonium" transition is forbidden for the additive

law but allowed for the multiplicative law. A similar situation obtains in the case of the process⁸

$$e^- + e^- \rightarrow \mu^- + \mu^- \quad (4)$$

These reactions have so far proved to be inconclusive concerning the additive-multiplicative question.

We propose to use the reaction



to detect electron-neutrinos, a technique first suggested by Pontecorvo, elaborated on by Alvarez and developed by Davis.

This reaction is allowed by both the additive and multiplicative laws whereas the reaction



is forbidden by both (as well as having been shown experimentally not to occur). We propose to use the IAMPF beam dump as a source of electron-neutrinos from reaction (1). Pions of both charges are produced in the beam dump by hadronic interaction of the primary proton beam. Of those pions which do not interact before stopping, only the positive pions will survive to decay into positive muons. The stopping negative pions will effectively all be captured on the heavy nuclei in the beam dump before decaying. The beam dump is, therefore, a source of stopped positive muons. These positive muons will all stop and decay via the mode (1) if the additive lepton conservation law holds and by both (1) and (2) if the multiplicative law holds. It has been proposed by many others to search for reactions characteristic of (2). A null result would indicate the non-occurrence of (2). To complete the logic, an affirmation of (1) is required which our proposed experiment would provide, as well as a verification of the existence of the electron-neutrino. Our experiment also provides a calibration of the neutrino flux useful in the electron-antineutrino searches as well.

The Cl^{37} neutrino capture reaction is a very important one for astrophysics. The IAMPF measurement provides a terrestrial test of the physics of the reaction itself, independent of the astrophysical context.

Another question which will be probed by this experiment concerns the detailed nature of reaction (1). At the 1965 International Conference on Weak Interactions at Argonne Prof. V. Telegdi¹⁰ pointed out the "circularity" of many arguments designed to verify the V-A theory. He quoted the conclusion of Mrs. C. Jarlskog to the effect that we would not understand muon decay until the neutrino and anti-neutrino spectra were measured. We do not here propose a measurement of the spectrum but, rather, a check on our assumptions about the spectrum. We use V-A theory (and nuclear physics) to tell us what the cross-section is, as a function of energy.

We use V-A theory to form the convolution of the cross section and flux. This yields a prediction involving the fundamental assumptions of the V-A theory. Experimental disagreement would be more interesting but would require other measurements¹² to localize the source of the disagreement.

Some Details

In Figure 1 we plot the expected spectrum of electron neutrinos (ν_e) from μ^+ decay: $\mu^+ \rightarrow e^+ + \nu_e + \bar{\nu}_\mu$

where we have assumed an additive lepton conservation law and the usual Fermi theory of weak interactions.

The cross section for the reaction: $\nu_e + \text{Cl}^{37} \rightarrow \text{Ar}^{37} + e^-$ goes up roughly as the square of the neutrino energy

$$\sigma = \sigma_0 (M_{1f})^2 F(Z, E) p_e E_e$$

where p_e , E_e are measured in units of m_e and

$$\sigma = 4.5 \times 10^{-45} \text{ cm}^2/\text{Cl}^{37} \text{ atom.}$$

The Fermi function $F(Z, E)$ is approximated by the constant value 1.5 over any neutrino energy range. The matrix element $(M_{1f})^2 = (1)^2 + (\frac{C_A}{C_V})^2 (g)^2$

For $\text{Cl}^{37} \rightarrow \text{Ar}^{37}$ ($T = 3/2$, $J = 3/2^+$)

$$(1)^2 = 3$$

$$(g)^2 = 1/5$$

$$(C_A/C_V)^2 = (1.18)^2 \approx 1.4 \text{ and}$$

$$(M)^2 \approx 3.3$$

The cross section for the analog state transition is, therefore, increased over the solar neutrino case because the higher energy ν_e from μ^+ decay on average are ~ 95 times as effective as ν_e from B^8 decay as seen from the following simple calculation assuming all the energy dependence of the cross section may be well-approximated as

$$\sigma = K (E_\nu - \Delta)^2$$

where Δ is the energy threshold for the reaction.

The average cross section for a B^8 neutrino is $\langle \sigma \rangle_{\text{B}^8} =$

$$K \frac{\int_{\Delta}^{\text{E}_{\text{max}}} (E_\nu - \Delta)^2 f(E_\nu) dE_\nu}{\int_{\Delta}^{\text{E}_{\text{max}}} f(E_\nu) dE_\nu} = K (E_\nu - \Delta)^2$$

The ν_e spectrum from a decay such as that of B^8 may be written in a normalized form as

$$\frac{dN}{dE_\nu} = 30 (1 - E_\nu)^2 E_\nu^2$$

where $E_\nu = 1$ at the maximum of the neutrino spectrum.

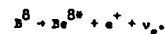
$$\langle \sigma \rangle_{\text{B}^8} = K (E_{\nu \text{max}})^2 30 \int_{\frac{\Delta}{E_{\nu \text{max}}}}^1 (E_\nu - \frac{\Delta}{E_{\nu \text{max}}})^2 (1 - E_\nu)^2 E_\nu^2 dE_\nu$$

For ν_e from μ^+ decay, we may calculate the spectrum of Figure 1 from the relation $\frac{dN}{dE_\nu} = 12 E_\nu^2 (1 - E_\nu)$

and

$$\langle \sigma \rangle_{\mu} = K (E_{\nu \text{max}})^2 12 \int_{\frac{\Delta}{E_{\nu \text{max}}}}^1 (E_\nu - \frac{\Delta}{E_{\nu \text{max}}})^2 E_\nu^2 (1 - E_\nu) dE_\nu$$

In this form, we may now scale up all the transitions of interest using the published calculations of Bahcall¹³ for the neutrinos from the boron decay



The cross sections averaged over the boron spectrum (labelled B) and the muon spectrum (labelled M) are as follows:

State	Energy threshold	B (from Bahcall)	M/B ratio	M
2nd	0.303	0.745×10^{-43}	21.6	16.1×10^{-43}
$\frac{1}{2}^+ + \frac{1}{2}^-$	1.72	$1.69 \times "$	29.6	$55.9 \times "$
$\frac{3}{2}^+, \frac{1}{2}^-$	1.91	$2.46 \times "$	31.0	$77.1 \times "$
$\frac{3}{2}^+, \frac{3}{2}^-$	5.30	$7.83 \times "$	95.5	$747.8 \times "$
Sum		1.3×10^{-42}		0.9×10^{-40}

The ratio of the averaged boron cross section to the averaged muon cross section is thus about 69.

Rate

The absolute rate is obtained from the cross section averaged over the μ^+ decay spectrum:

$$\langle \sigma \rangle_{\mu} = 69 \langle \sigma \rangle_{\text{B}^8} = 69 (1.35 \times 10^{-42} \text{ cm}^2) = 0.9 \times 10^{-40} \text{ cm}^2/\text{Cl}^{37} \text{ atom.}$$

Let us calculate the signal rate for a modest amount of C_2Cl_4 , say 6000 kilograms which corresponds roughly to 1000 gallons.

$$N = \# \text{ of } Cl^{37} \text{ atoms} = \frac{6 \times 10^6 \text{ gm}}{154 \text{ gm/mole}} \times 6.03 \times 10^{23} \times 4 \times 0.25$$

where the number of chlorine atoms and the isotopic abundance of Cl^{37} just cancel in the last two factors.

$$= 2.4 \times 10^{28} \text{ atoms of } Cl^{37}.$$

Let us take the flux of ν_e at 10 meters from the beam stop to be

$$\phi = 4 \times 10^7 / \text{cm}^2 - \text{sec}$$

which is consistent with other discussions but less than the "Blue Book." ¹⁴

The count rate is, therefore,

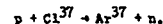
$$\begin{aligned} R &= \phi \sigma N \\ &= 4 \times 10^7 \text{ cm}^{-2} - \text{sec}^{-1} \times 0.9 \times 10^{-40} \text{ cm}^2 / \text{atom} \times 2.4 \times 10^{28} \text{ atoms} \\ &= 8.6 \times 10^{-5} \text{ events/sec.} \end{aligned}$$

$$R = 7.5 \text{ events/day-1000 gallons.}$$

This is quite clearly a feasible counting rate although calculated for a small detector. One might well think of disposing the detector liquid around the beam dump so as to increase the flux over that assumed.

Background

The nucleonic component of the cosmic radiation must be removed by shielding to avoid the reaction



Likewise, fast neutrons from the beam dump and from upstream targets must be prevented from entering the detection tank lest knock-on protons be produced in the Cl^{37} . The shielding from the beam dump may be less than two meters of iron equivalent and the overhead shielding required is the same since it is the number of interaction lengths which is of interest rather than the range. Cosmic-ray muons still produce background events and we estimate these to be of the order of 60/kilogallon-day. If the additive law holds and our calculations of cross-section and flux prove correct, we shall require

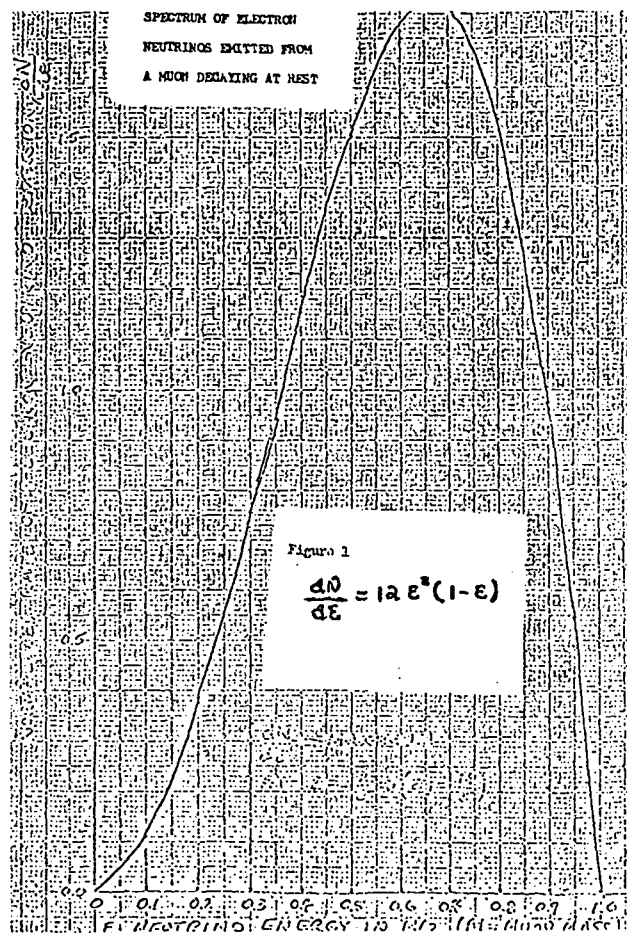
$$(3.4/\epsilon^2) \times 10^4 \text{ kilogallon-days}$$

of running to determine the cross-section to 5%. E.g. a 4000-gallon experiment could measure the cross-section of 20% in 21 days of running and about the same amount of time with the beam off.

References

1. E. Fermi, *Z. Physik* **88**, 161 (1934).
2. F. Reines and C.L. Cowan, *Science* **124**, 103 (1956).
3. R. Davis, *Phys. Rev.* **27**, 766 (1955).
4. G. Danby, *et. al.*, *Phys. Rev. Letters* **9**, 36 (1962).
5. See, B. Pontecorvo, *Soviet Physics JETP* **26**, 984 (1968).
6. G. Feinberg and S. Weinberg, *Phys. Rev. Letters* **6**, 381 (1961).
7. J.J. Amato *et. al.*, *Phys. Rev. Letters* **21**, 1709 (1968).
8. W.C. Barber *et. al.*, *Phys. Rev. Letters* **22**, 902 (1969).
9. a) J. Bahcall, *Sci. Amer.* **221**, 28 (1969).
b) E.E. Salpeter, *Comments on Nucl. and Part. Phys.* **II**, 87 (1968).
c) J. Bahcall and G. Shaviv, *Astrophysics Journ.* **153**, 133 (1968).
d) R. Davis, Jr., D.S. Harner, and K.C. Hoffmann, *Phys. Rev. Letters* **20**, 1205 (1968).
e) J. Bahcall, W.A. Bahcall and G. Shaviv, *Phys. Rev. Lett.* **20**, 1209 (1968).
f) V. Gribov and B. Pontecorvo, *Physics Lett.* **28**, 493 (1969).
g) B. Pontecorvo, *Soviet Physics, JETP* **26**, 984 (1968).

10. Proc. of the International Conference on Weak Interactions, October 25-27, 1965, Argonne National Laboratory ANL-7130, pp. 350-1, 364.
11. C. Jarlskog, *Nuclear Phys.* **72**, 699 (1966).
12. For example, the detection of electron neutrinos in Deuterium or Carbon ¹² would have a different dependence of cross-section on neutrino energy and hence would be sensitive, together with the Chlorine measurement, to the energy spectrum of neutrinos from muon decay. These reactions are discussed in United States Naval Ordnance Laboratory Report number NOL TR 66-221, *Neutrino Absorption in H^2 and C^{12}* by Francis J. Kelly.
See also Kelly and Uberall, *Phys. Rev. Letters* **16**, 145 (1966).
For Li^7 and B^{10} see Reines and Woods, *Phys. Rev. Letters* **14**, 20 (1965) and Reines and Knapp, *Phys. Rev. Letters* **12**, 457 (1964).
13. J. Bahcall, *Phys. Rev.* **135**, B137 (1964).
14. H.S. Butler and D.R.F. Cochran, *Proposal for a High Flux Meson Facility at Los Alamos*, p. 36.



Appendix A: Additive and Multiplicative Laws

Define N_e = electron number

N_μ = muon number

N_L = lepton number

ADDITIVE LAW:

DN_μ and DN_e are separately conserved.

The assignment is as follows:

	$\frac{N_\mu}{DN_\mu}$	$\frac{N_e}{DN_e}$	$\frac{N_L}{DN_L}$
μ^-	+1	+1	0
μ^+	-1	-1	0
ν_μ	+1	+1	0
$\bar{\nu}_\mu$	-1	-1	0
e^-	0	+1	+1
e^+	0	-1	-1
ν_e	0	+1	+1
$\bar{\nu}_e$	0	-1	-1

The reaction $\mu^+ + e^+ + \nu_e + \bar{\nu}_\mu$ conserves DN_μ , DN_e and DN_L .

The reaction $\mu^+ + e^+ + \bar{\nu}_e + \nu_\mu$ conserves DN_L but does not conserve

DN_μ (-1 \rightarrow +1) nor DN_e (0 \rightarrow -2).

The reaction $\nu_e + Cl^{37} \rightarrow Ar^{37} + e^-$ conserves DN_μ , DN_e and DN_L .

The reaction $\bar{\nu}_e + Cl^{37} \rightarrow Ar^{37} + e^-$ conserves DN_μ but violates conservation of DN_e (-1 \rightarrow +1) and DN_L (-1 \rightarrow +1).

The reaction $\mu^+ + e^- \rightarrow \mu^- + e^+$ conserves DN_L but violates conservation of DN_μ (-1 \rightarrow +1) and DN_e (+1 \rightarrow -1).

MULTIPLICATIVE LAW:

This says that $\Sigma (N_\mu + N_e)$ is conserved and the sign $(-1)^{DN_\mu}$ is con-

served. (Also the sign $(-1)^{DN_e}$ is conserved).

The assignment is as follows:

	$\frac{N_\mu}{DN_\mu}$	$\frac{N_e}{DN_e}$	$\frac{N_L}{DN_L}$
μ^-	+1	+1	-1
μ^+	+1	-1	-1
ν_μ	+1	+1	-1
$\bar{\nu}_\mu$	+1	-1	-1
e^-	-1	+1	+1
e^+	-1	-1	+1
ν_e	-1	+1	+1
$\bar{\nu}_e$	-1	-1	+1

The reaction $\mu^+ + e^+ + \nu_e + \bar{\nu}_\mu$ conserves $\Sigma(N_\mu + N_e)$ (lepton number) and conserves the sign $(-1)^{DN_\mu}$ (-1 \rightarrow -1).

The reaction $\mu^+ + e^+ + \bar{\nu}_e + \nu_\mu$ conserves lepton number $\Sigma(N_\mu + N_e)$ and conserves the sign $(-1)^{DN_\mu}$ (-1 \rightarrow -1).

Likewise, $\nu_e + Cl^{37} \rightarrow Ar^{37} + e^-$ is allowed by the multiplicative rule but $\bar{\nu}_e + Cl^{37} \rightarrow Ar^{37} + e^-$ is forbidden.

The transition $\mu^+ + e^- \rightarrow \mu^- + e^+$ is allowed by the multiplicative rule (+1 \rightarrow +1).

In summary, then:

Reaction	Additive	Multiplicative
$\mu^+ + e^+ + \nu_e + \bar{\nu}_\mu$	Allowed	Allowed
$\mu^+ + e^+ + \bar{\nu}_e + \nu_\mu$	Forbidden	Allowed
$\nu_e + Cl^{37} \rightarrow Ar^{37} + e^-$	Allowed	Allowed
$\bar{\nu}_e + Cl^{37} \rightarrow Ar^{37} + e^-$	Forbidden	Forbidden

Reaction	Additive	Multiplicative
$\mu^+ + e^- \rightarrow \mu^- + e^+$	Forbidden	Allowed
$e^- + e^- \rightarrow \mu^- + \mu^-$	Forbidden	Allowed

KT/pt: 770 (500)